Potential use of the *Oncorhynchus mykiss* checkpoint proteins Rad1 and Hus1 as genotoxicity biomarkers

by

Johny Bozdarov

A thesis
presented to the University of Waterloo
in fulfillment of the
thesis requirement for the degree of
Master of Science
in
Biology

Waterloo, Ontario, Canada, 2010

AUTHOR'S DECLARATION

I hereby declare that I am the sole author of this thesis. This is a true copy of the thesis, including any required final revisions, as accepted by my examiners.

I understand that my thesis may be made electronically available to the public.

Abstract

Cell-cycle checkpoint proteins help maintain genomic integrity by sensing damaged DNA and initiating DNA repair or apoptosis. Checkpoint protein activation to cell-cycle damaging agents can involve post-translational modifications and these alterations provide a means to determine whether DNA in a cell is damaged or not. Steinmoeller *et al*. (2009) showed that checkpoint proteins are suitable biomarkers for detecting genotoxins in *Oncorhynchus mykiss* (rainbow trout). In this project, two evolutionarily conserved checkpoint proteins, Rad1 and Hus1, have been cloned from rainbow trout and antibodies against these proteins were developed. This is the first time that either Rad1 or Hus1 has been characterized in rainbow trout. For rtRad1, it was determined that the open-reading frame was 840bp, which encodes 279aa with a predicted protein size of 31kDa. The rtRad1 amino-acid sequence is highly conserved and contains conserved exonuclease and leucine zipper domains. RT-PCR was used to identify alternatively spliced variants of rtRad1 and it appears that these variants encode different sized Rad1 proteins that are tissue and cell-line specific. A Rad1 splice variant that encodes an 18kDa protein appears to be abundant only in heart tissue and in the RTgill-W1 and RTbrain-W1 cell-lines. A genotoxicity study was completed where RTgill-W1 and RTbrain-W1 cells were treated with bleomycin, which induces double-stranded DNA breaks. In RTgill-W1, levels of an 18kDa Rad1 protein increased in a dose-dependent manner while in RTbrain-W1 the Rad1 levels remained the same. It appears that this 18kDa Rad1 protein may be directly involved in maintaining genomic integrity and shows potential to be used as a genotoxicity biomarker. This is the first time that an isoform of Rad1 has shown to be modified in the presence of a damaging agent. Both Rad1 and Hus1 need to be further characterized to determine their usefulness as genotoxicity biomarkers.

Acknowledgements

For the last two years, I have encountered amazing people who have helped me on my journey and I would like to send out my gratitude. This list is in no particular order.

I would like to thank my supervisor Dr. Brian Dixon for giving me this opportunity and for being a great leader. I will always thank you for entrusting me to make my own decisions and for allowing me to work at my own pace. You didn't take the fun out of science by constantly putting pressure on "getting results" and I hope that the effort I gave is reflected in my thesis and that they meet your standards. I would also like to thank you for allowing two students to work under my guidance. Because of it, I had the privilege of learning important leadership, organization and communication skills that not all Master students get to learn. I am not sure if I will continue in academia, but if I do I hope that we can collaborate on many future projects together.

I would like to thank my co-supervisors, Dr. Bernard Duncker and Dr. Niels Bols for their guidance and leadership. I appreciate the many sit-downs we have had to discuss this project and the excitement you both have shown in Rad1 and Hus1. I appreciate the expertise given by Dr. Duncker on all things molecular and on cell-cycle checkpoints. Thank you Dr. Bols for the many exciting discussions we have had on Rad1 and I look forward to working with you in January. It was great having three supervisors because I got to learn from three different specialists.

I had the privilege of having two undergrad students help me with this project, Daniel Zicherman and John Chi. Thank you Daniel for your help in discovering the cDNA sequence of rtRad1 and for cloning the open-reading frame of rtHus1 into an expression vector. John Chi was one of the hardest working people I have ever met and because of his work ethic we were able to overexpress and purify 17mg of rtHus1 recombinant protein in just 2 months. Both Daniel and John were great researchers and I am sure that they will have successful futures.

I would like to thank my colleagues in the biology department that have helped me throughout the years. A special thank you goes to Linda Zepf and Mila Kaufman who are two of the nicest people I have met and their helping hand made my two years a lot easier and enjoyable. All the members of the Brian Dixon lab have made these two years fun and exciting. I have made great friendships with many of you that will last forever and I appreciate all the help received throughout the years. I would like to thank Katja Engel for her help throughout the years. You have been a great friend and colleague and the help you gave me during my protein expression period will always be appreciated. I would like to thank Michelle Liu and Fanxing Zeng for preparing the bleomycin and hydroxyurea studies, respectively. I

received a lot of great advice from a great friend, Zhenyu Cheng, throughout the years that saved me a lot of time and for that I thank him. I would like to thank my colleague, Spence Macdonald, for the many stimulating discussions on biology that we have had over beers.

Last but definitely not least I would like to thank my partner Kimberley Le Sueur and my family. Kim, you are the best girlfriend a guy could ask for. I appreciate all the effort you made driving me to lab late at night, especially on Sundays to grow overnight cultures, or picking me up when it was cold out so that I didn't get sick when I walked home. You kept me company during many of the late nights and would entertain me on my breaks. Best of all, you never complained that my Masters was ruining weekends or holidays and you were always supportive. You are always there for me and I will always love you.

To my big brother Atanas Bozdarov, you're the best role model a brother could ask for. You're a beauty, a pillar of strength that I lean on like the big bear that I am. Without you, this Masters would not have happened, thanks for all your help. Also, thank you for all the graphic design work you did for my poster. To my uncle, Dragan Bozdarov, you have helped educate me since I was a child and it is because of your advice that I am where I am today. To my mother, the strongest women I know, thanks for all the motherly things you have done for me during my Masters; like doing my laundry when I was too busy and making me amazing food to keep me going. I owe you and love you more than you know.

Everyone I have mentioned has helped me greatly. I apologize to anyone that I have forgotten.

Thank you!

Sincerely,

Your friendly neighborhood scientist,
Johny Bozdarov

Table of Contents

List of Figures

List of Abbreviations

Cyclin-dependent kinases	**CDKs**
Cell-division cycle 6	**CDC6**
Retinoblastoma protein	**pRb**
Anaphase-promoting complex	**APC**
Spindle assembly checkpoint	**SAC**
Origin replication complex	**ORC**
Chromatin licensing and DNA replication factor 1	**CDT1**
Minichromosome maintenance proteins 2-7	**MCM2-7**
Replication protein A	**RPA**
Cell division cycle protein 45	**Cdc45**
Go-inchi-ni-san	**GIN**
DNA polymerase α-primase	**pol-prim**
Topoisomerase I	**TopI**
Replication factor C	**RFC**
Flap endonuclease 1	**Fen1**
Polo-like kinase 1	**PLK1**
Topoisomerase II	**TopII**
Single-stranded DNA breaks	**SSBs**
Double-stranded DNA breaks	**DSBs**
Rad9, Rad1 and Hus1	**9-1-1 complex**
BRCA1 C-terminus repeat	**BRCT**
Ataxia telangiectasia mutated	**ATM**
p53 binding protein 1	**53BP1**
Mediator of DNA damage checkpoint 1	**MDC1**
Breast cancer susceptibility gene 1	**BRCA1**
Phosphoinositide 3-kinase related kinases	**PIKKs**
Ataxia Telangiectesia Rad3-related	**ATR**
ATR-Interacting-Protein	**ATRIP**

Variant histone H2AX	**γH2AX**
Centromere associated protein E	**CENP-E**
deoxyribonucleotide triphosphate	**dNTP**
Radiation-sensitive	**RAD**
Proliferating cell nuclear antigen	**PCNA**
Jun-activation domain-binding protein 1	**Jab1**
Alternative lengthening of telomeres	**ALT**
Promyelocytic leukemia	**PML**
7,12-Dimethylbenz[a]anthracene	**DMBA**
Polycyclic aromatic hydrocarbons	**PAH**
Real-Time	**RT**
Rainbow trout Rad1	**rtRad1**
Polymerase chain reaction	**PCR**
Ultraviolet	**UV**
Phosphate buffered saline	**PBS**
Tris-buffered-saline	**TBS**
Enzyme-linked-immunosorbent-assay	**ELISA**
Human embryonic kidney	**HEK**
Open reading frame	**ORF**
Untranslated regions	**UTRs**
Hydroxyurea	**HU**
Hydroxyurea sensitve	**HUS**
Mouse embryonic fibroblasts	**MEF**
Diethyl pyrocarbonate	**DEPC**
Luria-Bertani	**LB**
Mre11/Rad50/Nbs1	**MRN**

Chapter 1
General Introduction

1.1 An overview of the cell-cycle

In 1953, Howard and Pelc first described the eukaryotic cell-cycle time-course using ^{32}P isotope labeled *Vicia faba* L. plants. The authors proposed that cells had a pre-DNA synthesis phase (G1), a DNA synthesis phase (S), a pre-cell division phase (G2) and cell division phase (D), which is known today as M or Mitosis (Steel, 1986). Since this time the individual phases have been characterized more thoroughly and a new phase (G0) has been introduced. Summarizing the cell-cycle in four phases does not do its intrinsic complexity justice. Intricate biochemical pathways regulate the transition from phase-to-phase to ensure the integrity of DNA (Hartwell and Weinert, 1989). There are many abbreviations used when explaining the cell-cycle and cell-cycle checkpoints and a list of all abbreviations are given on page III/IV.

1.1.1 Cell-cycle phases

The five stages of the cell-cycle are G0, G1, S, G2, and M. The three gap (G) phases, G0, G1 and G2, are preparation phases which allow the cell to transition into the next step. DNA is replicated during S-phase and in M-phase the duplicated DNA is separate into different nuclei and the cell splits equally forming two identical daughter cells (Johnson and Walker, 1999; Malumbres and Barbacid, 2009). M-phase includes 5 sub-phases: (1) prophase; (2) prometaphase; (3) metaphase; (4) anaphase; (5) telephase or cytokinesis. Furthermore, all phase transitions are driven by the family of proteins referred to as cyclins, which activate cyclin-dependent kinases (CDKs) (Coller, 2007; Malumbres and Barbacid, 2009). A diagrammatic representation of the cell-cycle can be seen in Figure 1.1.

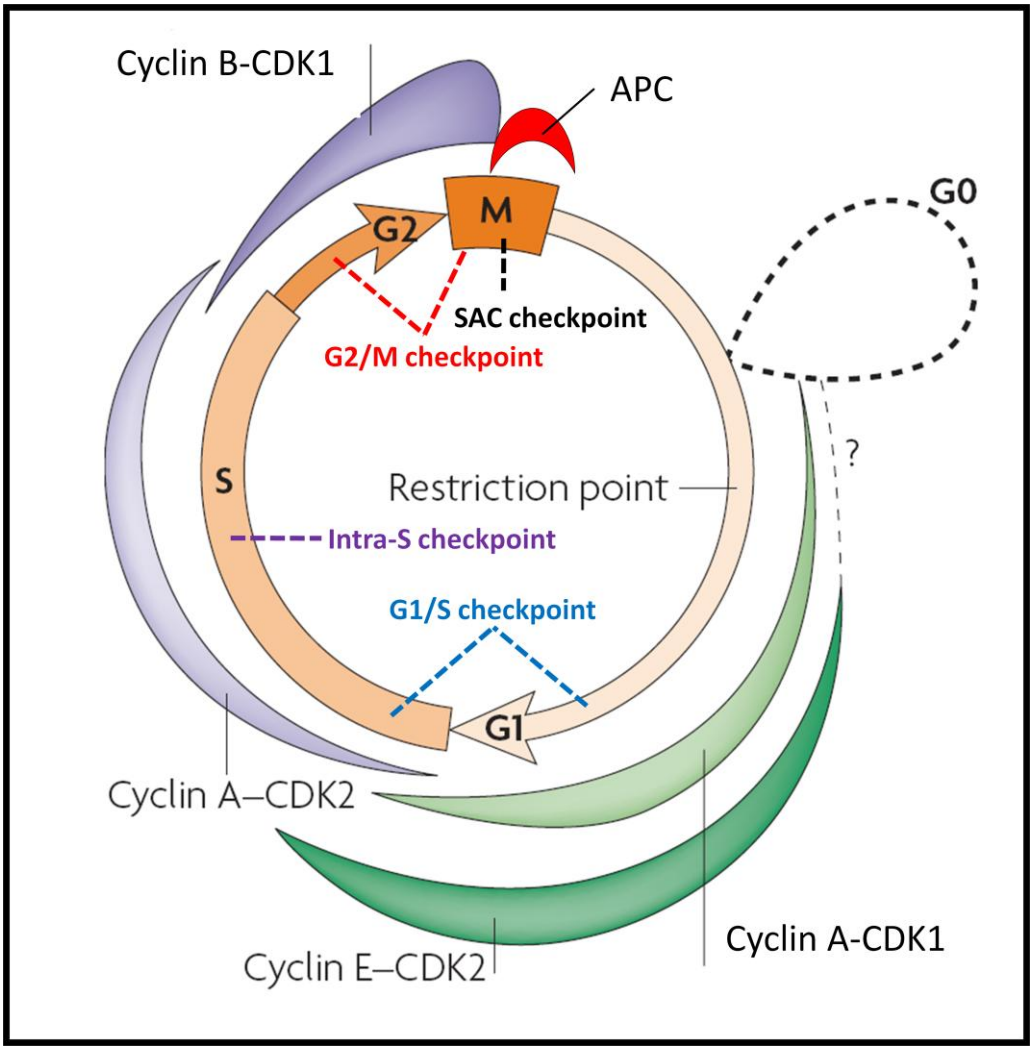

Figure 1.1: The eukaryotic cell-cycle: as the clock ticks
The four phases of the cell-cycle G1, S, G2 and M are shown. The out of cycle phase (dotted loop), G0, is placed prior to the G1 restriction point. Cyclin and cyclin-dependent complexes (CDKs) drive the phase transitions. Cyclin A/E-CDK1 drive the G1 phase while cyclin A-CDK1 drives S phase. The transition from G2 to M-phase requires the degradation of A-type cyclins and the formation of B-type cyclins. Cell progression up until metaphase is driven by CDK1-cyclin B. Afterwards, progression involves the anaphase-promoting complex (APC). The 4 cell-cycle checkpoints (1) G1/S checkpoint; (2) Intra-S checkpoint; (3) G2/M checkpoint; (4) spindle assembly checkpoint (SAC) are indicated. This figure was adapted from (Coller, 2007).

1.1.2 G0-phase

The quiescent phase, called G0, refers to the 'out-of-cycle' state that cells remain in before proceeding to G1-phase. How the G0 phase operates and its direct role has been under scrutiny for many years (reviewed in Coller, 2007). G0 occurs right after Mitosis and before the restriction point in G1 phase. The restriction point is the point of the cell-cycle where cells are no longer influenced by external signals, such as stress and nutrient levels, and are 100% committed to completing the cell-cycle (Coller, 2007). Prior to the restriction point the cell may remain in the G0-phase if they are not needed. E2F proteins are transcription factors that regulate expression of essential genes needed for DNA synthesis (Johnson and Walker, 1999; Sun *et al.,* 2007). Cell-division cycle 6 (CDC6), is an E2F target that is essential for DNA synthesis. The loading of CDC6 onto chromatin allows for origin firing and is the determining factor behind a cell's future (Coller, 2007; Borlado and Mendez, 2008). Details on origin firing and CDC6 will be discussed in section 1.1.3.

The re-entry of quiescent cells into the cell-cycle is determined mainly by retinoblastoma protein (pRb). Unphosphorylated pRb binds to E2F making it a transcriptional repressor (Johnson and Walker, 1999; Sun *et al.,* 2007). When the cell is needed, external signals increase levels of E-type cyclins which work with CDK2 to phosphorylate pRb. Phosphorylated pRb disconnects from E2F which allows E2F to promote the transcription of genes involved in the cell-cycle. The pRb works with E2F to ensure that expression of genes required for synthesis are repressed until S-phase (Sun *et al.,* 2007).

1.1.3 G1-phase

The initiation of DNA synthesis and the firing of replication origins occur in G1-phase. It is here that CDC6 in association with the origin replication complex (ORC), chromatin licensing and DNA replication factor 1 (CDT1) and minichromosome maintenance proteins 2-7 (MCM2-7) control the firing of replication origins. The transition from G1 to S-phase is controlled by CDK2's association with E-type cyclins. The CDK2-cyclin-E complex phosphorylates pBr which disconnects it from E2F and leaves E2F

active to promote the transcription of genes which are necessary for DNA replication (Johnson and Walker, 1999; Coller, 2007; Malumbres and Barbacid, 2009).

1.1.4 S-phase

The objective of S-phase is to replicate DNA only once and to ensure that no errors have occurred. DNA replication is initiated when the multi-subunit ORC recruits CDC6 and CDT1 and forms the CDC6-CDT1-ORC- DNA complex. This complex loads the MCM2-7 complex onto chromatin and at this stage the combined proteins are called the pre-replication complex (preRC). The preRC activates the initiation complex which consists of replication protein A (RPA), cell division cycle protein 45 (Cdc45) and the go-inchi-ni-san (GIN) complex (Broderick and Nasheuer, 2009; Malumbres and Barbacid, 2009). The initiation complex activates DNA polymerase α-primase (Pol-prim) and the replicative helicase complex: essentially, this is the start of DNA replication. As the replicative helicase complex unwinds DNA, topoisomerase 1 (TOP1) nicks the upstream DNA backbone strands to ease the stress of supercoiled DNA allowing pol-prim to elongate the DNA by adding RNA primers (Broderick and Nasheuer, 2009; Maya-Mendoza *et al.*, 2009). The replication factor C (RFC) complex loads the proliferating cell nuclear antigen (PCNA) onto DNA at which time pol-prim gets replaced by the proofreading polymerase, pol-δ. Discontinuous synthesis on the lagging strand occurs due to this replacement and creates Okazaki fragments. The fragments are joined together by RNAse H, flap endonuclease 1 (Fen1) and DNA ligase 1 (Broderick and Nasheuer, 2009). After replication is complete, CDKs promote the phosphorylation of CDT1 and CDC6 causing degradation of CDT1 by proteasomes and nuclear export of CDC6 into the cytoplasm, where it cannot initiate replication firing until the next cell-cycle (Coller, 2007). The completion of S-phase results in two identical DNA duplexes which are maintained in the nucleus. The transition from S-phase to G2 involves phosphorylation of cyclin-A by CDK2 (Malumbres and Barbacid, 2009).

1.1.5 G2-phase

During G2, the processes needed for mitosis are finalized to ensure chromosome stability. The precentriol, which was synthesized in G1 and S-phase, duplicate and become two functional pairs of centrosomes. Centrosomes are non-membranous organelles that form the bipolar spindles which are responsible for the separation of sister chromatid during mitosis (Wang *et al.,* 2009). The transition from G2 to mitosis requires the degradation of A-type cyclins and the formation of B-type cyclins (Malumbres and Barbacid, 2009).

1.1.6 Mitosis

Sister chromatids are held together by cohesin, a multiprotein complex, as they travel from G2 to the first step in mitosis, prophase. This transition activates CDK1, Polo-like kinase 1 (PLK1) and Aurora B5, which in turn form the mitotic spindles. The transition from prophase to the second step in mitosis, premetaphase, involves the degradation of A-type cyclins and the formation of CDK1-cyclin B. CDK1-cyclin-B breaks down the nuclear envelope and allows chromatin to condense with the help of the condensing complex and DNA topoisomerase II (TOPII: Wollmann *et al.,* 2007; Malumbres and Barbacid, 2009). The condensed chromosomes align in the middle of the cell during the transition from premetaphase to the third step of mitosis, metaphase. Cell progression up until metaphase is driven by CDK1-cyclin B. Afterwards, progression involves the anaphase-promoting complex (APC). APC is an ubiquitin-protein ligase which ubiquitinates many regulatory proteins for proteasome degradation (Sullivan and Morgan, 2007; Yanagida, 2009). In metaphase, the spindles get retracted and begin to be pulled to the poles of the cell by the kinetochore-associated microtubule as they transition to anaphase. The APC ubiquitinates securin which causes it to be degraded and removed from the protease called separase. Separase then cleaves the protein cohesin which allows for sister chromatids to separate to the opposite poles of a cell (Hagting *et al.,* 2002; Yanagida, 2009). During cytokinesis, the CDKs in the cell are dephosphorylated by phosphatases which influences the disassembly of spindles, the formation of

nuclei and the decondensation of chromatin allowing for the completion of the cell-cycle (Sullivan and Morgan, 2007; Malumbres and Barbacid, 2009; Yanagida, 2009).

1.2 Checkpoint proteins

Checkpoints are present during the cell-cycle to ensure that future events in the cell-cycle are not hindered due to previous events (Hartwell and Weinert, 1989). There are 4 checkpoints: (1) G1/S checkpoint; (2) Intra-S checkpoint; (3) G2/M checkpoint; (4) spindle assembly checkpoint (SAC: (Sancar *et al.*, 2004; Clarke and Allan, 2009). The details of each checkpoint will be discussed in section 1.3. Cell-cycle checkpoints operate via a signal transduction pathway involving proteins, termed "checkpoint proteins". Checkpoint proteins are organized into 4 different categories based on their function: (1) sensors; (2) mediators; (3) transducers; (4) effectors. The categories are used to simplify a rather complex biochemical pathway and it should be noted that many proteins have ubiquitous functions in the cell-cycle. Checkpoint proteins are involved in cross-talking mechanism and function in different groups. A breakdown of the four different categories and some of the major players involved is provided below.

1.2.1 Sensors

Sensors directly or indirectly recognize DNA damage or cellular abnormalities and parlay the information to the mediators (Sancar *et al.*, 2004; Niida and Nakanishi, 2006). Different sensor proteins are activated depending on the damage; examples include, single-stranded and double-stranded DNA breaks (Nyberg *et al.*, 2002). The 9-1-1 complex is a heterotrimeric ring composed of three evolutionary conserved proteins Rad9, Rad1 and Hus1 (9-1-1) and is grouped as a sensor protein. The complex is loaded onto DNA by the RAD17-RFC complex and its interaction has been shown to be active in damaged and undamaged cells (Parrilla-Castellar *et al.*, 2004). Upon detecting damage, the 9-1-1 complex has been shown to phosphorylate other checkpoint proteins; for example, in response to UV damage the 9-1-1

complex phosphorylates the serine/threonine-protein kinase Chk1 (Venclovas *et al.,* 2002; Parrilla-Castellar *et al.,* 2004).

1.2.2 Mediators

Mediators function as a molecular bridge from the sensors to the transducers to complete checkpoint activation and DNA repair. Four main types of mediator proteins in mammals contain twin BRCA1 C-terminus repeat (BRCT) domains and it is this unique domain that allows for protein-phosporylation interactions (Sancar *et al.,* 2004; Niida and Nakanishi, 2006; Wilson and Stern, 2008). Furthermore, BRCT proteins mediate a damage response by attracting proteins of interest, such as ataxia telangiectasia mutated ATM, to the site without directly recruiting them (Eliezer *et al.,* 2009). The p53 binding protein 1 (53BP1) and the mediator of DNA damage checkpoint 1 (MDC1) are required for the repair of DNA break sites as well as in the regulation of mitosis (Eliezer *et al.,* 2009). Breast cancer susceptibility gene 1 (BRCA1) is a tumor suppressor gene that participates in multiple DNA repair pathways and plays a pivotal role as a mediator (Niida and Nakanishi, 2006; Reguart *et al.,* 2008).

1.2.3 Transducers

Transducers initiate a molecular cascade which amplifies the signal to the effectors. They are mainly a group of kinases, which includes the phosphoinositide 3-kinase related kinases (PIKKs) ATM and ATR (Ataxia Telangiectesia Rad3-related) and the serine-threonine kinases CHK1 and CHK2 (Sancar *et al.,* 2004; Niida and Nakanishi, 2006). ATM and ATR are large proteins that work by phosphorylating many substrates involved in the checkpoint pathway. ATM phosphorylates CHK2 during a double-stranded DNA break (DSB) response, while ATR, with the help of the ATR-Interacting-Protein (ATRIP), phosphorylates CHK1 in a single-stranded DNA break (SSB) response. CHK1/CHK2 phosphorylate downstream components to prevent damaged DNA from entering mitosis (Sancar *et al.,* 2004; Niida and Nakanishi, 2006).

1.2.4 Effectors

Effectors phosphorylate and dephosphorylate CDKs thereby controlling the transition stages of the cell-cycle. There are three phosphotyrosine phosphatases, Cdc25-A, Cdc25-B and Cdc25-C, and a transcriptional factor protein, p53, which are the main effectors in human checkpoints. Cdc25 group of proteins dephosphorylate CDKs and directly disrupt cell-cycle transitions. While p53 is a transcription factor that promotes the expression of CDK inhibitors (Sancar *et al.*, 2004).

1.3 Cell-cycle checkpoints

The cell-cycle checkpoints are important in preserving the integrity of the DNA from DNA damaging agents and from an erroneous repair mechanism. There are 4 checkpoints: (1) G1/S checkpoint; (2) Intra-S checkpoint; (3) G2/M checkpoint; (4) spindle assembly checkpoint (SAC). Figure 1.2 is a diagrammatic representation of the G1/S, Intra-S and G2/M checkpoints. The G1/S checkpoint ensures that proper origin firing is prepared and that DNA is not damaged. The Intra-S checkpoint prevents damaged DNA from replication and blocks replication if synthesis is unusual; i.e. replication fork stalling. G2/M checkpoint prepares necessary adjustments for mitosis and is the last line of defense for the prevention of damaged DNA. The SAC ensures proper spindle attachment to the kinetochore for the separation of sister chromatid (Sancar *et al.*, 2004; Clarke and Allan, 2009). If the repair mechanisms cannot isolate the problem then the cell will undergo apoptosis or cell suicide.

1.3.1 G1/S checkpoint

If DNA damage is detected then the cell becomes arrested which prevents the firing of replication origins until the problem becomes resolved. Under normal conditions, the transition from G1 to S-phase requires the dephosphorylation of CDK2 which prevents the phosphorylation of CDC25A. Under SSBs and DSBs, two different pathways are used that involve keeping CDK2 phosphorylated to stop the transition (Houtgraaf *et al.*, 2006).

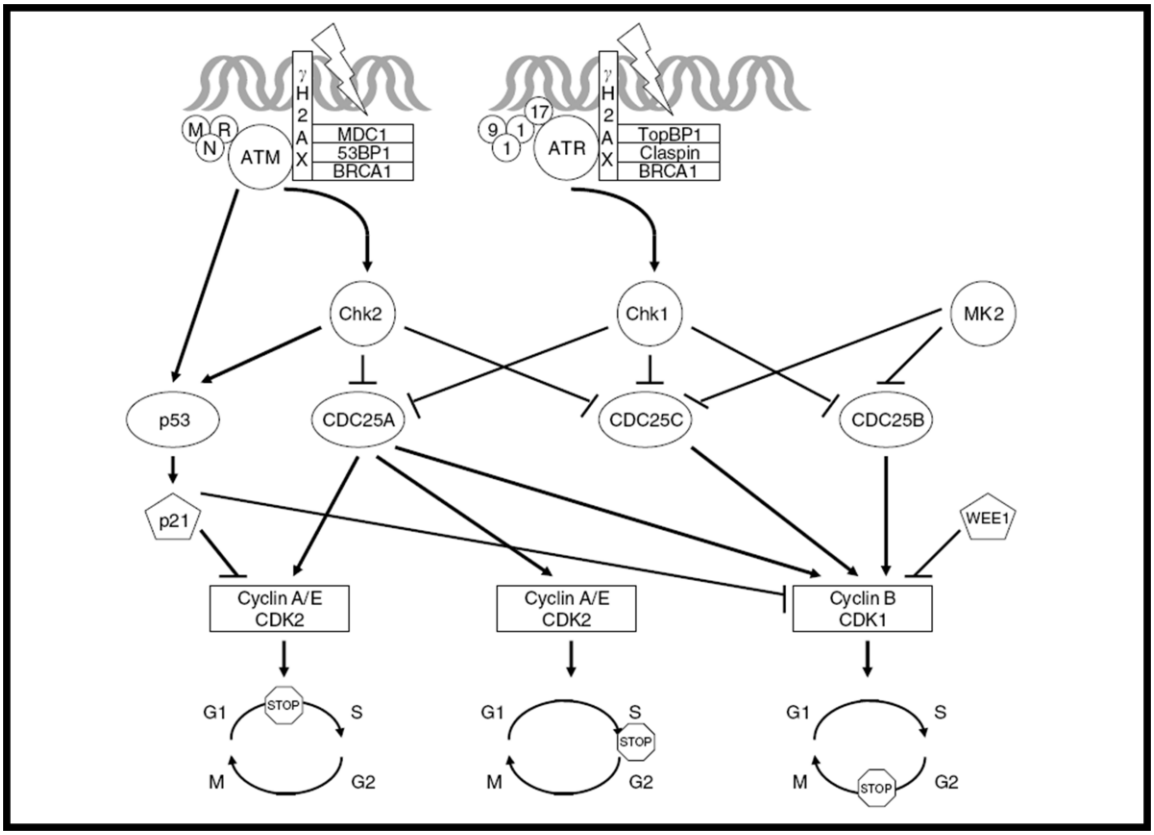

Figure 1.2: A summary of the cell-cycle checkpoints: G1/S, intra-S and G2/M
To the top left (ATM) is the pathway involved in a double stranded break response, while the pathway to the right (ATR) is of a single-stranded break response. The lightning rod at the top is indication of irradiation on DNA. These pathways can lead to cell-cycle arrest during any of the three checkpoints, G1/S, intra-S and G2/M. This figure is adapted from (Bucher and Britten, 2008).

In pathway 1, a DSB is recognized by the Mre11/Rad50/Nbs1 (MRN) sensor complex sensor and MRN recruits ATM, in an ATP dependent manner, leading to self-phosphorylation of ATM, phosphorylation of MRN and phosphorylation of the variant histone H2AX (γH2AX). This subsequently leads to the phosphorylation of chromatin-bound proteins (Wang *et al.*, 2000; Bucher and Britten, 2008; Clarke and Allan, 2009). The phosphorylated γH2AX recruits Mdc1 and together they recruit Rnf8-Ubc12- an E3 ubiquitin ligase. Rnf8-Ubc12 ubiquitylates γH2AX and recruits the mediator proteins 53BP1 and BRCA1(Ashwell and Zabludoff, 2008). This causes DNA to unravel from the tightly bound histone complex. ATM phosphorylates the transducers CHK2 and p53 which leads to the phosphorylation of CDC25A leading to G1 arrest. Phosphporylated CDC25A inactivates itself leading to nuclear export and proteolytic ubiquitin-mediated degradation ((Bucher and Britten, 2008).

In pathway 2, phosphorylated p53 is stabilized and accumulates where it promotes and facilitates the transcription of p21 (Shimada and Nakanishi, 2006). CDK2 activity is inhibited by p21 which allows pRB to remain attached to E2F and transcription of DNA is prohibited (Bucher and Britten, 2008; Clarke and Allan, 2009; Malumbres and Barbacid, 2009). Furthermore, during SSB response, phosphorylated CHK1 can also phosphorylate CDC25A, however, this pathway is used only past the restriction point to halt G1 in the late stages (Ashwell and Zabludoff, 2008).

1.3.2 Intra-S checkpoint

The intra-S checkpoint will arrest the cell-cycle and allow for repair if the replication complex is stalled or if there is damaged DNA. It is the second line of defense for DNA damage not corrected in the G1-phase. The DSB pathway (mentioned in section 1.3.1) works in parallel with the SSB pathway. To repair damage or to fix a stalled replication fork, a DSB response is initiated and S-phase is arrested by degrading CDC25A. The SSB response occurs when ssDNA is exposed during synthesis. RPA labels single-stranded DNA. The 9-1-1 complex and Rad17-RFC signal to ATRIP to recruit ATR. The 9-1-1 complex, Rad17-RFC, TopBI, and RPA signal to ATRIP and ATR to phosphorylate CHK1 which in turn

phosphorylates CDC25A. CDC25A becomes down-regulated when it is phosphorylated causing CDK2 activity to be suppressed which inhibits synthesis of DNA by blocking the loading of CDC45 onto chromatin. CDC45 is necessary for new origin firing and without being loading onto chromatin, DNA synthesis is prohibited allowing for cellular repair (Parrilla-Castellar *et al.,* 2004; Xu *et al.,* 2009).

1.3.3 G2/M checkpoint

The G2/M checkpoint prepares necessary adjustments for mitosis and is the last line of defense for the prevention of damaged DNA. The DSB and SSB repair pathways are initiated in the same manner as described above except with the end goal of phosphorylating CDC25B/C to arrest the cycle. CHK1/CHK2 phosphorylates CDC25B/C which in turn causes it to be exported into the cytoplasm by 14-3-3 proteins (Ashwell and Zabludoff, 2008; Malumbres and Barbacid, 2009; Wang *et al.,* 2009). Loss of CDC25B/C prevents CDK1-cyclin-B activation thereby arresting G2 transition into mitosis until the problem is resolved (Ashwell and Zabludoff, 2008; Malumbres and Barbacid, 2009; Wang *et al.,* 2009). New evidence suggests that the centrosome helps to regulate the G2/M checkpoint. It has been shown that various proteins involved in the cell-cycle have can traffic in and out of the centrosomes, such as CDKs, cyclins, p53, ATR/ATM and others (Wang *et al.,* 2009).

1.3.4 The spindle assembly checkpoint

The spindle assembly checkpoint (SAC) ensures that proper attachment of chromosomes to the spindle microtubules has occurred as well as proper chromosome alignment during metaphase. The SAC works by regulating APC, the complex which transitions metaphase to telophase (Yen and Kao, 2005; Musacchio and Salmon, 2007; Wood *et al.,* 2008). The kinetochore is formed on the centromere and it attaches to spindle microtubules to allow for proper separation. Many kinetochore proteins are involved with SAC but the centromere associated protein E (CENP-E) works directly by inhibiting APC. During G1-phase, CENP-E is exported to the cytosol and can only begin inhibiting APC following the

breakdown of the nucleus during prophase (Wood *et al.,* 2008). The mitotic checkpoint complex (consisting of BubR1, Bub3, Mad2 and Cdc20) works in association with CENP-E to inhibit APC until proper attachment has occurred. When a microtubule is connected to CENP-E the mitotic checkpoint complex gets phosphorylated releasing it from the kinetochore. The APC ubiquitinates cyclin-B and securin leading to their degradation which allows the transition of mitosis to continue. Proper attachment of the kinetochore with spindle microtubules represses the inhibitory signal on APC allowing for the proper transition past metaphase (Musacchio and Salmon, 2007).

1.4 Cell-cycle damaging agents

On a daily basis cells are affected by external factors that interfere with DNA integrity and the cell-cycle. These substances stimulate a checkpoint response signaling for cellular repair or apoptosis. Damaging agents have been categorized based on how they affect the cell-cycle: such as, DNA damaging agents, microtubule inhibitors, ribonucleotide pool depletors, topoisomerase inhibitors and antimetabolites (Hartwell and Kastan, 1994; Johnson and Walker, 1999). Key points explaining the categories will be mentioned below.

1.4.1 DNA damaging agents

Clastogenic agents that induce DNA cross links and or SSBs/DSBs are typically termed DNA damaging agents (Johnson and Walker, 1999; Li *et al.,* 2008). For example, UV-radiation, γ-radiation and X-rays bombard cells with energy and cause free oxygen radicals to alter the DNA structure (Sinha and Hader, 2002). Ionizing radiation causes thymine-dimers, thymine-cytosine-dimers and base adducts to form which signals a base-excision repair response in the SSB/DSB pathway. Irradiation is used often when studying SSB pathway because it inevitably elicits a response from checkpoint proteins (Sinha and Hader, 2002; Stephan *et al.,* 2009). Bleomycin is a DNA damaging agent that creates DNA strand scissions leading to DSBs and a DSB response. Bleomycin induces arrest/apoptosis of G1/S/G2 phases by

phosphorylation of a CDC25 protein via the MRN/ATM/CHK2/p53 pathway (pathway mentioned in detail in section 1.3.1: Steighner and Povirk, 1990; Claussen and Long, 1999).

1.4.2 Microtubule inhibitors

These inhibitors disrupt the cell-cycle during M-phase which sets off the SAC response. Essentially, tubulin polymerization is inhibited which therefore disrupts spindle formation (Johnson and Walker, 1999). Paclitaxel (Taxol) is a chemical that binds to microtubules and represses microtubule dynamics. This repression inhibits the kinetochore from binding to the spindles and arrest the cell-cycle in pre-metaphase (Wang *et al.*, 2009). Similar to Taxol, Colchicine is a chemical that forms a complex with β-tubulin causing inhibition of microtubules assembly (Cerquaglia *et al.*, 2005).

1.4.3 Ribonucleotide pool depletors

These chemical substances are purine nucleoside analogs that deplete ribonucleotide pools. The exact mechanism of action is unknown but in some way the purine nucleoside analogs interfere with ribonucleotide reductase and DNA polymerase which stops the extension of DNA (Nabhan *et al.*, 2004). In response, the G1/S checkpoint attempts to excise the addition of the purine nucleoside analog and if the problem is not fixed then the intra-S checkpoint will signal for apoptosis (Johnson and Walker, 1999). Hydroxyurea and gemcitabine are chemicals that both deplete purine deoxyribonucleotide triphosphate (dNTP) pools and by doing so inhibiting ribonucleotide reductase which inhibits DNA replication (Johnson and Walker, 1999; Koc *et al.*, 2004).

1.4.4 Topoisomerase inhibitors

The enzyme, topoisomerase, relaxes DNA from its supercoiled state by unwinding it. This process is vital for replication so that DNA is not compacted around its histone complex. There are two topoisomerases, topoisomerase I which relaxes negatively and positively supercoiled DNA domains and topoisomerase II which relaxes supercoiled DNA and condenses DNA during M-phase (Wang, 1991; Johnson and Walker,

1999). The chemical etoposide inhibits topoisomerase II by blocking the catalytic mechanism necessary for DNA re-ligation. This prevents enzyme turnover and therefore inhibits transcripton and replication. Etoposide induces high levels of cellular damage and has been termed a topoisomerase poison (Nitiss, 2009).

1.4.5 Antimetabolites

Antimetabolites are chemicals that have structures that resemble metabolites and are processed in the cell by the same route. This prevents cell growth by outperforming proper cell functions, such as DNA replication. Methotrexate and 5-fluorouracil are antimetabolites that act as a metabolic decoy. These compounds inhibit DNA synthesis and create a p53-dependent S-phase arrest (Johnson and Walker, 1999; Peters *et al.,* 2000).

1.5 Checkpoint proteins as genotoxicity biomarkers

Currently, there are no genotoxicity assays or biomarkers that can accurately determine the type of damage occurring in a cell. As mentioned above, there are a variety of ways the cell-cycle can be damaged and altered but an assay that determines where or how the damage has occurred doesn't exist. For example, DNA integrity is often assessed using the comet assay (Singh *et al.,* 1988; McArt *et al.,* 2009). In the comet assay, cells are encapsulated in agarose and lysed using a salt solution to remove all cellular components except DNA. The agarose is then subjected to electrophoresis where the DNA migrates based on size and charge. Undamaged DNA will run slowly and remain as the "head" while damaged DNA will run faster and form a "tail" similar to the head and tail of a comet. The length and intensity of the "tail" is what determines the severity of damage (Singh *et al.,* 1988; McArt *et al.,* 2009). The comet assay cannot specify whether or not the DNA damage is single-stranded or double-stranded; in the past, an alkaline and neutral method was used to determine whether the type of DNA damage was single or double-stranded but that method has now been debunked (Collins *et al.,* 2008; McArt *et al.,*

2009). Furthermore, one of the biggest limitations is that the comet assay is not sensitive enough to detect low levels of DNA damage (McArt *et al.,* 2009).

There is a need in biology for a genotoxicity biomarker that is able to detect low levels of single-stranded or double-stranded DNA damage. Recent evidence suggests that checkpoint proteins can be used as genotoxicity biomarkers. For example, the checkpoint protein CHK2 (checkpoint kinase 2) was characterized in rainbow trout and used a genotoxicity biomarker (Steinmoeller *et al.,* 2009). The authors treated rainbow trout cell-lines with bleomycin (see section 1.4.1) and examined the expression levels of CHK2 on a western blot using polyclonal anti-rtCHK2 antibodies. Bleomycin is known to create DSBs and CHK2 is known to be activated during the formation of DSBs. The authors observed that expression levels of rainbow trout CHK2 increased with an increase of bleomycin concentration (Steinmoeller *et al.,* 2009). This suggests that checkpoint proteins can be used as genotoxicity biomarkers. Furthermore, since certain checkpoint proteins respond to a specific type of damage, i.e. CHK2 response to DSBs, then a variety of them could be used to determine whether there is a SSB or DSB or whether the spindles are attached properly during mitosis or whether a damaging agent is causing more than one event.

1.6 Rainbow trout as a model organism

The boom in industrialization has caused more toxicants and cell-cycle damaging agents to be released into the environment. A lot of these toxicants end up in the water and have been shown to have adverse affects on aquatic species. For example, endocrine disrupters have shown to alter the normal bodily functions of a fish (Johnson *et al.,* 2007), while low concentrations of "the pill" have made an entire fish population sterile (Kidd *et al.,* 2007). *Oncorhynchus mykiss* (rainbow trout) is often used in toxicology studies (Fairchild *et al.,* 2009; Wassmur *et al.,* 2010) and is considered a model organism (Carvan *et al.,* 2007). Rainbow trout are very sensitive to genotoxins which makes them good indicators for the surrounding wildlife (Adams *et al.,* 1999). Furthermore, they are easily maintained at an affordable cost and their size is large enough to conduct physiological experiments where enough tissue can be extracted

to complete assays of viability (Carvan *et al.*, 2007). Although the genome has not yet been sequenced, a few genetic maps are available (Rexroad *et al.*, 2008) and there are many rainbow trout partial and full sequences accessible from NCBI and The Gene Index. Most importantly, there are many rainbow trout cell-lines (Fryer and Lannan, 1994) which have been used in past genotoxicity studies and have been shown to be effective in modeling *in vivo* biology (Pichardo *et al.*, 2007; Steinmoeller *et al.*, 2009). Also, the use of cell-lines eliminates any ethical issues surrounding the use of whole fish in genotoxic studies.

1.7 Research Aims

The main objective of this project was to characterize the checkpoint proteins Rad1 and Hus1 in rainbow trout and to determine their potential as genotoxicity biomarkers. To do this for Rad1, the cDNA sequence was determined, a recombinant rtRad1 protein was purified, and polyclonal antibodies were made against the rtRad1 recombinant protein. Anti-rtRad1 antibodies were used in western blots to characterize the protein levels of Rad1 in each tissue and to determine whether or not the activity of Rad1 is influenced when damaging agents are added to cell-lines. As for Hus1, the recombinant rtHus1 protein was purified and used to developed polyclonal anti-rtHus1 antibodies. The antiserum was then used to determine the specificity of Hus1 in each rainbow trout tissue using western blots. If these genes or proteins can be used as markers of genotoxicity, they will provide valuable tools for screening aquatic environments for DNA damaging agents

Chapter 2
Characterization of Rad1 in Rainbow Trout

2.1 Introduction to Rad1

The screening of radiation-sensitive (RAD) mutants from *Saccharomyces cerevisiae* (*Sc* or budding yeast) led to the discovery of $RAD17^{Sc}$, a mutant strain at loci 17 that was unable to arrest the cell-cycle in response to DNA damage induced by ultraviolet-light (UV: Prakash, 1976; Walworth *et al.,* 1993). In *Schizosaccharomyces pombe* (*Sp* or fission yeast), RAD mutants were also examined and a UV-sensitive mutant that was deficient in DNA repair and has a reduced recombination frequency, called $RAD1^{Sp}$, was isolated (Grossenbacher-Grunder and Thuriaux, 1981). Even though budding yeast and fission yeast are evolutionarily distant, the checkpoint mechanism involved in each yeast is conserved (Carr and Hoekstra, 1995). The mutant yeast stains $RAD17^{Sc}$ and $RAD1^{Sp}$ contain genes, $Rad17^{Sc}$ and $Rad1^{Sp}$, which are mutated and non-functional. In their normal state, $Rad17^{Sc}$ and $Rad1^{Sp}$ are checkpoint proteins involved in the cell-cycle and are homologs of one another (Sunnerhagen *et al.*, 1990; Siede *et al.,* 1996; Freire *et al.*, 1998). The nomenclature of checkpoint proteins from *S. pombe* is used in higher eukaryotes.

In 1998, six different research groups identified the human homolog of $Rad1^{Sp}$, called hRad, which codes for a 282aa protein which has a molecular weight of 32kDa (Bluyssen *et al.,* 1998; Dean *et al.,* 1998; Freire *et al.,* 1998; Marathi *et al.,* 1998; Parker *et al.,* 1998; Udell *et al.,* 1998). Four out of the five groups concluded that human Rad1 isoforms exist. Three of the four groups concluded that two isoforms exist, Rad1A and Rad1B (Freire *et al.,* 1998; Parker *et al.,* 1998) while the other group identified three isforms, Rad1A, Rad1B and Rad1C (Marathi *et al.,* 1998). Human Rad1A is the "canonical" sequence that all the other isoforms are based on and the sequence was the same from all six groups. However, hRad1B did not have the same sequence from all four groups, in fact, each group determined a different splice site for hRad1B. Furthermore, northern blots were completed by the same three groups and all three identified hRad1 transcripts of different sizes. The identity of Rad1 is hard to determine since past

literature was contradictory. For example, two groups (Freire *et al.,* 1998; Parker *et al.,* 1998) determined that the hRad1 protein sequence contains domains that suggest it has 3'-5' exonuclease activity, similar to that of the checkpoint protein Rec1. However after conducting an assay (Parker *et al.,* 1998) determined that hRad1A, but not hRad1B, possess 3'-5' exonuclease activity, while (Freire *et al.,* 1998) determined that hRad1A does not exhibit 3'-5' exonuclease activity. The contradictions in Rad1 literature makes it hard to determine the exact role of Rad1, none the less, the role of Rad1 while be explored in the sections below.

2.1.1 The role of Rad1

$Rad1^{Sp}$ has been shown to transmit information to other checkpoint proteins when DNA is damaged. In the presence of a DNA damaging agents (γ irradiation) or a ribonucleotide pool depletory (hydroxyurea) the mutant $Rad1^{Sp}$ strain is unable to arrest the cell-cycle in S-phase or G2 (Rowley *et al.,* 1992). This suggests that under normal conditions $Rad1^{Sp}$ plays a pivotal role in the cell-cycle checkpoint response. Furthermore, $Rad1^{Sp}$ comprises 3 exons which encode a 37kDa protein (Long *et al.,* 1994). High transcript levels of hRad1 are seen in the testis which suggest that hRad1 is involved in meiosis which would be consistent with $Rad17^{Sc}$ function (Freire *et al.,* 1998; Marathi *et al.,* 1998; Parker *et al.,* 1998). Furthermore, hRad1 is expressed at higher levels in proliferating tissue where it is localized in the nucleus (Freire *et al.,* 1998). It appears that Rad1 plays an important role in the cell-cycle since $Rad1^{-/-}$ mice are embryonic lethal while $Rad1^{+/-}$ mice had high levels of skin tumors than wild-type mice (Han *et al.,* 2010). This suggest that mRad1 normally plays a role in the prevention of cancerous cells by helping maintain DNA integrity.

2.1.2 Rad1 in the 9-1-1 complex

A heterotrimeric ring composed of Rad9, Rad1 and Hus1 (9-1-1 complex) detects DNA damage and signals for arrest/repair (Volkmer and Karnitz, 1999). The heterotrimeric ring is similar to the PCNA

homotrimeric ring complex that encircles DNA and is involved in replication and post replication repair (Parrilla-Castellar *et al.,* 2004; Lehmann and Fuchs, 2006). The 9-1-1 complex is present in damaged and undamaged cells and is loaded onto damaged DNA by RAD17-RFC clamp-complex in response to genotoxic stresses such as alkylation, UV light, ionizing radiation and replication inhibition (Parrilla-Castellar *et al.,* 2004). Research suggests that during SSBs and DSBs the 9-1-1 complex unites ATR/ATM to facilitate CHK1/CHK2 to arrest the cell-cycle during the intra-S and G2 checkpoints (Roos-Mattjus *et al.,* 2002; Parrilla-Castellar *et al.,* 2004; Sorensen *et al.,* 2004). Localization of hRad1 into nucleus from the cytoplasm is hRad9 dependent and lack of hRad9 has been shown to create an accumulation of hRad1 in the cytoplasm in G2-phase (Hirai and Wang, 2002). However, it appears that the expression of hHus1 is dependent on hRad1 as hRad1 is believed to act as a chaperone and bind to hHus1 in the cytoplasm preventing its proteasomal degradation (Hirai *et al.,* 2004). Rad1 acting as a chaperone correlates with expression patterns seen in mice where Hus1 transcript levels were only present with Rad1 transcript levels (Wang *et al.,* 2004). New evidence suggests that the 9-1-1 complex is removed from the site of damage, in a Rad9 dependent manner, once the repair mechanisms have arrived (Furuya *et al.,* 2010). Once the 9-1-1 complex is no longer needed it appears that the Jun-activation domain-binding protein 1 (Jab1), which is known to help with the degradation of proteins, interacts directly with Rad1 causing the dissociation of the 9-1-1 complex which induces the nuclear export of the 9-1-1 complex to the cytoplasm where it is degraded by the 26 S proteasome (Huang *et al.,* 2007).

2.1.3 Rad1 and telomeres

Although the exact mechanism is unknown, it appears that the 9-1-1 complex is a critical component in mouse and human telomeres where it helps maintain telomere length (Francia *et al.,* 2006; Francia *et al.,* 2007; Meyerkord *et al.,* 2008). The $Rad1^{Sp}$ mutant strain, which is unable to produce the Rad1 protein, has shorter telomere lengths than that of wild-type. Furthermore, overexpression of the Rad1 gene caused a slight increase in telomere length of the $Rad1^{Sp}$ mutant strain suggesting Rad1 may be associated with

another component to maintain telomere length (Dahlen *et al.,* 1998). In fission yeast, it has been determined that Rad1 binds to telomeres and that it may be involved in telomere maintenance (Nakamura *et al.,* 2002). In HeLa cells it has been shown that Rad1 (possibly with the 9-1-1 complex) associates with telomerase, the enzyme that extends the length of telomeres (Francia *et al.,* 2006; Francia *et al.,* 2007). Immortal cells avoid cellular senescence (HAYFLICK and MOORHEAD, 1961) by maintaining telomere length using telomerase or by activating a telomerase-independent mechanism termed alternative lengthening of telomeres (ALT) (Bryan *et al.,* 1995; Bryan and Reddel, 1997). The exact mechanism of ALT is unknown but it appears that Rad1 (the 9-1-1 complex) is involved with some of the key components, such as promyelocytic leukemia (PML) body, APBs and telomere binding proteins hTRF1 and hTRF2, suggesting it has a pivotal role in telomere maintenance no matter which mechanism is employed (Nabetani *et al.,* 2004; Jegou *et al.,* 2009).

2.1.4 Rad1 in genotoxic studies

In *Xenopus*, the potential phosphorylation sites of xRad1 were mapped to positions T5, T135, T215 and T217 (TQ motifs). The *Xenopus* egg extract system was used to determine that position T5 is the phosphorylation site of xRad1, the sequence of which is also conserved in humans, mice, and zebrafish. Furthermore, *Xenopus* Rad1 became phosphorylated in the presence of exoIII-treated plasmid but the phosphorylation was abrogated with the addition of caffeine, an inhibitor of phosphatidylinositol 3-kinase-related protein kinases, giving evidence that xRad1 is phosphorylated at site T5 in an ATR-dependent manner (Lupardus and Cimprich, 2006). Human Rad1 has been shown to become phosphorylated when Human K562 erythroleukemia cells were treated with the Ionizing Radiation, 4-Nitroquinoline oxide (4-NQO) and Hydroxyurea (HU: Roos-Mattjus *et al.,* 2002).

Nogueira *et al.,* (2009) treated whole *Anguilla anguilla* L. (European eel) with 7,12-Dimethylbenz[a]anthracene (DMBA), which is a prototype synthetic polycyclic aromatic hydrocarbon (PAH) known to create bulky adducts of DNA, at high and low concentrations for a variety of days. Eels

were sampled prior to the addition of DMBA and 1, 3, 7, 14, 28 and 90 days after the addition of DMBA. The authors wanted to determine if Rad1 could be used as a genotoxicity biomarker to detect genotoxins in aquaculture. The expression levels of Rad1 mRNA in liver were examined using real-time qPCR and it was determined that Rad1 expression did not increase with the increase in DMBA. Since the comet assay showed that DMBA did induce DNA damage, the authors concluded that Rad1 is not a good biomarker. However, the data is not conclusive since the protein levels or states were not examined and Rad1 phosphorylation has been shown to occur in response to genotoxic damage (as stated above). For this study the use of rainbow trout Rad1 (rtRad1) as a genotoxicity biomarker will be examined.

2.2 Materials and methods

2.2.1 Isolation of rtRad1 partial sequence from cDNA library

A pair of gene specific primers was designed from two conserved nucleotide regions (Rad1For1 5-CGGGTTGAAAGTCACTGTGGAGG-3' and Rad1Rev2 5'-CCTCTTCCACTTCCTCATCCGG-3') based on the alignment of two rainbow trout Rad1A expressed sequence tags [TC133098 and BX082263.2] with human [AJ004974.1], Atlantic salmon [TC116181] and zebrafish [NM_200898.1] Rad1A homologs found on Dana Fabar Gene Index, Genbank and NCBI. PCR was performed using 2.5µl of 10X Incubation Mix Taq Polymerase without $MgCl_2$, 0.5µl of 10mM each dNTP mix, 1.5µl of 25mM $MgCl_2$, 1µl of each primer (10µM), 0.1µl Taq DNA Polymerase (5U/µl) (MP Biomedical: Solon, OH), 1µl of rainbow trout head kidney cDNA library (245 ng/µl) and 16.4µl H_2O. A PCR thermocyler gradient (Eppendorf Mastercycler gradient: Hamburg, Germany) was used with the following conditions, 95°C 5min, 35 cycles (95°C 40sec, 59°C 1min, 72°C 1min) and 72°C 15min. The PCR product was run on a 1% agarose gel containing 1X GelRed™ (Hayward, CA) and visualized with a UV transilluminator and Alpha Imager HP program (Alpha Innotech Flourochem 8000 Chemiluminescence and Visable Imaging system: Santa Clara, CA). The amplicon was gel purified using QIAquick Gel Extraction Kit

(Qiagen: Mississauga, ON), ligated into pGEM T-easy vector according to the product manual (Promega: Madison, WI) and subcloned into XL1-Blue MRF' *E.coli* competent cells. Clones containing the insert were sequenced at the University of Waterloo core facility. The sequence was placed into BLAST to determine the sequence identity and aligned with the aforementioned Rad1A homolog.

2.2.2 Isolation of rtRad1 full-length cDNA sequence

A headkidney cDNA library was developed by Kazuhiro Fujiki and was directionally cloned into vector pcDNA™3.1(+) (Invitrogen: Carlsbad, CA). "Anchored PCR" was used to amplify the rest of the coding sequence as well as both untranslated regions of rtRad1A. Gene-specific sense (Rad1For3 5-CCAGGAGCCAGAGGAGCC-3') and antisense (Rad1Rev2 5'-CCTCTTCCACTTCCTCATCCG-3') primers were developed based on the rtRad1 partial sequence and 'anchor' sense (pcDNA.T7 5'-CGACTCACTATAGGGAGACCCAAGC-3' and antisense (pcDNA.BGH 5' CTAGAAGGCACAGTCGAGGCTG-3') primers were developed based on the pcDNA™3.1(+) vector sequence (Invitrogen: Carlsbad, CA). Primer set 2 (pcDNA.BGH and Rad1Rev2) and primer set 4 (Rad1For3 and pcDNA.T7) were used to amplify the rest of the 5' and 3' regions, respectively. Primer sets were arranged so that each amplicon would have an overlapping sequence with the others. PCR was performed as described in section 2.2.1. The thermocyler (Bio-Rad DNA Engine: Mississauga, ON) conditions were as follows 95°C 5min, 36 cycles (95°C 40sec, 60°C 1min, 72°C 1min) and 72°C 15min). Procedures for cloning and sequences of each amplicon were the same as in section 2.2.1. Using the BioEdit software (http://www.mbio.ncsu.edu/BioEdit/bioedit.html) the overlapping sequences were spliced together to obtained the full-length rtRAD1 cDNA sequence. The protein sequence was determined using the Translate tool from ExPASy (http://expasy.org/tools/dna.html). Nucleotide and protein sequences from human [AJ004974.1; AAC95466.1], Atlantic salmon [NM_001141832.1; ACI66420.1], European eel [FJ438472.1; ACO52465.1] and zebrafish [NM_200898.1; NP_957192.1]

Rad1A homologs were aligned with the determined rtRad1A nucleotide and protein sequences using ClustalW.

2.2.3 Cloning of rtRad1 open reading frame into an expression vector

The rainbow trout Rad1A open reading frame (ORF) was amplified using sense (Rad1-ORF.For 5' GGATCCATGCCCTTGTCTACTCAGTCTCAG- 3') and antisense (Rad1-ORF.Rev 5'AAGCTTCTACTCCTCTTCCACTTCCTCATC-3') primer-adapters. The restriction sites *BamH*I and *Hin*dIII were included in the sense and antisense primers, respectively. Two different restriction sites were used to allow for directional cloning into the pRSET(A) expression vector (Invitrogen: Carlsbad, CA). Furthermore, each restriction site is not present in rtRAD1 sequence therefore preventing digestion of the amplicon. PCR was performed using 2.5µl of 10X Incubation Mix Taq Polymerase without $MgCl_2$, 0.5µl of 10mM each dNTP mix, 1.5µl of 25mM $MgCl_2$, 1.5µl of each primer (10µM), 0.1µl Taq DNA Polymerase (5U/µl) (MP Biomedical: Solon, OH), 0.5µl of rainbow trout head kidney cDNA library (245 ng/µl) and 16.9µl H_2O. The thermocyler (Bio-Rad DNA Engine: Mississauga, ON) conditions were as follows 95°C 5min, 35 cycles (95°C 40sec, 55°C 1min, 72°C 1min) and 72°C 15min. The amplicon was gel-purified, cloned and sequenced as stated in section 2.1.1.

The clone containing rtRad1 ORF (pGEM T-easy:rtRAD1) and the pRSET (A) expression vector (Invitrogen: Carlsbad, CA) were both digested with *BamH*I and *Hin*dIII restriction enzymes and run on an agarose gel. Bands corresponding to rtRad1ORF(*B*/*H*) and pRSET(A)(*B*/*H*) were gel purified using using the QIAquick Gel Extraction Kit (Qiagen: Mississauga, ON) then ligated together using T4 DNA ligase (Promega: Madison, WI) for 1hr at room temperature and sequenced at TCAG Sequencing Center (Toronto,ON) to verify that the ORF was in frame with the N-terminal 6x His-tag. The expression vector construct [pRSET(A):rtRAD1ORF(*B*/*H*)] was transformed into the *E. coli* bacterial strain, BL21 (DE3) pLysS (Promega: Madison, WI). During a pilot study it was revealed that over-expression of rtRAD1 was minimal, potentially due to codon bias. Therefore the [pRSET(A):rtRAD1ORF(*B*/*H*)] construct was

transformed into BL21-CodonPlus®(DE3)-*RIPL* strain (Stratagene: Aurora, ON) to relieve the codon bias.

2.2.4 Expression and purification of rtRad1 recombinant protein

Overnight cultures were grown in 4ml SOB containing 50µg/ml ampicillin and 35µg/ml chloroamphenical at 37°C and 220rpm shaking. Two 4ml overnight cultures were used to inoculate 1L of SOB. At an OD600 of 0.4-0.6 cultures were induced by the addition of isopropyl-beta-D-thiogalactopyranoside at 0.5mM. After 5h of induction, cells were harvested by centrifugation at 10,000×*g* for 25min.

Lysis buffer 1 (1X PBS (pH 7.4), 5% Triton X-100, 0.5mg Lysozyme and 5X "complete" Protease Inhibitor cocktail-EDTA free (Roche: Mississauga, ON) was added to the cells and then sonicated (Microson™ Ultra Sonic Cell Disrupter, Misonix: Farmingdale, NY) on level 5 for 1min at 4°C. The supernatant (i.e. soluable fraction) was collected and removed after centrifugation of cells in a Sorvall® RC5B Plus centrifuge (Buckinghamshire, England) at 10,000×*g* for 25min. Solubilizing buffer (1mM B-mercaptoethanol, 0.5M NaCl, 20mM Tris-HCl, 1% Tween 20, 5mM Imidazole, 6M Urea, 0.5mg Lysozyme and 5X "complete" Protease Inhibitor cocktail-EDTA free: pH 8) was added to remaining pellet (i.e. insoluble fraction) and sonicated on level 5 for 1 min at 4°C and set to rotate overnight at 4°C. The cells were centrifuged at 10,000×*g* for 25min and the supernatant (the "solubilised insoluble fraction") was collected and purified using Ni-NTA Agarose (Qiagen: Mississauga, ON) as per the manufacturer's instructions. To summarize, 50ml of the "solubilised insoluable" fraction was added to 1.5ml of equilibrated Ni-NTA resin on an econo-column (Bio-Rad Laboratories: Mississauga, ON) 4°C. The urea was removed from the resin by washing the column once with 10ml 4M Urea Wash (1mM B-mercaptoethanol, 0.5M NaCl, 20mM Tris-HCl, 4M Urea: pH 8), once with 10ml 2M Urea Wash(1mM B-mercaptoethanol, 0.5M NaCl, 20mM Tris-HCl, 2M Urea: pH 8) and once with 0M Urea Wash (1mM B-mercaptoethanol, 0.5M NaCl, 20mM Tris-HCl: pH 8).The column was then subjected to 10 washes

(1mM B-mercaptoethanol , 0.5M NaCl, 20mM Tris-HCl, 30mM Imidazole: pH 8) of 10X the volume of the resin. The recombinant protein was eluted in five 1ml aliquots of elution buffer (1mM B-mercaptoethanol , 0.5M NaCl, 20mM Tris-HCl, 0.5M Imidazole: pH 8).

Each elution was separated on a 12% sodium dodecyle sulfate (SDS) gel and stained with Coomassie Brilliant Blue G-250 (ThermoFisher Scientific: Nepean, ON) to determine purity and background proteins. High purity elutions were dialyzed in 1xPBS (pH 7.4) overnight at 4°C and again in 1XPBS (pH 7.4) the following day for 4h. A Bradford (Bio-Rad: Mississauga, ON) assay was performed following dialysis to determine the protein concentration. The dialyzed protein was concentrated using VivaSpin6 10,000 MWCO columns (Sartorius Stedim Biotech: Aubagne, France) to 1mg/ml and stored at -80°C. One microgram of the final batch of recombinant rtRad1 (1mg/ml) was run on a 12% SDS-PAGE and analyzed through Coomassie staining and western blot. Please refer to Appendix A for the western blot protocol. Western blots were probed with the following primary antibodies; Anti-polyhistidine (Sigma: St. Louis, MO), Anti-Xpress™ (Invitrogen: Carlsbad, CA), Anti-Human-Rad1A (ProteinTech Group: Chicago, IL- Catalog No: 11726-2-AP), and no primary antibody. Western blot results confirmed that the recombinant protein made was indeed rtRad1. The total amount of recombinant rtRad1 protein made was 21mg.

2.2.5 Immunization of rabbits

An emulsion of 1.2ml recombinant rtRad1A protein (1mg/ml) and 1.2ml of Freund's Complete Adjuvant (Sigma: MO, USA) was created. Two female New Zealand white rabbits (Charles River Canada: Wilmington, MA) were immunized subcutaneously with 200ul of the emulsion. Prior to every boost, blood samples were collected from the marginal ear vein to measure antibody titres. Blood was left at 4°C overnight to clot and serum was separated by centrifugation at 3,000xg for 10min at 4°C (Eppendorf Centrifuge 5810R: Hamburg, Germany), collected and stored at -80°C. The above process was repeated using Feund's Incomplete Adjuvant (Sigma: St. Louis, MO) every three weeks for 12 weeks. After week

12, the rabbits were exsanguinated by carotid cannulation and 'final bleed' serum was stored at -80°C. Injections and exsanguinations were performed by Martin Ryan, the veterinary technician of the Biology department at the University of Waterloo.

2.2.6 Monitoring Rad1 antibody titres

Serum collected prior to each boost was used to assess antibody titre by performing an enzyme-linked-immunosorbent-assay (ELISA). Each well of a 96-well plate were coated with 100ul of 10µg/ml recombinant rtRad1 protein diluted in coating buffer (15mM Na_2CO_3, 34mM $NaHCO_3$, 0.02% NaN_3, pH9.3) for 18hrs at room temperature. The wells were emptied and washed three times with TBS-T (Tris Buffer Saline and 1% Tween-20). Wells were blocked with 300µl of blocking buffer (1% bovine serum albumin [BSA] in TBS-T) at 37°C for 1h. The wells were emptied and washed three times as previously stated. Anti-rtRad1 serum was diluted in blocking buffer to 1:100, 1:500, 1:1000, 1:5000, 1:10000, 1:50000, 1:100000 and 100µl of each dilution was added in triplicate and incubated for 1h at room temperature. Goat anti-rabbit IgG antibody conjugated to alkaline phosphatase (Sigma: St. Louis, MO) was diluted in blocking buffer to 1:5000 and 100µl was added to each well for incubation at room temperature for 1h. For detection, 50µl of SIGMAFAST™ p-Nitrophenyl phosphate (Sigma: St. Louis, MO) stock solution was added to each well and incubated in the dark for 20min at room temperature. Absorbance was measured at 405nm using the Versamax microplate reader and the SOFTmax PRO 2.6.1 program (Molecular Devices: Sunnyvale, CA). Values were corrected by subtracting the background readings.

2.2.7 Whole fish RNA and protein lysate preparation

Rainbow trout (*Oncorhynchus mykiss*) were purchased from Silver Creek Aquaculture (ON, Canada) and held in well-water flow-through tanks at the University of Waterloo. Fish were kept at 12-13°C and fed Classic Floating Trout 5pt Regular pellets (Martin Mills: ON, Canada) daily. Fish were then euthanized

by overdose with Phenoxyethanol (0.001%). Spleen, heart, gill, brain, liver, head kidney, thymus, muscle and gonad tissue along with eggs (when available) were extracted and placed into 10ml of RNA*later* and stored in -20°C. The tissues were cut into smaller pieces before adding them to the RNA*later* to better preserve the RNA and protein. These tissues were used for both RNA and protein extractions.

For RNA extraction, 120mg of tissue was used for RNA extraction using the "Trizol Method" (Appendix B). The isolated RNA was subjected to DNase disgestion and "RNA cleanup" according to the protocol of *QIAGEN® RNeasy®* mini kit (Qiagen: Mississauga, ON). RNA concentration was determined using NANODROP® Spetrophotometer ND-100 (Thermo Scientific: Wilmington, DE) and the quality of RNA was evaluated by running 10µg of each samples on a formaldehyde-agarose gel. The RNA samples were stored at -80°C.

For protein extraction, 100mg of tissue was added to 250µl NP-40 lysis buffer (1% Nonident P40, 50mM Tris-HCl; pH 8, 150mM NaCl) and 50µl "complete" Protease Inhibitor cocktail (Sigma: St. Louis, MO). The tissue was homogenized using a hand held electric pestle, sonicated (Microson™ Ultra Sonic Cell Disrupter, Misonix: Farmingdale, NY) at level 5 intensity for 30s and centrifuged at 13,000rpm for 10min at 4°C in a Biofuge-Pico centrifuge (Heraeus: AZ, USA). The lysate was collected and subjected to a Bradford Assay. Sample Buffer (60mM Tris-HCl, pH 6.8, 25% glycerol, 2% SDS, 14.4mM β-mercaptoethanol, 2% bromophenol blue) was added to create a 5ug/µl protein stock prior to storage at -20°C.

2.2.8 Cell-line RNA and protein lysate preparation

RTbrain-W1 and RTgill-W1 cell-lines were obtained from Dr. Niels C. Bols (University of Waterloo). The cell lines were maintained in 75cm^2 flasks at 18°C in L-15 media (Sigma: St. Louis, MO) supplemented with 1% penicillin-streptomycin solution (100 µg/ml streptomycin, 100 IU/ml penicillin; Sigma: St. Louis, MO). RTgill-W1 and RTbrain-W1 cell-lines used in the bleomycin study (described below) contained 10% FBS and 15% FBS respectively. RTgill-W1 cell-lines used in the hydroxyurea

study (described below) did not contain any FBS. Cells were harvested using scraper and centrifugated at 1,000Xg. RNA was extracted from the cells using *QIAGEN® RNeasy®* mini kit (Qiagen: Mississauga, ON) according to the manufacturer's instructions. Protein was extracted as stated in section 2.2.7 except that a handheld homogenizer was not used.

2.2.9 Determining anti-rtRad1 specificity

Results from the ELISA analysis of the final bleed determined that serum diluted to 1:1000 from rabbit 1Z1 was sufficient for anti-rtRad1 to recognize rtRad1 protein. Protein lysates from rainbow trout spleen, gill, heart, brain, liver, head kidney, eggs, thymus and muscle were boiled with 5X sample buffer (60mM Tris-HCl, pH 6.8, 25% glycerol, 2% SDS, 14.4mM β-mercaptoethanol, 2% bromophenol blue) and 50µg of each sample was loaded, then run in four replicates on a 12% SDS-PAGE and transferred to 0.2 µm nitrocellulose membrane (Bio-Rad: Mississauga, ON). Western (1) was probed with Anti-actin (1:200; Sigma: St. Louis, MO), (2) was probed with pre-immune serum (1:1000), (3) was probed with anti-rtRad1 (1:1000), (4) was probed with anti-rtRad1 (1:1000) that had been pre-incubated with 1mg rtRad1. Following washes, the blots were probed with Goat anti-rabbit IgG antibody conjugated to alkaline phosphatase (Sigma: St. Louis, MO) at 1:3000 and then detected with an alkaline phosphate solution (as stated in the Appendix) until bands became visible. The blot was visualized using a Hewlett Packard ScanJet 3300C (Mississauga, ON) scanner and Adobe® Photoshop® 7.0.

2.2.10 Whole fish and cell-line tissue distribution

Protein lysates were extracted from the same tissues described above, from three different fish. Fifty micrograms of each sample was run on 12% SDS-PAGE gel and used in a western blot, as described above. Anti-rtRad1A (1:1000) was used to detect rtRad1 in each tissue while Anti-actin (1:200; Sigma: St. Louis, MO) was used as a control. Following washes, the blots were probed with Goat anti-rabbit IgG

antibody conjugated to alkaline phosphatase (Sigma: St. Louis, MO) at 1:3000 and detected with alkaline phosphatase detection solution as stated in Appendix A. Blots were visualized as stated above.

Protein lysates were extracted from RTgill-W1, RTbrain-W1 and human embryonic kidney (HEK)-293 cell-lines and prepared as described above. Twenty micrograms of RTgill-W1 and RTbrain-W1 and 40µg of HEK 293 was loaded on the same gel. The samples were run, transferred and detected as stated above.

2.2.11 Rad1 mRNA distribution in rainbow trout tissues

One microgram of spleen, heart, gill, brain, liver, head kidney, thymus, and egg RNA was transcribed into cDNA using *RevertAid™ H Minus First Strand* cDNA *Synthesis* Kit (Fermentas: ON, Canada) according to the manufacturer's instructions. RT-PCR was performed using 2.5µl of 10X Incubation Mix Taq Polymerase without $MgCl_2$, 0.5µl of 10mM each dNTP mix, 1.5µl of 25mM $MgCl_2$, 1.5µl of each primer (10µM), 0.1µl Taq DNA Polymerase (5U/µl) (MP Biomedical: Solon, OH), 1µl of cDNA template and 16.4µl H_2O. The primers used were Rad1For1 and Rad1Rev2. Ten RT-PCR reactions were completed, one for each tissue and one for a positive and a negative control (NTC). The thermocyler (Bio-Rad DNA Engine: Mississauga, ON) conditions were as follows 95°C 5min, 35 cycles (95°C 40sec, 59°C 1min, 72°C 1min) and 72°C 15min. Equal amounts of each RT-PCR product (5 µl) were run on a 1% agarose gel containing 1X GelRed™ (CA, USA) and visualized with a UV transilluminator and Alpha Imager HP program (Alpha Innotech Flourochem 8000 Chemiluminescence and Visable Imaging system: Santa Clara, CA).

2.2.12 Bleomycin treatment on RTbrain-W1 and RTgill-W1 cell-lines

RTbrain-W1 and RTgill-W1 cell lines were maintained in Leibovitz's L-15 culture medium supplemented with 1% penicillin-streptomycin solution (100 µg/ml streptomycin, 100 IU/ml penicillin; Sigma: St. Louis, MO), with 10% fetal bovine serum (FBS; Sigma: St. Louis, MO) for RTgill-W1 and 15% FBS for

RTbrain-W1 in 75cm2 flasks at 18°C. Cells were seeded in 25cm^2 flasks at either 1.5 x 10^6 (RTbrain-W1) or 3 x 10^6 (RTgill-W1) cells per flask, 24 hours prior to treatment. Cells were treated indirectly with 20µg/ml, 100µg/ml and 200µg/ml bleomycin (final concentration: Calbiochem) in L-15 medium. Control cells were treated with fresh media only. Flasks were then incubated in the dark at room temperature for the indicated time points of exposure. Maintenance and dosage of cell-lines was completed by Michelle Liu from Dr. Duncker's lab at the University of Waterloo.

2.2.13 Hydroxyurea treatment on RTgill-W1 cell-line

The RTgill-W1 cell-line was treated indirectly with 200mM hydroxyurea (final concentration) in L-15 culture medium with 1% penicillin-streptomycin solution (100 µg/ml streptomycin, 100 IU/ml penicillin; Sigma: St. Louis, MO). Each dish (100X15mm Petri dish) contained 2 million cells and were harvested at days 1, 3, and 6. The control used was an RTgill-W1 cell-line not treated with hydroxyurea and was harvested during the same days. Dosing and maintenance of cell cultures was completed by Fanxing Zang from the Dr. Bols lab at the University of Waterloo. Protein lysates were harvested and the concentration was determined as described above. Twenty micrograms of each sample was loaded on a 12% SDS-PAGE and transferred as described above. Samples were detected with anti-rtRad1 (1:1000), probed with Goat anti-rabbit IgG antibody conjugated to alkaline phosphatase (Sigma: St. Louis, MO) at 1:3000 and detected as stated above. The western blots were visualized as stated previously.

2.2.14 Determining the splice variants of rtRad1 using RT-PCR

RT-PCR was used to determine if alternative forms of rainbow trout Rad1 exist. One microgram of RNA from rainbow trout heart, brain, and RTgill-W1 cell-line was transcribed into cDNA as stated above. Primer set A (Rad1start 5'-GAAAGCTCAGATGGCG- 3' and Rad1stop 5'-CAATATTCCTATTCTCCCTACTC - 3') and primer set B (Rad1-5UTR 5'-GTCAACAGACTTTGATACATCAAG - 3' and Rad1-3UTR 5'-CATTTGAGCCTCGTATTC -3') were

the two primer sets used. RT-PCR was performed using 2.5µl of 10X Incubation Mix Taq Polymerase without $MgCl_2$, 1µl of 10mM each dNTP mix, 2µl of 25mM $MgCl_2$, 1.5µl of each primer (10µM), 0.15µl Taq DNA Polymerase (5U/µl) (MP Biomedical: Solon, OH), 1µl of cDNA template and 15.35µl H_2O. The thermocyler (Bio-Rad DNA Engine: Mississauga, ON) conditions were as follows 95°C 5min, 35 cycles (95°C 40sec, 59°C 1min, 72°C 1.15min) and 72°C 15min. The product (5 µl) was run on a 1% agarose gel containing 1X GelRed™ (CA, USA) and visualized with a UV transilluminator Alpha Imager HP program (Alpha Innotech Flourochem 8000 Chemiluminescence and Visable Imaging system: Santa Clara, CA). Another gel was made to excise the different bands present in each PCR sample. For the heart sample, two bands were gel excised one at 840bp and one at 668bp. For the brain sample a band at approximately 1.1kb and another at 900kb were excised from the gel. Lastly, two bands at around 400bp and one band at 840bp were excised from the RTgill-W1 samples. These bands were purified and sequenced as stated in section 2.1.1. The nucleotide and translated protein sequences of all the samples were aligned together to determine if the excised bands were Rad1 splice variants.

2.3 Results

2.3.1 Determining the full-length cDNA sequence of rainbow trout Rad1

Gradient PCR was performed to amplify a 721bp fragment of Rad1 from a rainbow trout head kidney cDNA library (Figure 2.1). The product from the 57°C reaction was cloned and sequenced. When placed into BLAST it was revealed to be a rainbow trout homolog of Rad1. The 721bp sequence was used to develop gene-specific sense and antisense primer necessary for Anchored PCR.

Five different primer sets were used to amplify the remaining ORF and untranslated regions (UTRs: Figure 2.2). Amplicons from primer set two and four were cloned and sequenced. The size of the amplicons from primer sets 2 and 4 were 755bp and 795bp, respectively. Each amplicon sequence had a section that overlapped with the other. The overlapping sequences were spliced together to obtain the full-

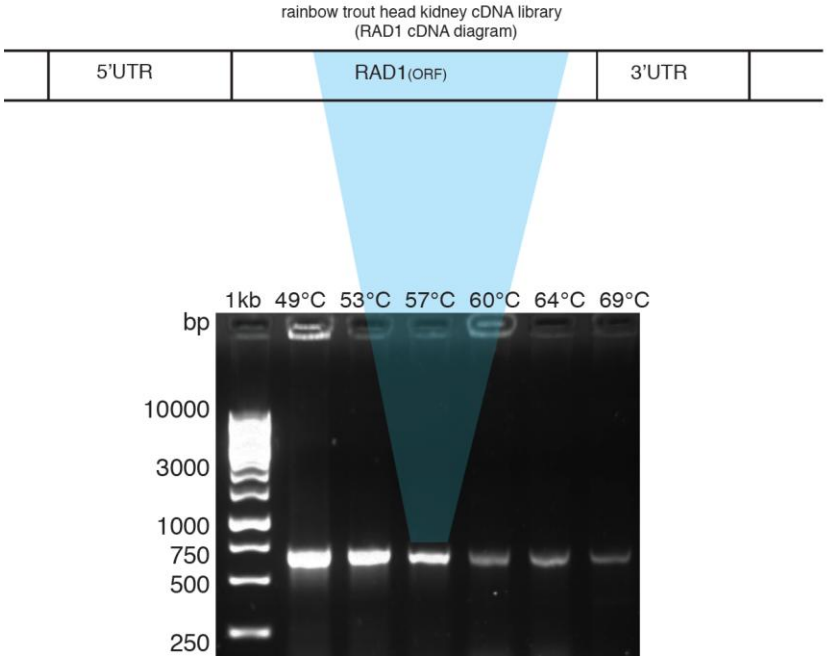

Figure 2.1: Amplification of a 721bp portion of rtRad1
A 721bp fragment of Rad1 was amplified from the open reading frame (ORF) of the head kidney cDNA library. The lanes of the 1% agarose gel are labeled according to the annealing temperature used in the gradient PCR reaction. The amplicon from the 57°C reaction was cloned, sequenced and it was identified as Rad1. Above the gel is a diagram of the Rad1 cDNA. Highlighted in blue is a visual interpretation of the amplicon's location on the diagram.

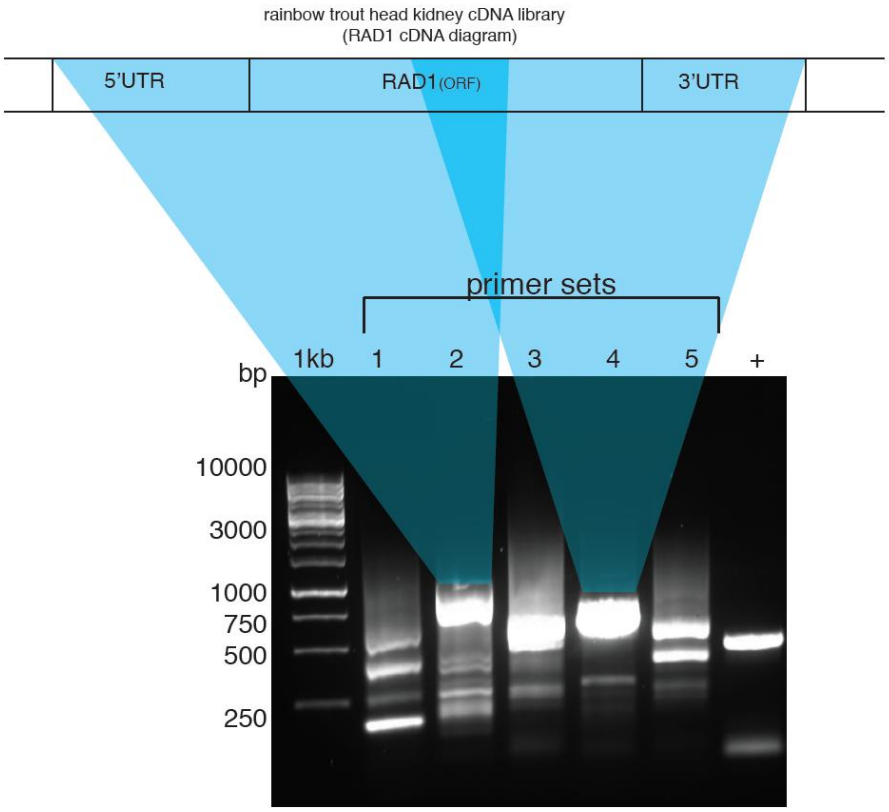

Figure 2.2: Amplification of the full-length cDNA of rtRad1
Anchored PCR was used to amplify the remaining cDNA sequence of rtRad1. The lanes of the 1% agarose gel are labeled according to the primer sets used. Primer set 2 was used to amplify a portion of the remaining ORF and the 5'UTR while primer set 4 was used to amplify the remaining ORF and the 3'UTR. The size of the amplicon from primer sets 2 and 4 was 755bp and 795bp, respectively. Above the gel is a diagram of the Rad1 cDNA. Highlighted in blue is a visual interpretation of the amplicon's location on the diagram. Each amplicon sequence had a section that overlapped the other. This overlapping region is highlighted as a darker blue colour on the diagram.

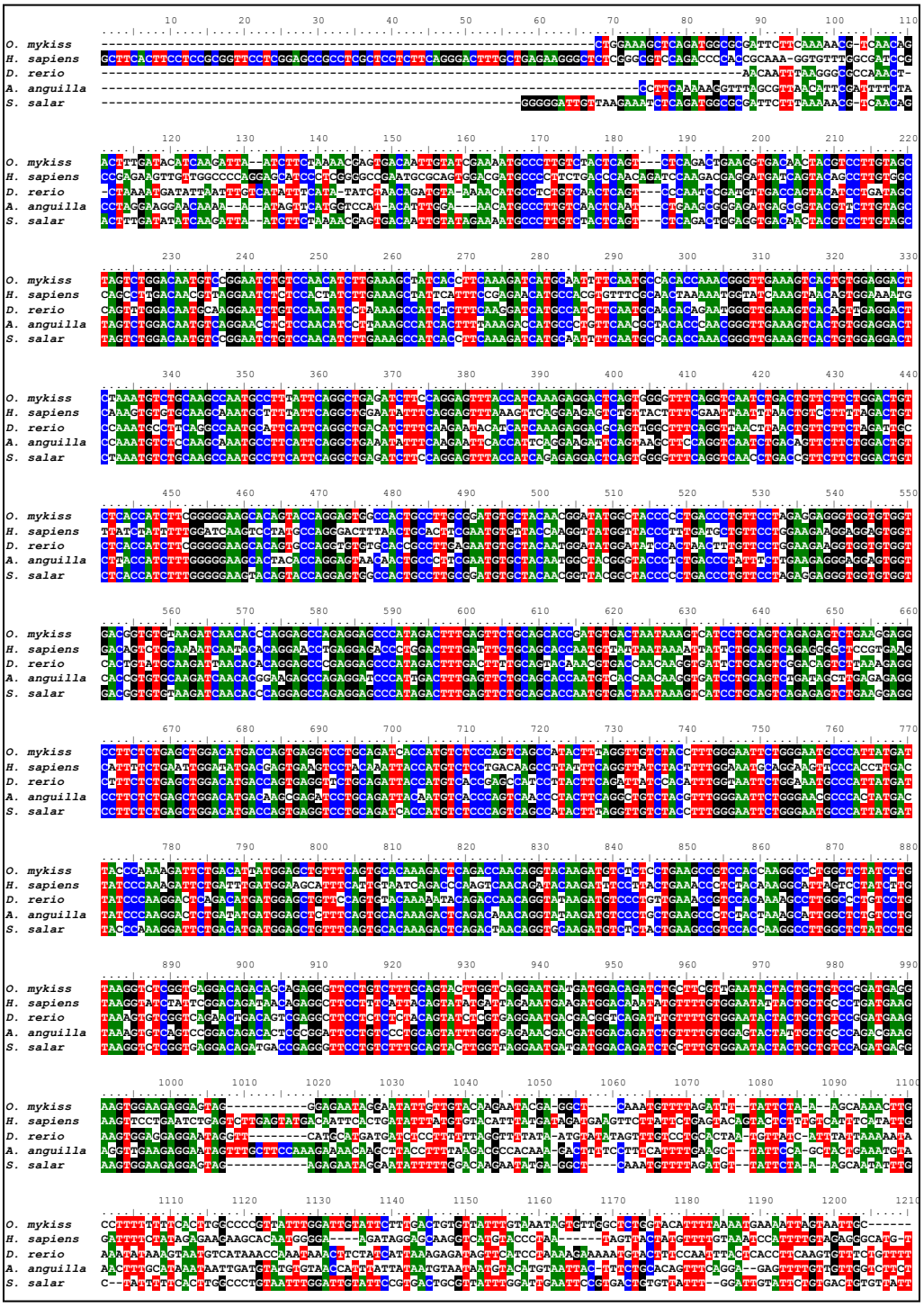

Figure 2.3: Nucleotide alignment of rtRad1 and Rad1 homologs
The cDNA sequence of rtRad1 and Rad1 homologs are aligned and the conserved regions are highlighted in colour (A=green, G=black, C=blue, T=red). The species names are listed to the left.

length rtRAD1 cDNA sequence, which was subsequently amplified as a single product to confirm that it was a real sequence (see Figure 2.3). The isolated rtRad1 cDNA sequence was 1,110bp (excluding the polyA-tail) with a 5'UTR of 94bp, a 3'UTR of 176bp and an ORF of 840bp which encodes a 279 amino-acid protein. The nucleotide (Figure 2.3) and protein (Figure 2.4) sequence of rtRad1 were aligned with homologs which revealed conserved domains.

2.3.2 Cloning of rtRad1 open reading frame into an expression vector

PCR was performed to amplify the 840bp ORF of rtRAD1 (Figure 2.5). The ORF was cloned into pGEM T-easy vector and then digested out using the restriction sites incorporated into the ORF (*BamH*I and *Hin*dIII). The digested ORF and pRSET(A) were both gel purified (Figure 2.6A) and ligated together. The new construct was sequenced to confirm that proper ligation occurred and that the ORF was in frame with the 6XHIS and XPRESS™ epitope N-terminal tags (Figure 2.6B). The construct [pRSET(A):rtRAD1ORF(*B*/*H*)] was transformed into BL21-CodonPlus®(DE3)-*RIPL* strain (Stratagene: Aurora, ON) to begin over expression of rtRad1 recombinant protein.

2.3.3 Expression and purification of rtRad1 recombinant protein

The theoretical molecular weight of rtRad1 is 31kDa but due to the addition of the 6XHIS and Xpress™ epitope (3kDa) the recombinant protein ran at 34kDa (Figure 2.6). Elutions which contained a thick band at 34kDa and with little background were collected and stored at -80°C (Figure 2.7). In the end, 21mg/ml of recombinant rtRad1 protein in 1XPBS (pH 7.4) was collected. A Coomassie stained gel containing 1µg/ml of the final stock of recombinant rtRad1 revealed the presence of a pure sample as there was no background bands present (Figure 2.8A). Four western blots containing 1µg/ml of the final stock of recombinant rtRad1 were probed with (1) anti-polyhistidine (Figure 2.8B), (2) anti-Xpress™ (Figure 2.8C), (3) anti-Human-Rad1A (Figure 2.8D) and (4) no primary antibody (Figure 2.8E) confirm that the recombinant protein made was indeed rtRad1 and it was highly pure (Figure 2.8). The western blots from

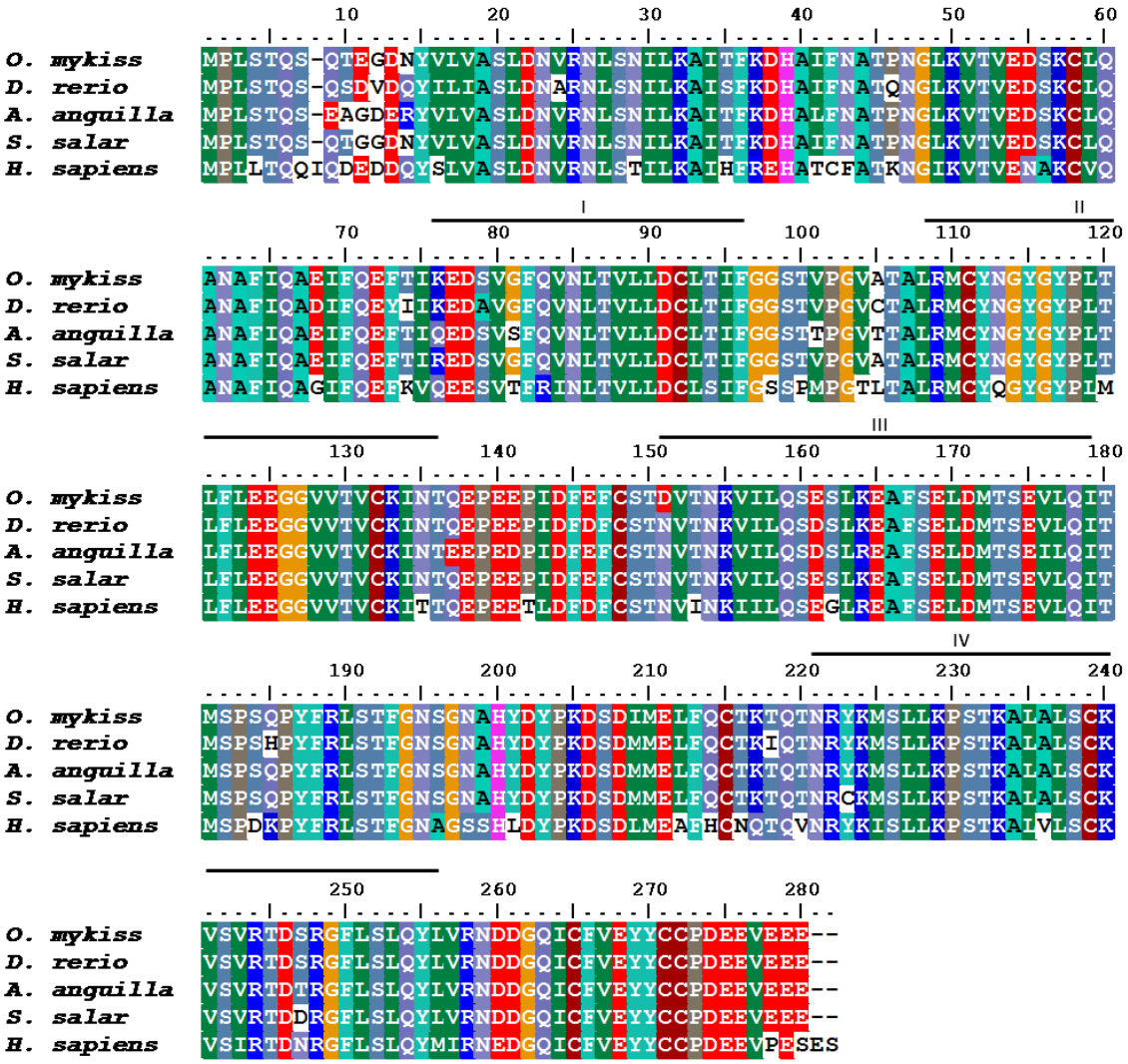

Figure 2.4: Multiple protein alignment of Rad1 sequences
The protein sequences of rtRad1 and Rad1 homologs are aligned and the conserved regions are highlighted. The species names are listed to the left. An overline is used to label the predicted conserved exonuclease domains (I, II, III) and the leucine zippers (III, IV) based on Nogueira *et al.*, (2009).

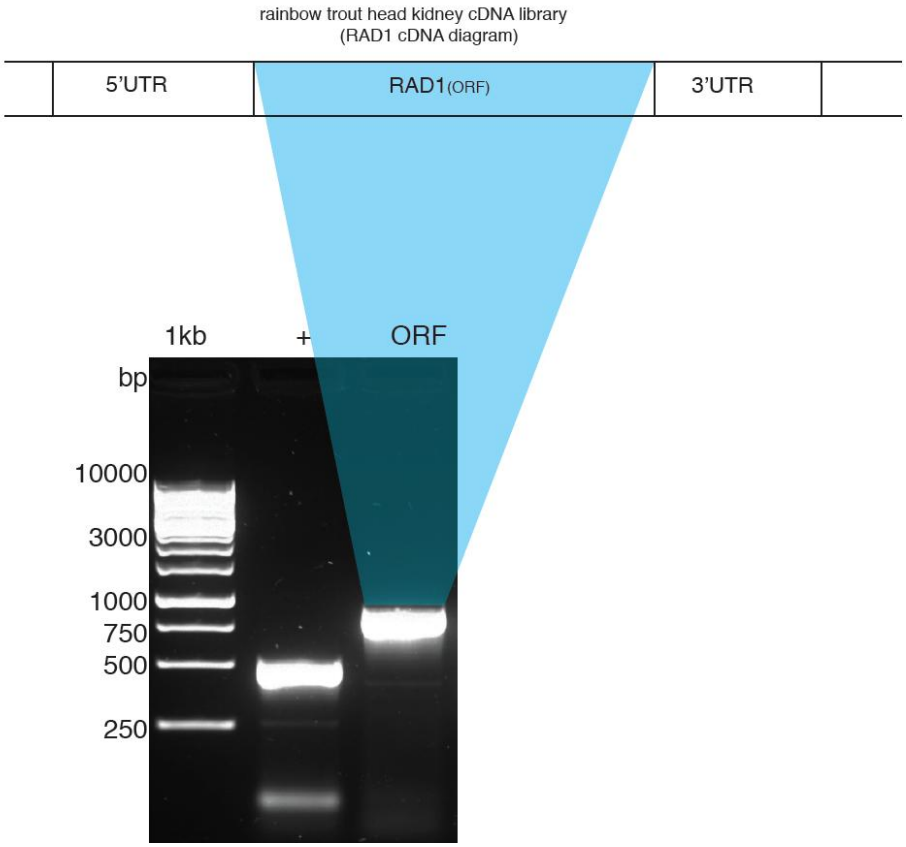

Figure 2.5: Amplification of rtRad1 open reading frame
The 840bp open reading frame (ORF) of rtRad1 was amplified using primer-adapters. The lanes of the 1% agarose gel are a positive control (+) and the ORF of rtRad1. Above the gel is a diagram of the Rad1 cDNA**.** Highlighted in blue is a visual interpretation of the amplicon's location on the diagram.

A

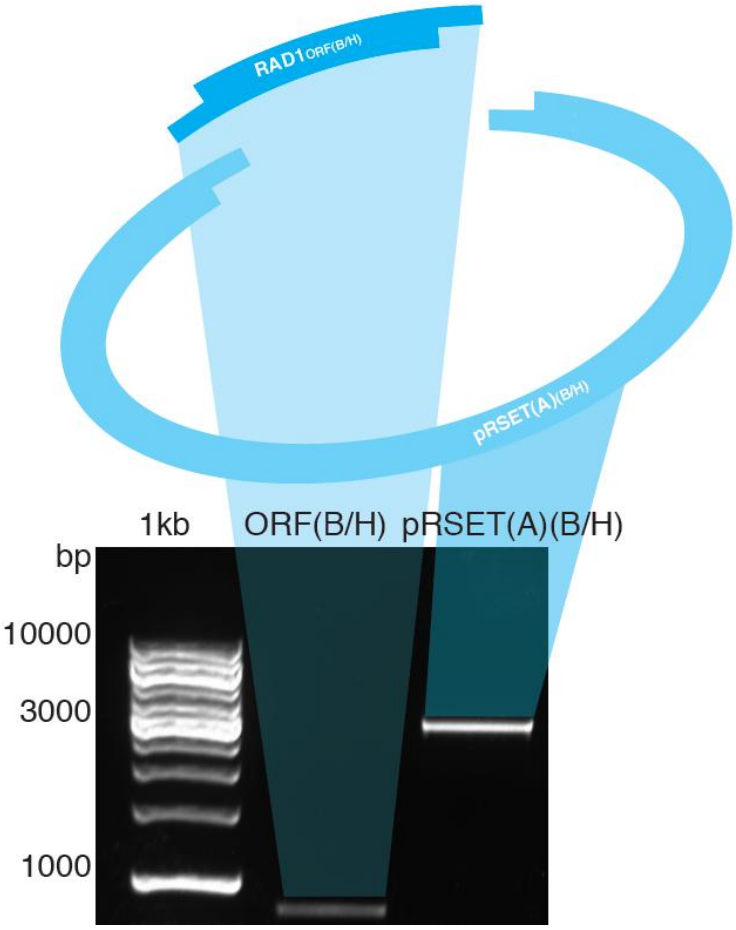

B

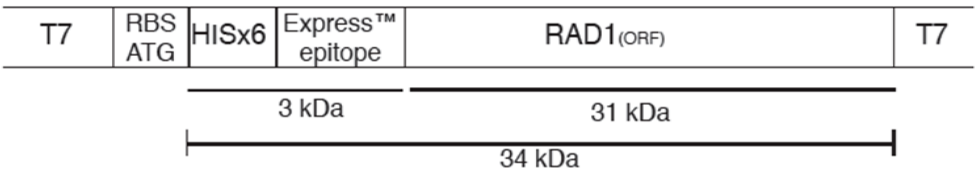

Figure 2.6: Ligation of rtRad1 ORF into an expression vector
(A) The 1% agarose gel shows the digested products of rtRad1 ORF (840bp) and pRSET(A) vector (2.9kb) with *BamH*I and *Hin*dIII (B/H). Above the gel is a schematic representation of the two digested products being ligated together. Highlighted in blue is a visual interpretation of the amplicon's location. **(B)** Diagram of the ligation construct created [pRSET(A):rtRAD1ORF(*B*/*H*)]. Expected protein sizes of the N-terminal tags, rtRad ORF and the expected size of the rtRad1 recombinant protein are labeled.

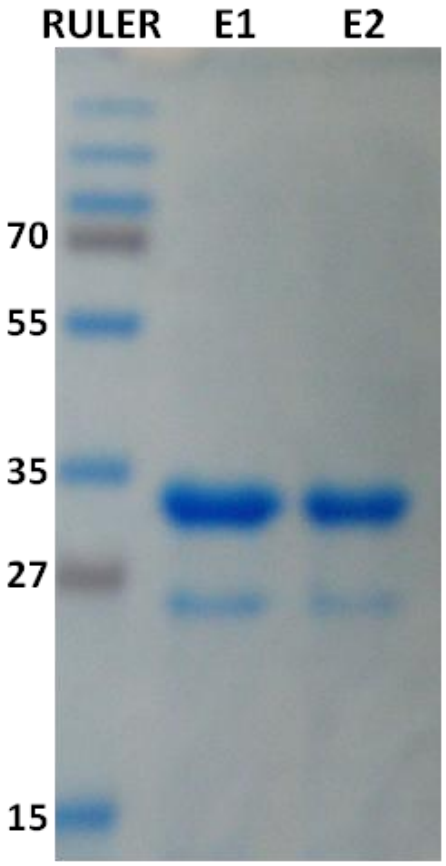

Figure 2.7: Coomassie staining of rtRad1 recombinant protein elution fractions
Ten micrograms of each elution was run on a 12% SDS-PAGE and stained with Coomassie Brilliant Blue G-250. Elution fractions 1-2 are labeled as E1 and E2, respectively. The expected size of the rtRad1 recombinant protein (34kDa) is seen in both E1 and E2.

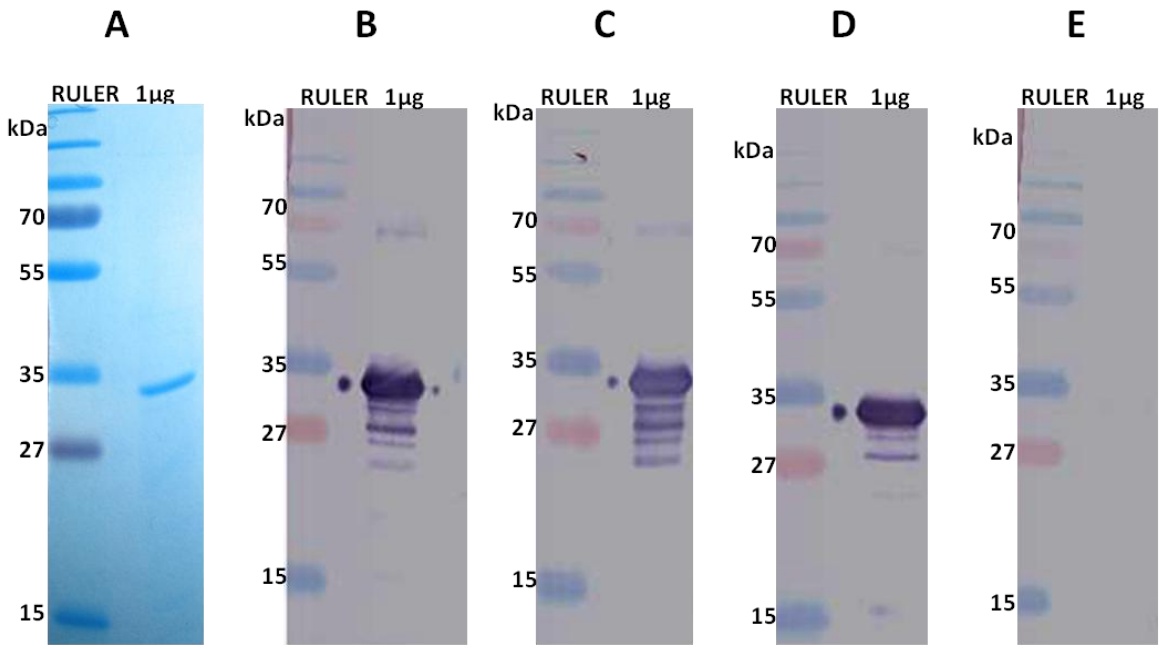

Figure 2.8: Analysis of the rtRad1 recombinant protein
One microgram of the final batch of recombinant rtRad1 was run on a 12% SDS-PAGE and analyzed through Coomassie staining (A) and western blot (B-E). **(A)** Comassie staining revealed a clear band at 34kDa with no background proteins visible. **(B)** A western blot probed with Anti-polyhistidine was used to detect the 6XHIS-TAG on the recombinant protein (34kDa). **(C)** A western blot showing the detection of the Xpress™ epitope tag on the recombinant protein (34kDa) using the primary antibody Anti-Xpress™. **(D)** A western blot probed with Anti-Human-Rad1A was used to detect the rtRad1 recombinant protein (34kDa). **(E)** Western blot showing that with no primary antibody added there were no proteins detected.

anti-polyhistidine, anti-Xpress™ and anti-hRad1A identified a fat band at 34kDa, a faint band at 68kDa and bands under 34kDa at around 30kDa, 28kDa, 27kDa, 26kDa. The thick band at 34kDa is the molecular weight of rtRad1 recombinant protein while the faint band at 68kDa appears to be a dimer. The bands below 34kDa appear to be degradation products of the rtRad1 recombinant protein.

2.3.4 Analysis of anti-rtRad1 antibody titre

The highly pure rtRad1 recombinant protein was used to inoculate two rabbits to develop anti-rtRad1 antibodies. The titre was monitored prior to each boost and it was revealed that anti-rtRad1 was being produced at a high titre for each rabbit (Figure 2.9). For each rabbit, there was an increase in titre strength from boost one to boost three. However, the final bleed had a titre that was lower than that of the previous boost. Both rabbits produced very strong antibodies that can be used at 1:1000 dilution for western blots. Serum for rabbit #1 was used for all westerns as it had a little less background than rabbit #2 (data not shown).

2.3.5 Determining anti-rtRad1 specificity

Anti-rtRad1 antisera from rabbit #1 recognize protein at different molecular weights than the predicted size of rtRad1. To confirm that these bands are rtRad1 and to confirm the specificity of the polyclonal antibodies four western blots were completed. Blot one had untreated final bleed anti-rtRad1 antiserum (1:1000), blot two used anti-rtRad1 antiserum (1:1000) that was pre-incubated with 1mg of recombinant rtRad1, blot three used antiserum prior to inoculation, and blot four used an anti-actin antibody as a control. Figure 2.10 shows that when anti-rtRad1 antiserum is blocked with the recombinant protein, that the bands around that were there prior to being blocked are absent. This is due to the excess recombinant protein blocking the anti-rtRad1 antibodies. This helps confirm that the bands that appear on the western blots probed with anti-rtRad1 are highly likely to be rtRad1. Furthermore, the blot with the pre-immune

A

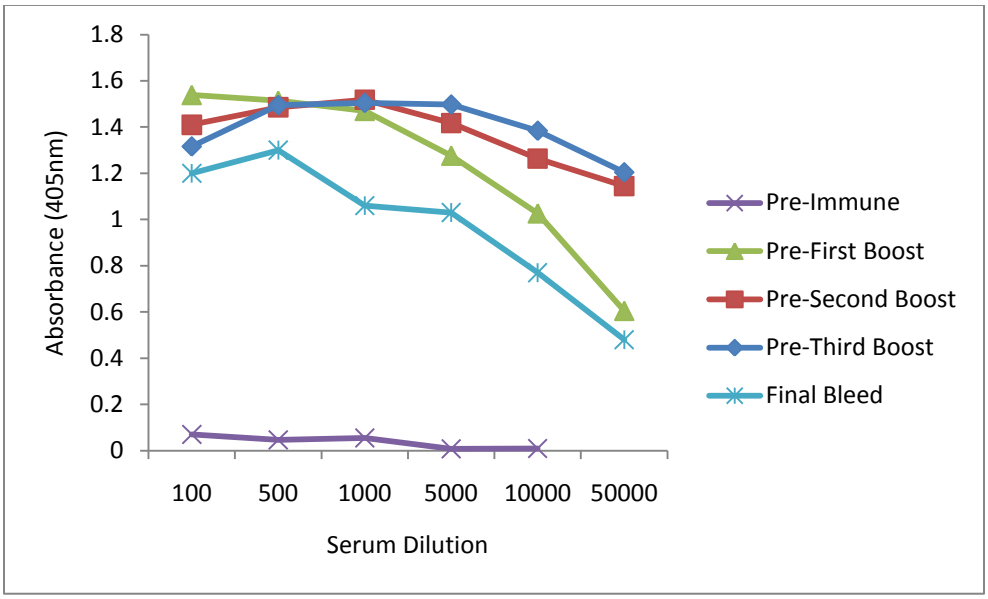

B

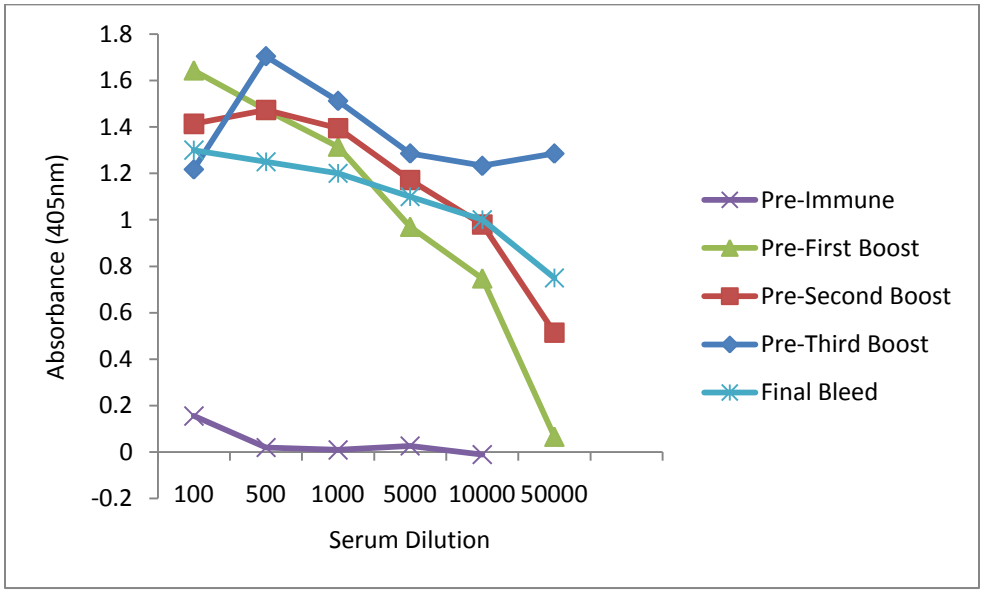

Figure 2.9: ELISA of anti-rtRad1 antiserum samples from rabbits #1 and #2
Serum was taken prior to each boost, as well as the final bleed, to examine the antibody's titre. **(A)** The dilution series of rabbit#1 shows that each boost had a high titre against the recombinant rtRad1 protein. **(B)** Serum from rabbit #2 had similar results to rabbit#1. For both rabbits, the final bleed had a titre that was less than that of the previous boost.

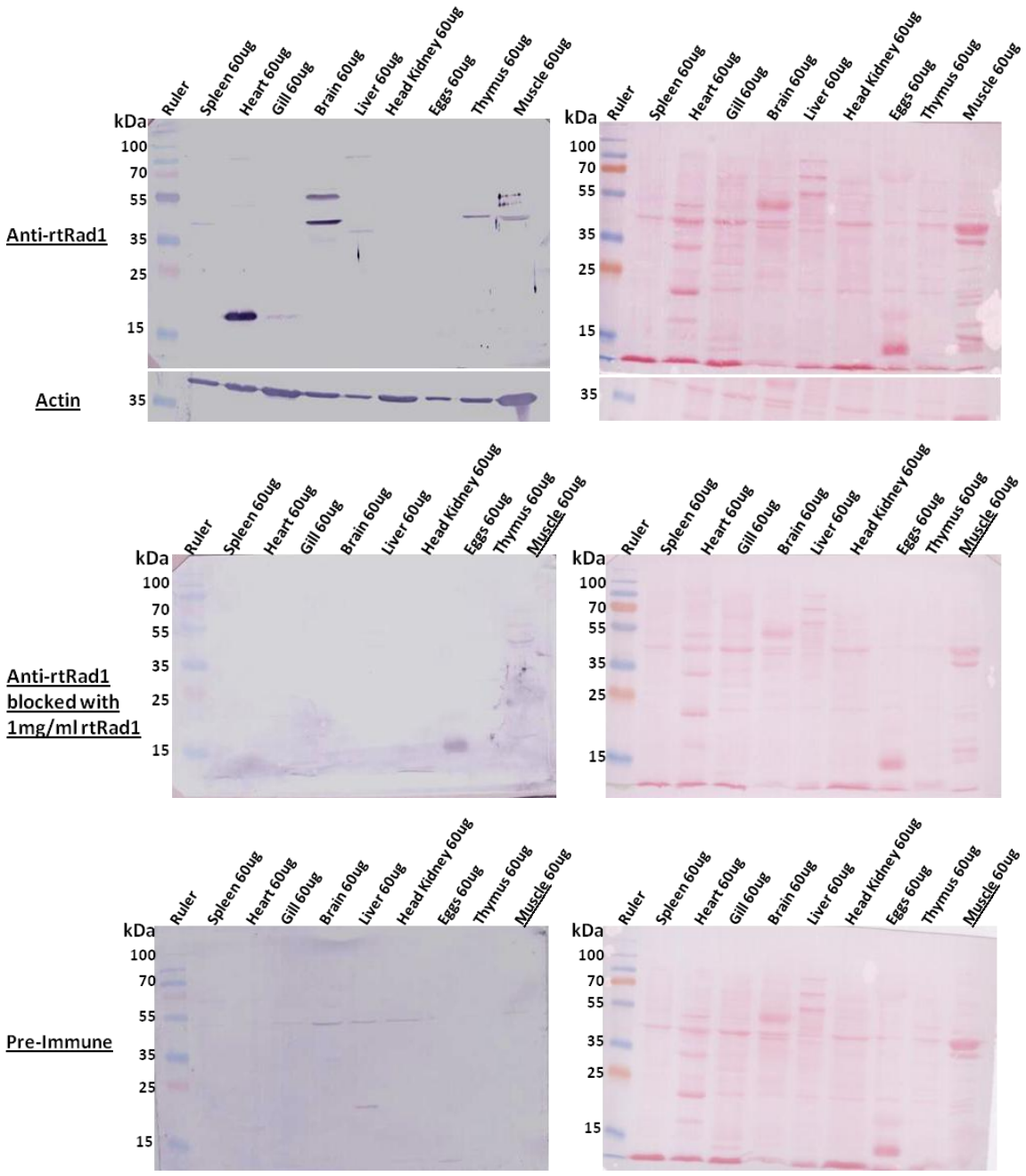

Figure 2.10: Analyzing the specificity of the anti-rtRad1 antibody
Western blots were used to verify the specificity of anti-rtRad1 antibody. Rainbow trout Rad1 protein was detected with the anti-rtRad1 antibody (1:1000) and anti-actin (1:500) was used as a control. Detection of Rad1 protein was absent when the anti-rtRad1 antiserum was pre-incubated (blocked) with 1mg of the recombinant rtRad1 protein. Pre-immune antiserum detected only a few background bands. Ponceau S staining is shown to the right of the western blot and is shown as a loading control.

antiserum shows that there is only a small amount of background bands that appear at 54kDa. Ponceau S staining is shown as a loading control.

2.3.6 Rad1 distribution in rainbow trout tissues and cell-lines

Rad1 protein levels were examined in different rainbow trout tissues from three different fish (Figure 2.11). The predicted size of rtRad1 is 31kDa but this size was never observed on any of the western blots. Band sizes ranging from 18kDa to 100kDa were visualized but the predicted size was never seen. In spleen tissue, a faint band at 18kDa and 48kDa appeared, while in heart and gill tissues only a band at 18kDa was visible. In heart, the band at 18kDa is very intense in all three of the fish- it is also the most intense band seen in any of the westerns to date. The detection of a Rad1 protein at 18kDa suggests that rtRad1 may be alternatively spliced into a functional protein that is almost half the size of the expected form. In brain tissue a faint band appeared at 35kDa, an intense band appeared at 48kDa and sometimes another intense band appeared at 55kDa. Interestingly, in RTbrain-W1 only one band appears at 18kDa suggesting that there may be different forms of rad1 present in brain tissue than in the cell-line. Liver had bands present around 48kDa and 100kDa. The band at 100kDa may potentially be rad1 in the 9-1-1 complex that has remained associated with each other even though denaturing of proteins has occurred. Rad1 was never detected in head kidney, while it has been detected at low intensities at 48kDa in thymus and muscle. The lane that contains lysate fromHEK-293-T had a strong band at 55kDa while RTgill-W1 had a band at 18kDa. Ponceau S staining is shown as a loading control.

2.3.7 Rad1 mRNA distribution in rainbow trout tissues

RT-PCR was used to determine the rtRad1 mRNA levels, using high-quality RNA (Figure 2.12A) from spleen, heart, gill, brain, liver, head kidney, gonad and thymus. The primers used created an amplicon of 721bp that was seen in each of the aforementioned tissues (Figure 2.12B). Since only a portion of Rad1 was amplified, the mRNA level could not accurately be calculated since there appears to be many alternatively spliced forms of rad1 (reviewed in section 2.2.14). However, the information is useful as

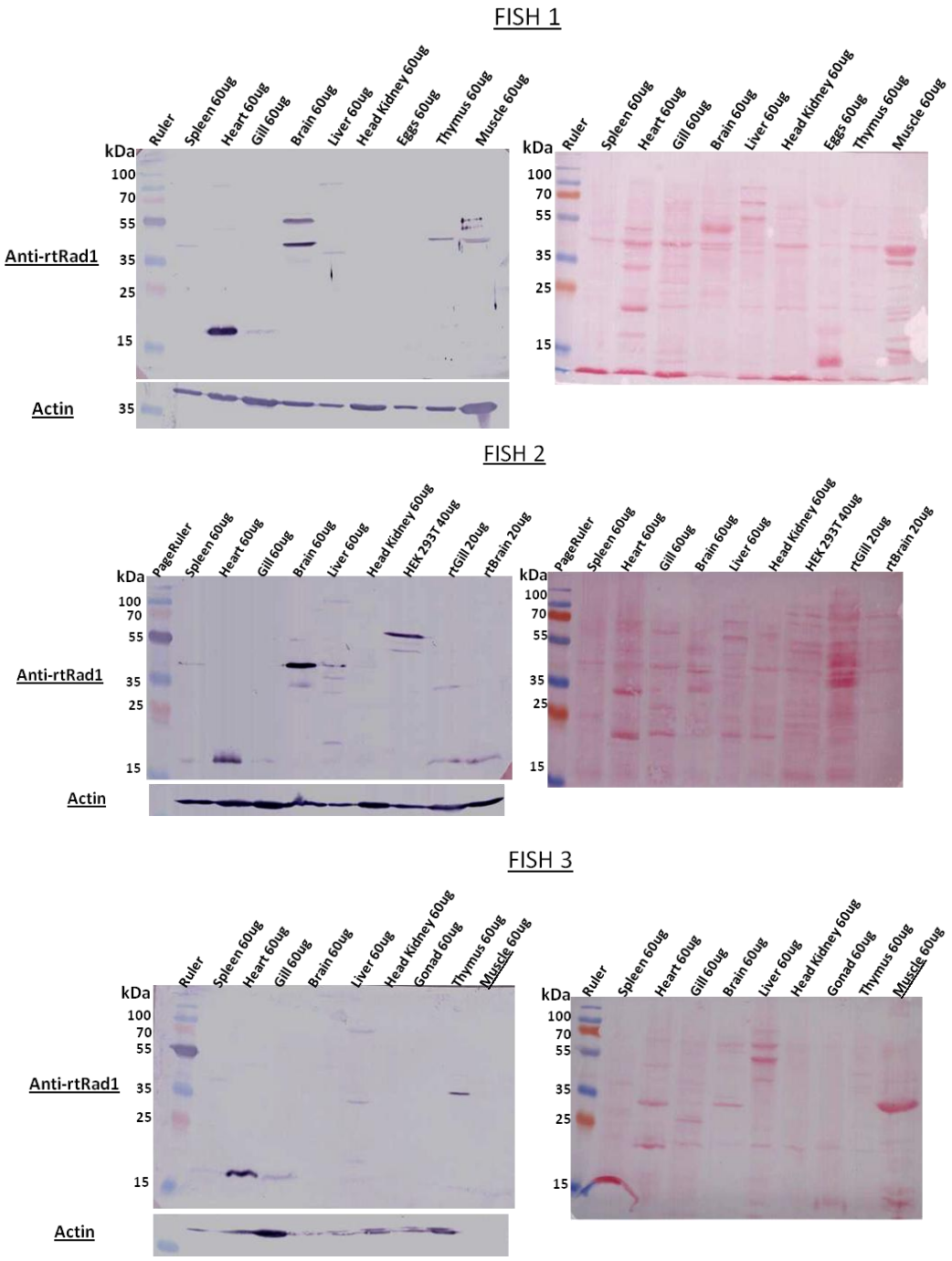

Figure 2.11: Assesment of Rad1 protein levels in three adult rainbow trout
Western blot of various rainbow trout tissue from three adult rainbow trout. Protein lysates (60µg) were probed with anti-rtRad1 antiserum (1:1000) and anti-actin antiserum (1:500). Each lane is labeled with the sample name and the amount loaded. Ponceau S staining is shown to the right of the western blot and is shown as a loading control. The western blot labeled "Fish 2" contains protein lysates from the HEK 293 T, RTgill-W1(labelled rtGill) and RTbrain-W1 (labelled rtBrain) cell-lines.

A

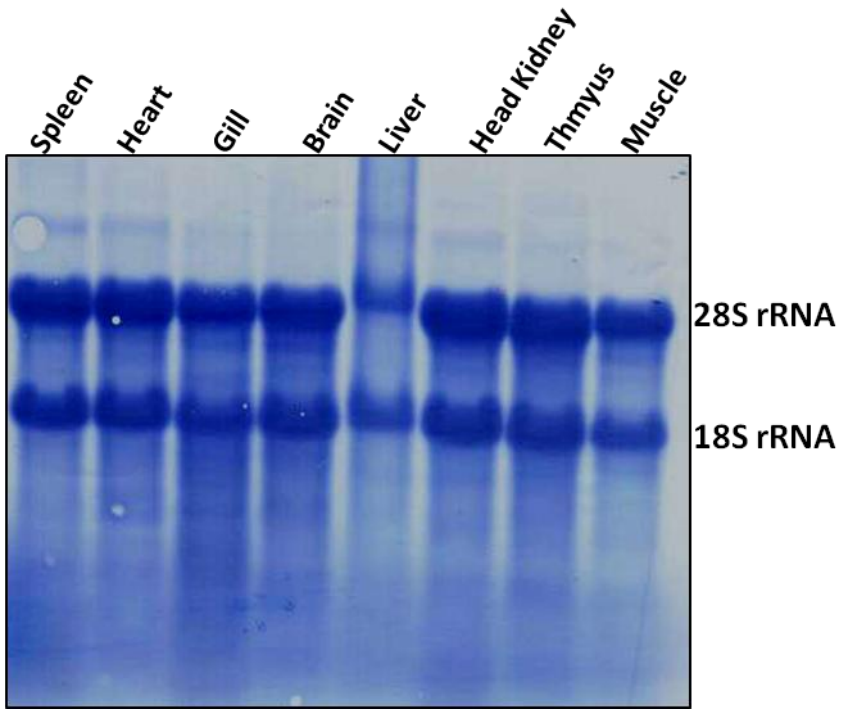

B

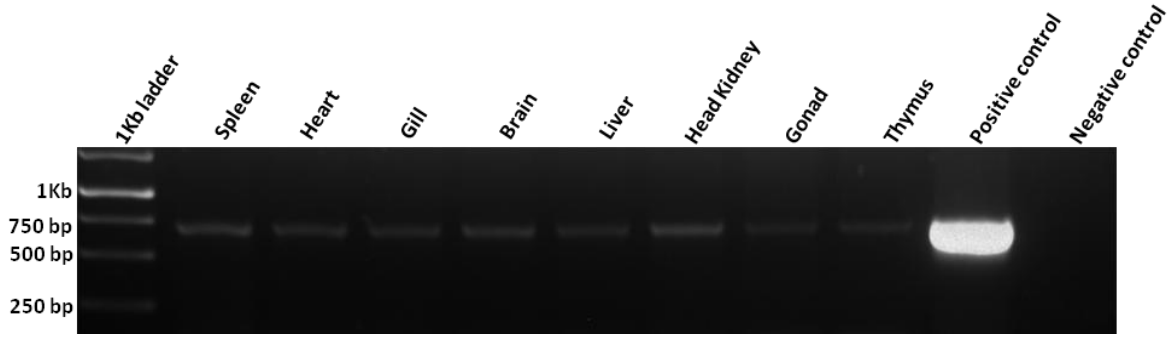

Figure 2.12: Expression of Rad1 mRNA transcripts in various rainbow trout tissues
(A) Negative stain of nitrocellulose membrane containing total RNA extracted from various rainbow trout tissues. Bands corresponding to the 28S and 18S rRNA are labeled. The negative stain was used to ascertain the quality of RNA to be used in the RT-PCR reaction. **(B)** The products of the RT-PCR were run on a 1% agarose gel and the lanes corresponding to the template cDNA used are labeled. The positive and negative controls were used according to the *RevertAid™ H Minus First Strand* cDNA *Synthesis* Kit (Fermentus: ON, Canada) protocol.

now it is known that some form of rad1 mRNA is expressed in each of the aforementioned tissues.

2.3.8 The effects of Bleomycin induced damage on Rad1 in RTbrain-W1 and RTgill-W1

Rad1 has been shown to be overexpressed (Hirai *et al.*, 2004) or phosphorylated (Lupardus and Cimprich, 2006) in response to ssDNA or dsDNA damage. RTbrain-W1 and RTgill-W1 cells were treated with bleomycin at various concentrations (0µg/ml, 20µg/ml, 100µg/ml, and 200µg/ml) for 24h. Bleomycin is a radiomimetic agent that induces double stranded breaks (Povirk *et al*., 1977). In Figure 2.13, experiment #1 shows that the increased concentration of bleomycin had no effects on rtRad1 in RTbrain-W1 since the band at 18kDa appeared to remain at the same relative intensity throughout the treatment and did not shift to a slower molecular weight. Rad1 may not be overexpressed nor phosphorylated in RTbrain-W1 cells. Note that a band at 48kDa is present in brain tissue but not in RTbrain-W1. However, it appears that the 18kDa band present in RTgill-W1 increases in intensity at 100µg/ml, and 200µg/ml. The only problem is that the bands are touching each other forming one large band which is impossible to quantify. The blot for experiment #1 could not be replicated due to insufficient samples.

For experiment #2, two replicates were made, one on a 12% SDS-PAGE (Figure 2.14A) and one on a 15% SDS-PAGE (Figure 2.14B) in order to better resolve the 18kDa band. Levels of Rad1 did not appear to increase in RTbrain-W1 nor in RTgill-W1. The increase in intensity of the 18kDa band in RTgill-W1 in experiment #1 was not seen again in experiment #2. However, it should be noted that the concentration loaded for the 200µg/ml bleomycin sample was lower than the others due to insufficient sample quantity. Note that the background bands were present in both the RTbrain-W1 and RTgill-W1 samples which could be detection of different Rad1 isoforms. Ponceau S staining is shown as a loading control.

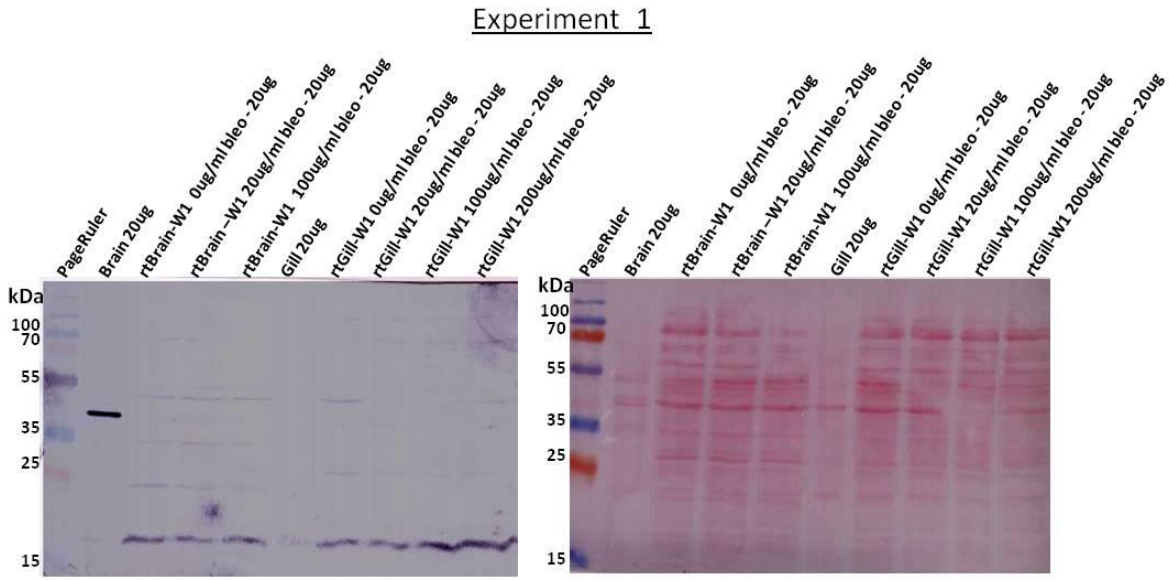

Figure 2.13: A first study of the expression of Rad1 polypeptides in rainbow trout cell-lines exposed to bleomycin

Experiment 1 had both RTbrain-W1 and RTgill-W1 cells treated with bleomycin (labelled as bleo) at various concentrations for 24h. The western blot was probed with anti-rtRad1 (1:1000) antiserum and contains samples from brain tissue, RTbrain-W1 cells treated with 0µg/ml, 20µg/ml, 100µg/ml of bleomycin, gill tissue, and RTgill-W1 cells treated with 0µg/ml, 20µg/ml, 100µg/ml, 200µg/ml of bleomycin. Rad1 was detected at 18kDa in the cell-lines but was detected at 48kDa in the brain tissue.

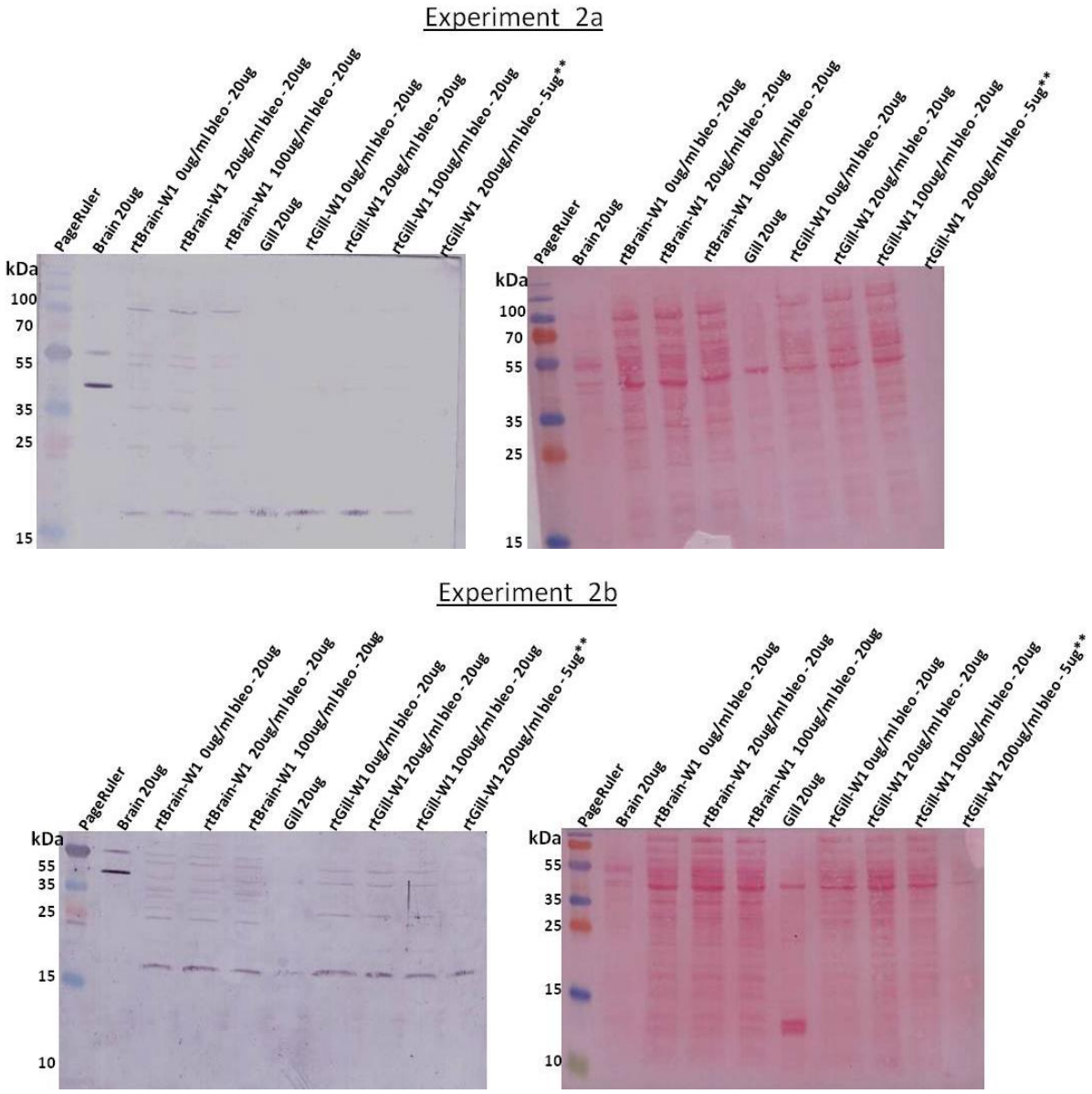

Figure 2.14: A second study of the expression of Rad1 polypeptides in rainbow trout cell-lines exposed to bleomycin

Experiment 2 had both RTbrain-W1 and RTgill-W1 cells treated with bleomycin (labelled as bleo) at various concentrations for 24h. The western blot was probed with anti-rtRad1 (1:1000) antiserum and contains samples from brain tissue, RTbrain-W1 cells treated with 0µg/ml, 20µg/ml, 100µg/ml of bleomycin, gill tissue, and RTgill-W1 cells treated with 0µg/ml, 20µg/ml, 100µg/ml, 200µg/ml of bleomycin. The samples were run on a 12% SDS-PAGE (Experiment 2a) and a 15% SDS-PAGE (Experiment 2b) Rad1 was detected at 18kDa in the cell-lines but was detected at 48kDa in the brain tissue. Ponceau S staining of the western blot is located to the right and is shown as a loading control.

2.3.9 The effects of hydroxyurea on Rad1 in RTgill-W1 during a 6 day time course

Hydroxyurea (HU) is an antineoplastic drug that inhibits ribonucleotide reductase which causes a depletion in purine dNTP levels causing the cell-cycle to arrest in S-phase (Johnson and Walker, 1999; Koc *et al.,* 2004). In HEK293-T cells, Rad1 expression levels increase slightly with the addition of HU to cell lines, which was the motive for using HU in this study (Hirai *et al.,* 2004). RTgill-W1 cells were treated with 200mM HU and were harvested at days one, three, and six. As shown in Figure 2.15, an intense band at 18kDa appears in all of the control and HU samples. A band at 21kDa appears above the 18kDa band in days one, three and six of the control samples, but is only present in day one of the HU samples. A phosphorylated protein has a slower mobility than that of the unphosphorylated form and therefore it appears slightly above the unphosphorylated form in a western blot. Also, it is known that Rad1 becomes phosphorylated during a checkpoint response (Lupardus and Cimprich, 2006). The double band that is visualized in Figure 2.15 may possibly be the unphosphorylated (18kDa) and phosphorylated (21kDa) forms of Rad1. Since the 21kDa band disappears at day 3 of the HU dosed cells, it may be likely that in rainbow trout the 18kDa form of Rad1 is normally phosphorylated and becomes dephosphorylated when induced with a damaging agent in S-phase.

2.3.10 Alternative splicing of rtRad1

Real-Time PCR (RT-PCR) has been shown to be an effective method to determine the splice variants of a gene (Vandenbroucke *et al.,* 2001). Here, RT-PCR was used to determine whether alternative spliced forms of Rad1 exist in rainbow trout. Two different primer sets were used to amplify heart, brain and RTgill-W1 cDNA. Primer set A amplifies Rad1 from start to stop, while primer set B amplifies Rad1 from the 5'UTR to the 3'UTR (Figure 2.16A). It was important to amplify the UTR as well as the ORF to determine whether or not the untranslated regions of Rad1 were being spliced to form different variants. Amplification of the UTR did not reveal that spliced variants arise from spliced UTR (Data not shown) so the sequence of the ORF is presented only. However, amplification of the open reading frames revealed

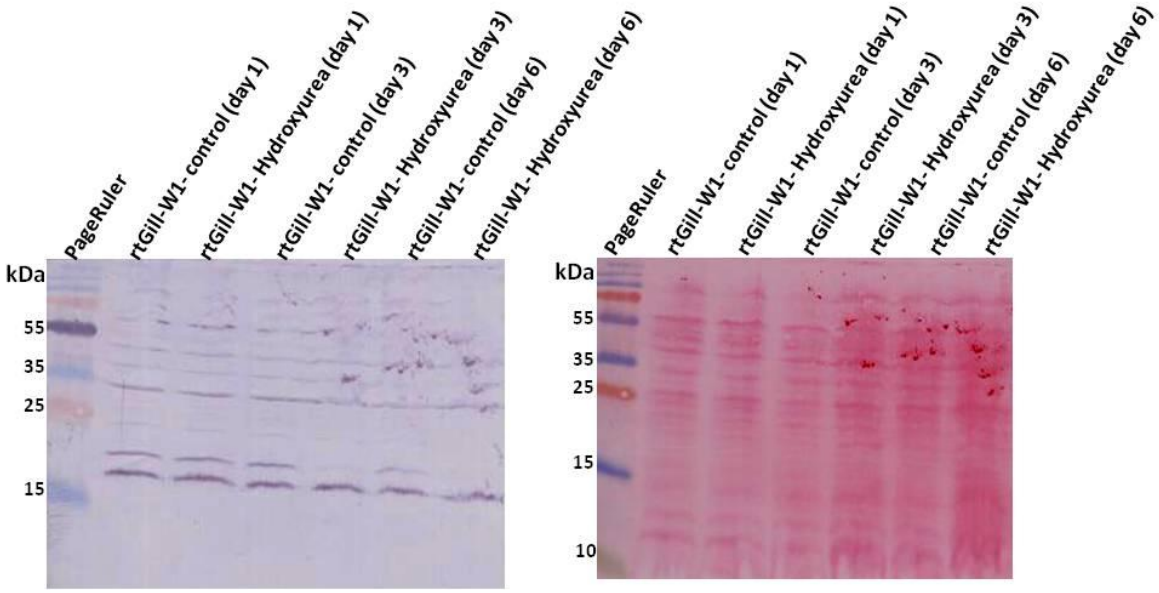

Figure 2.15: Detection of Rad1 in a 6-day time-course of RTgill-W1 treated with 0.2M hydroxyurea
Western blot showing a potential time dependent phosphorylation of Rad1 over 6 days of treatment with hydroxyurea (200mM). Rad1 is detected at 18kDa in all the samples. A protein at 21kDa is detected above the 18kDa band in the control samples (days 1, 3, 6) and the hydroxyurea samples (day 1). The 21kDa protein may be a phosphorylated form of Rad1 that becomes dephosphorylated during a checkpoint response. This could explain why the band is absent in days 3 and 6 of the hydroxyurea samples. Each lane contains 20µg of protein extracts and Ponceau S staining is shown as a loading control.

A

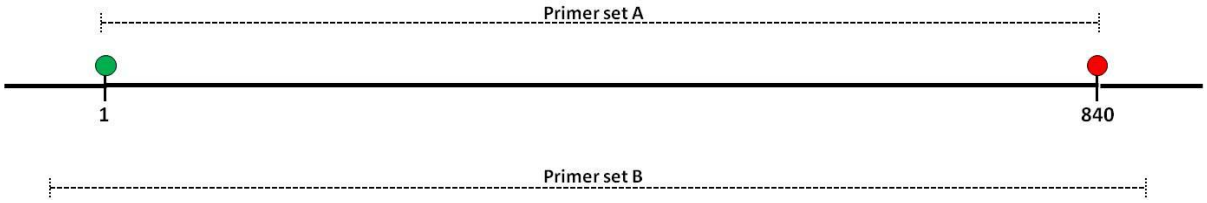

B

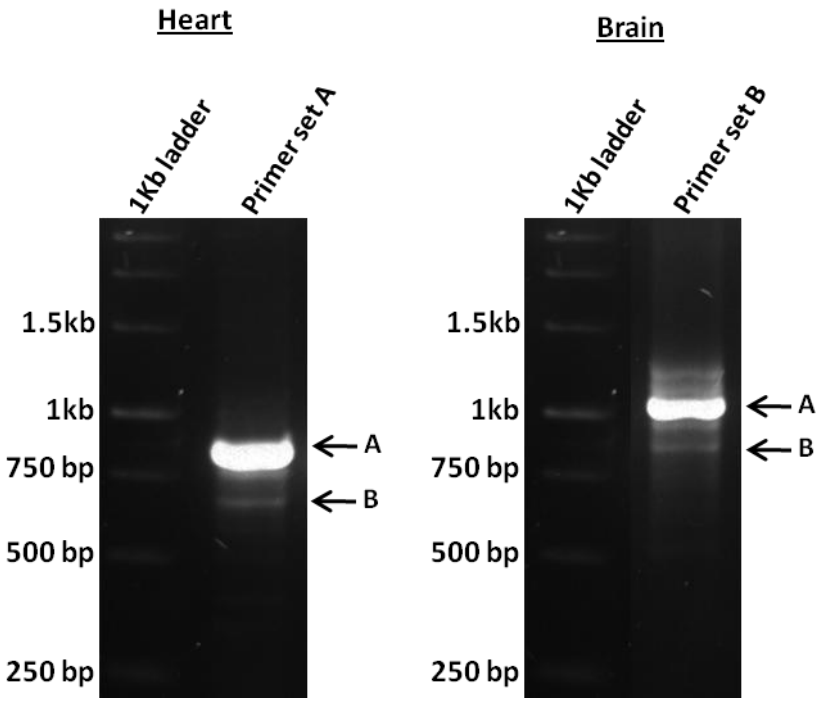

Figure 2.16: Detecting Rad1 splice variants in rainbow trout heart and brain using RT-PCR
(A) Schematic showing which Rad1 sections primer set A and primer set B amplify. Primer set A amplifies the ORF from start (green circle) and stop (red circle), while primer set B amplifies the ORF from the 5'UTR and 3'UTR. **(B)** Primer set A was used to amplify Rad1 in heart and primer set B was used to amplify Rad1 in brain. The band at 840bp, labeled "A", is the expected Rad1 ORF. The band at 664bp, labeled "B", is an isoform of Rad1 which is missing 176bp from the expected ORF.

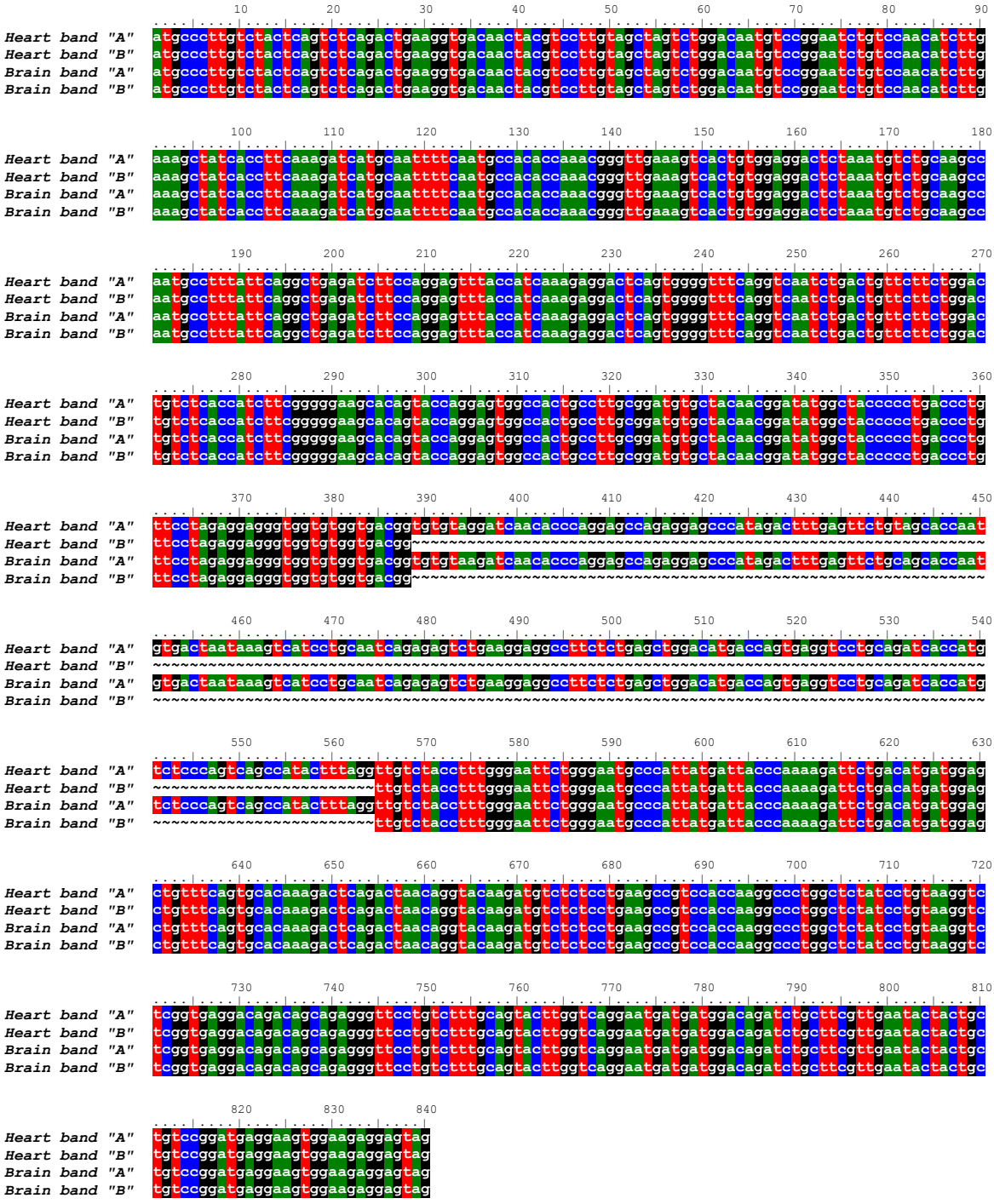

Figure 2.17: Nucleotide alignment of the Rad1 isoforms discovered in heart and brain
The ORF nucleotide sequences of band "A" and "B" that were isolated from heart and brain are aligned. Conserved regions are highlighted in colour (A=green, G=black, C=blue, T=red). The dash (~) in the alignment represents where the sequence is missing in band "B".

alternative spliced products in heart, brain and RTgill-W1. When amplifying the ORF in heart two products were revealed, one at 840bp (band A) and one at 664bp (band B: Figure 2.16). The nucleotide alignment (Figure 2.17) shows that the sequence of band A is that of the full rtRad1 ORF, while the sequence of band B is that of rtRad1 but with the removal of 176bp. The 176bp are removed from section 388bp to 564bp of the "canonical' Rad1 sequence. There are 279aa and 221aa in band "A" and band "B", respectively. The same spliced variant (band B) was isolated from brain cDNA(Figure 2.17). The amino-acid sequence from bands "A" and "B" from both heart and brain were aligned together (Figure 2.18). The protein product from band "B" does not produce a functional protein since there is a nonsense mutation at amino acid position 141.

The amplification of RTgill-W1 ORF revealed three products, one at 840bp (band A), one at 426bp (band C) and one at 405bp (band D: Figure 2.19). Band "C" and "D" are spliced variants of Rad1, where band "C" is missing 414bp from 267bp to 681bp and band "D" is missing 435bp from 102bp to 537bp (Figure 2.20.) An alignment of the amino-acid sequences from bands "A", "C", and "D" reveal that band "C" and "D" are splice variants of Rad1 that can form functional proteins. There are 279 amino acids in band "A", while there are 141aa and 134aa in band "C" and "D" respectively. The predicted molecular weight of band "C" and "D" are 15.7kDa and 15.1kDa which is approximately the molecular weight of the 18kDA band seen in many of the western blots detecting rtRad1. Figure 2.22 is a schematic illustrating the different splice forms of rtRad1 discovered and demonstrates that each of the variants are spliced at different locations.

2.4 Discussion of rtRad1

This is the first time the Rad1 gene has been cloned from rainbow trout. The open reading frame is 840bp with a predicted protein sequence of 279aa which is the same length as Rad1 in zebrafish. Rainbow trout Rad1 contains conserved exonuclease and leucine zipper domains which are also seen in humans, European eel and zebrafish (Nogueira *et al.,* 2009). The deduced amino-acid sequence has proliferating

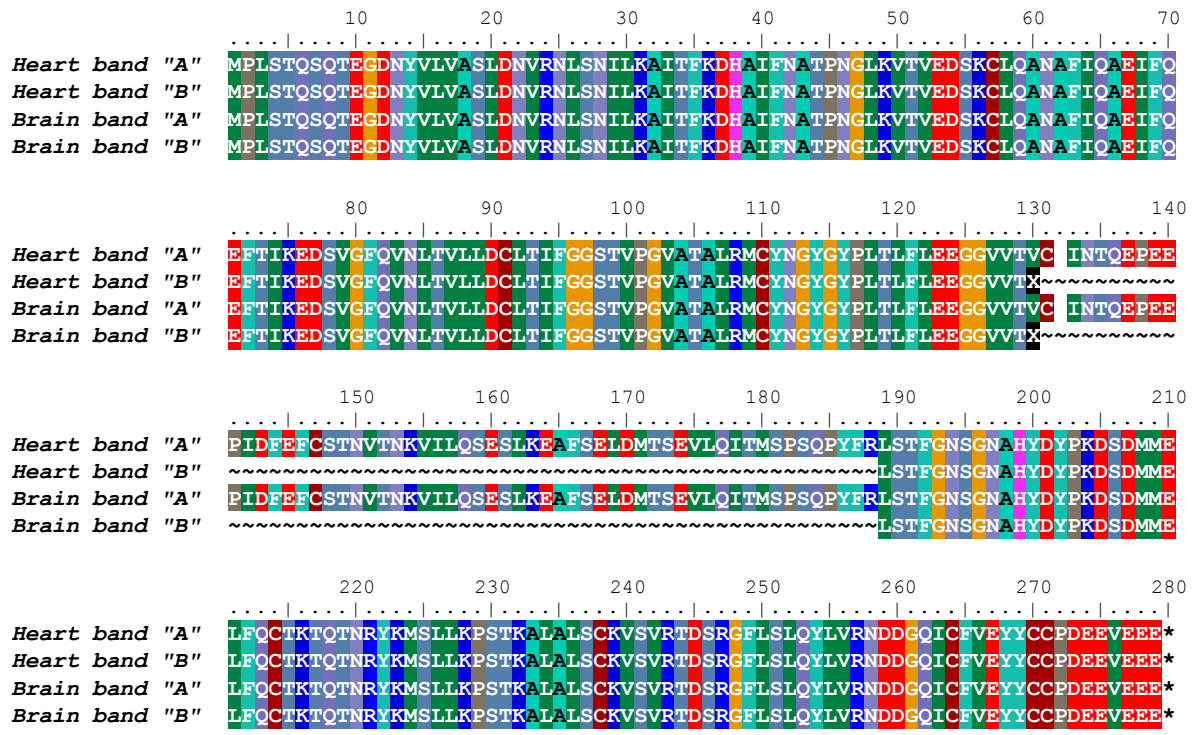

Figure 2.18: Protein alignment of the Rad1 isoforms isolated from heart and brain
The protein sequences of band "A" and "B" that were isolated from heart and brain are aligned. Conserved regions are highlighted. Band "B" does not make a functional protein and the letter "X" at amino acid #130 represents where the point mutation is located. The dash (~) in the alignment represents where the sequence is missing in band "B". The stop codon is indicated by a star (*). The amino-acid at position 132 is lysine (K).

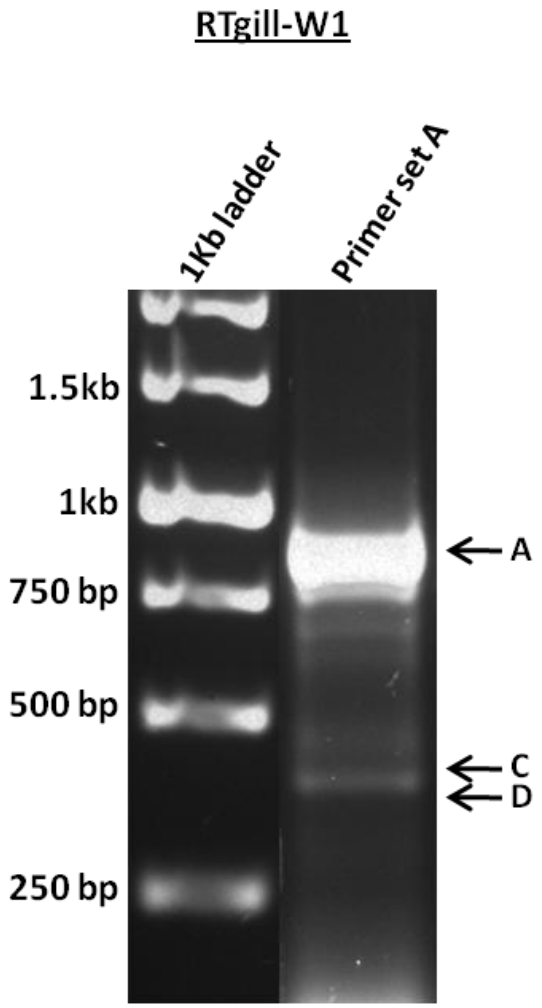

Figure 2.19: Detecting Rad1 spliced variants in RTgill-W1 cell-line using RT-PCR
Primer set A was used to amplify Rad1 in RTgill-W1. Please refer to Figure 2.17 for schematic on primer set A. The band at 840bp, labeled "A", is the expected Rad1 ORF. The band at 426bp (labeled "C") and the band at 405bp (labeled "D") are isoforms of Rad1 which are missing 414bp and 435bp, respectively, from the expected Rad1 ORF. There are other bands visible on this gel but they were at such low concentrations that they could not be excised from the gel.

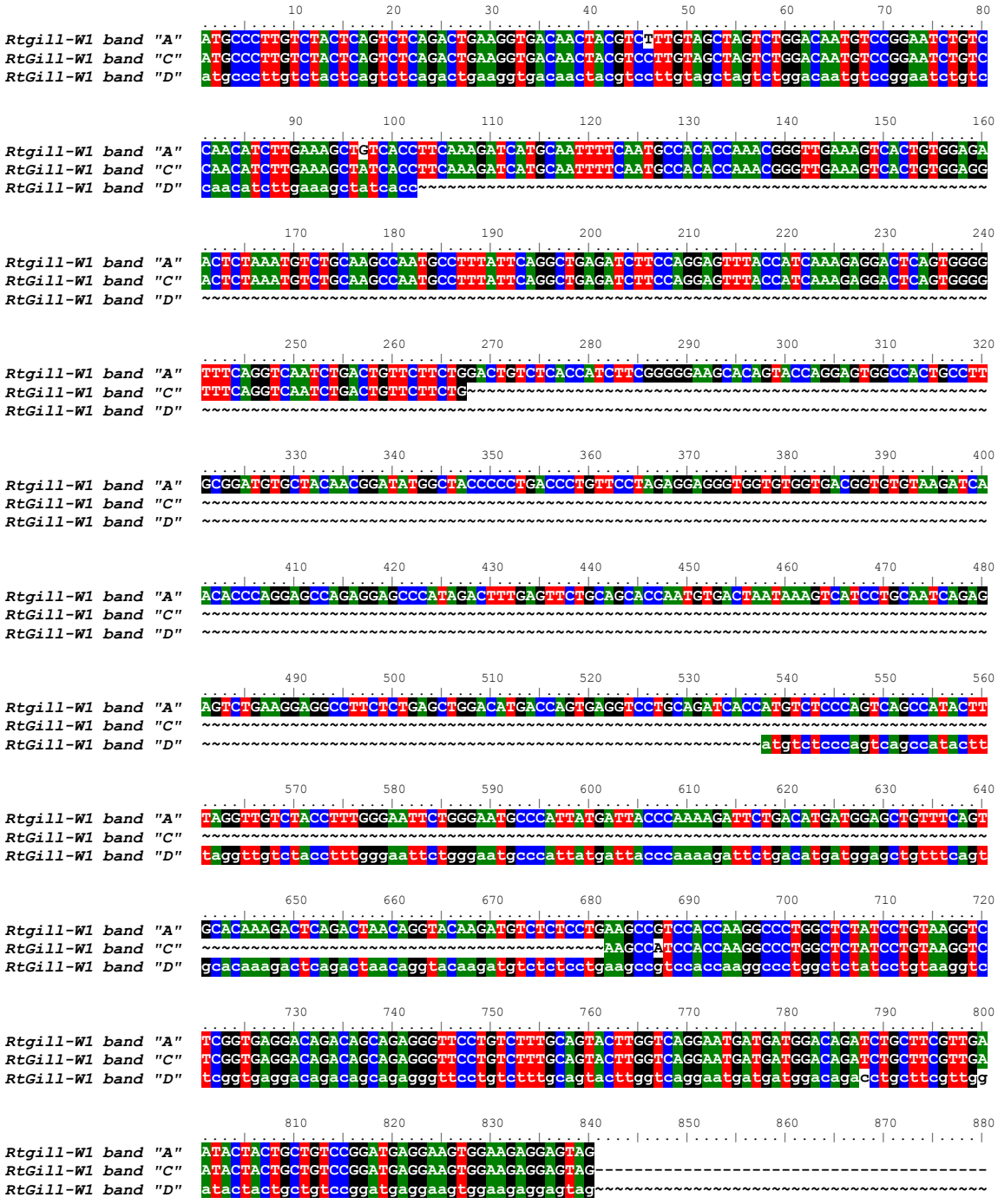

Figure 2.20: Nucleotide alignment of the Rad1 isoforms discovered RTgill-W1
The ORF nucleotide sequences of bands "A", "C", and "D" isolated from RTgill-W1 are aligned. Conserved regions are highlighted in colour (A=green, G=black, C=blue, T=red). The dash (~) in the alignment represents where the sequence is missing. White background around a nucleotide signifies that it is not conserved amongst the other two sequences. Band "D" is in lowercase letters to better display the spliced areas.

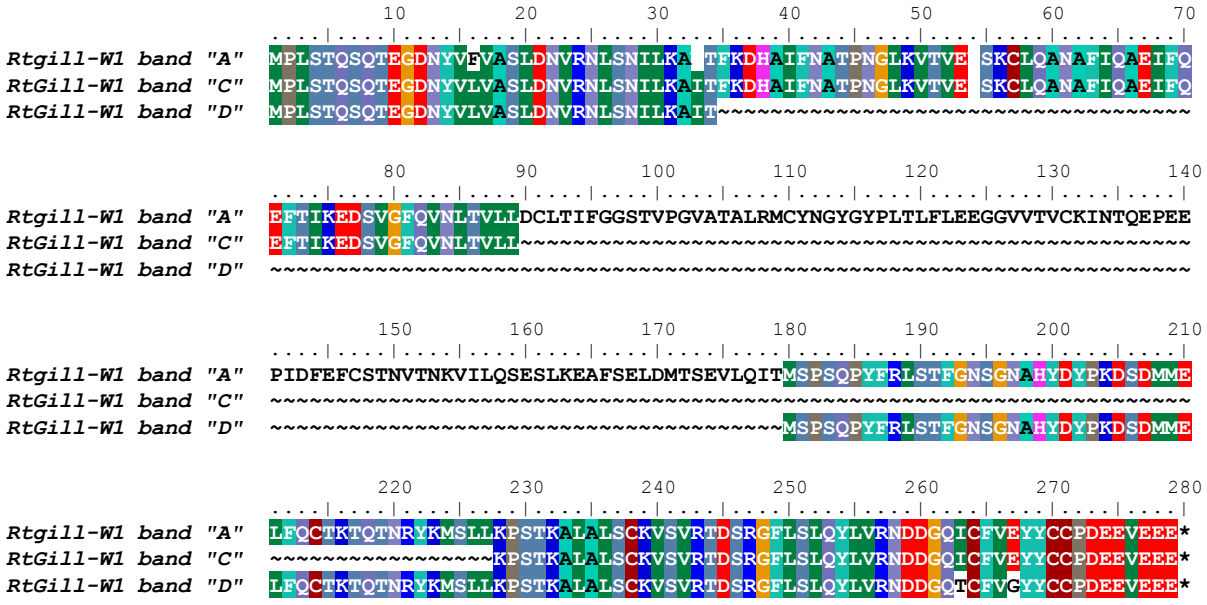

Figure 2.21: Protein alignment of the Rad1 isoforms isolated RTgill-W1
The protein sequences of band "A", "C" and "D" that were isolated from RTgill-W1 are aligned and conserved regions are highlighted. The dash (~) in the alignment represents where the sequences are missing. The stop codon is indicated by a star (*). The amino-acids at position 34 and 54 are valine (V) and Asparagine (N), respectively.

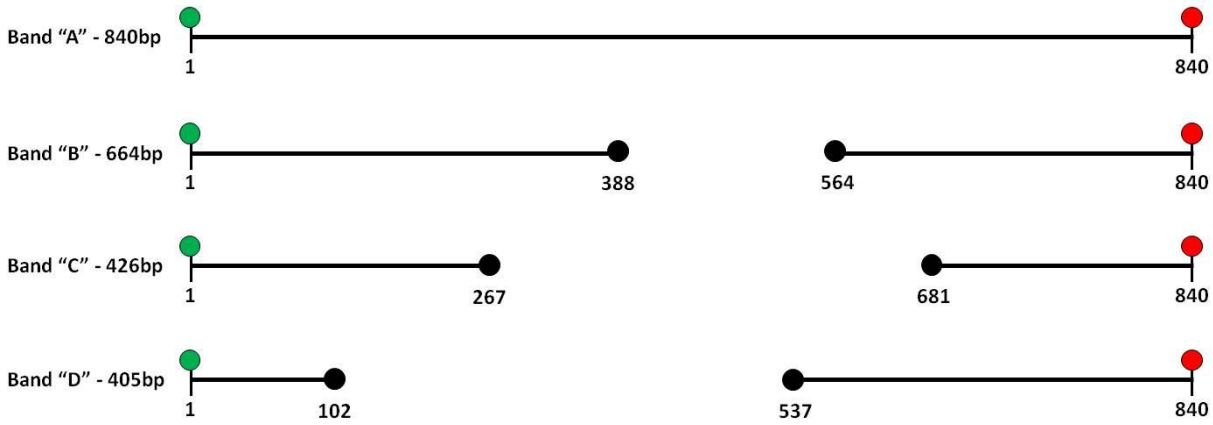

Figure 2.22: Schematic of the Rad1 isoforms isolated
The schematic shows the different splice variants of Rad1 discovered from start (green circle) to stop (red circle). The predicted splice junctions are labeled with a black circle and the nucleotide location is written. Band "A" is the expected Rad1 ORF sequence and is termed the "canonical" sequence. The nucleotide sequence of band "B" is 664bp and there are 176bp removed from sections 388bp to 564bp. The predicted amino-acid sequenced contains a nonsense mutation at position 388. Band "C" is missing 414bp from sections 267bp to 681bp and band "D" is missing 435bp from sections 102bp to 537bp. The location of the spliced area is based on the "canonical" Rad1 sequence.

cell nuclear antigen (PCNA) domains which show that Rad1 plays a role in DNA replications and repair. The rtRad1 protein sequence has a high identity with Rad1 sequences from higher eukaryotes: such as, 98% identical to *Salmo salar*, 93% identical to *Danio rerio*, 79% identical to *Xenopus laevis* and 78% identical to *Homo sapiens*. The high level of identity shows that Rad1 is an evolutionarily conserved checkpoint protein.

Characterization of Rad1 expression in rainbow trout spleen, gill, heart, brain, liver, head kidney, eggs, thymus and muscle tissues showed that the molecular weight of the detectable bands differs amongst the tissues. The expected size of rtRad1 is 31kDa but this size was never identified in any of the rainbow trout tissue samples where only strong bands at approximately 18kDa and 48kDa were visualized. Not being able to detect Rad1 at 31kDa is strange since this size is the predicted protein size from the Rad1 "canonical" sequence. However, the PageRuler™ is only an estimate of protein size and proteins can run at different sizes on an SDS-PAGE due to post-translational modifications such as glycosylation, acetylation, alkylation and phosphorylation (Walsh *et al.,* 2005). A molecular weight of approximately 48kDa has been seen for Rad1 previously in the literature when HEK 293T cells were transfected with a plasmid containing myc-hRad1 (Hirai *et al.,* 2004). The Rad1 recombinant protein was detected with anti-myc at around 48kDa which is 14kDa larger than the expected size of 34kDa – which includes the 1.5kDa myc-tag. It was mentioned that the slower migration of Rad1 could be due to modifications but the type of modification was not specified (Hirai *et al.,* 2004).

The detection of several different sized Rad1 proteins has been reported in *Mus musculus* (mouse: Freire *et al.,* 1998). A western blot containing protein lysates from mouse brain, uterus, kidney, spleen, muscle, liver, heart, lung, and HeLa cells was detected with anti-Rad1 and intense bands at 19kDa, 31kDa and 43kDa were visualized. Figure 2.23 compares the mouse western blot with the western blot from rainbow trout and shows that the bands at 19kDa and 43kDa seen in mouse are similar to the 18kDa and 48kDa bands seen in rainbow trout. The 31kDa Rad1 protein was only detected in uterus, spleen, heart,

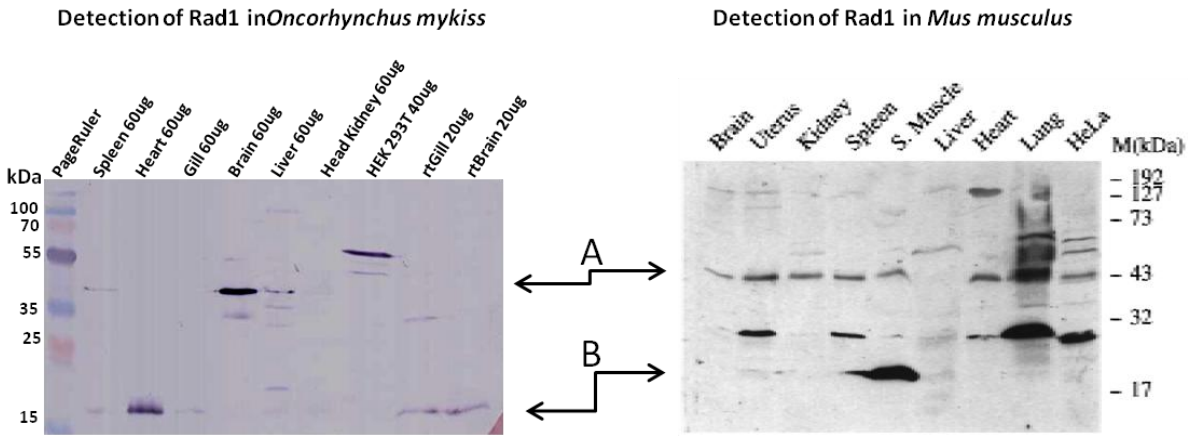

Figure 2.23: Comparison of Rad1 in rainbow trout and mouse
Western blots showing the detection of Rad1 in rainbow trout and mouse. (A) identifies the band at 48kDa and 43kDa in rainbow trout and mouse respectively. The 48kDa band is seen in gill, brain and liver in rainbow trout while it is seen in all the samples, except liver, in mouse. (B) shows the band at 18kDa seen in heart and RTgill-W1 and RTbrain-W1 in rainbow trout and the 19kDa band seen in s. muscle of mouse. The type of muscle is not specified. In mouse, the expected size of Rad1, 31kDa, is seen in some of the tissue but not all. The western blot from mouse is taken from (Freire *et al.*, 1998).

lung and HeLa cells. The 43kDa Rad1 protein was detected in mouse brain, uterus, kidney, spleen, muscle, heart, lung, and HeLa cells. The authors only focus on the 31kDa Rad1 protein and suggest that the other bands are background. However, by comparing the western blots from Figure 2.23, it is clear to see that the different sized Rad1 proteins are tissue specific and that they are more than just background. In mouse, the 19kDa protein was detected in high abundance in s. muscle but in low abundance in the testis (Freire *et al.,* 1998)), while in rainbow trout the 18kDa band was detected in high abundance in heart, RTgill-W1, RTbrain-W1 and in low abundance in spleen and gill. The type of muscle used from mouse was not specified and only an "s." was used to describe the type. It is possible that the "s." is an acronym for "smooth" or "skeletal" muscle. If mouse skeletal muscle was used than the 19kDa Rad1 protein detected correlates with the 18kDa protein detected in rainbow trout heart since skeletal muscle is present in the heart (Kilarski, 1967).

Furthermore, the molecular weight of Rad1 in rainbow trout brain is different than that seen in RTbrain-W1 cell-line (Figure 2.13). In brain, a strong band at 42kDa and a faint band at 55kDa are visible while in the cell-lines a strong band at 18kDa is visible with bands at 25kDa, 35kDa, 54kDa, 55kDa and 100kDa in the background. There is no evidence in the literature to explain why the *in vitro* results are different from those *in vivo*. However, since Rad1 has shown to play a role in telomere maintenance (Dahlen *et al.,* 1998; Nakamura *et al.,* 2002; Francia *et al.,* 2006; Jegou *et al.,* 2009) and the RTbrain-W1 cell-line is immortal with active telomerase (unpublished data), then there is a possibility that different Rad1 isoforms may be functioning in telomere maintenance. Future work that is needed on this topic will be explored in section 2.4.1.

Different isoforms of Rad1 mRNA were isolated from rainbow trout heart, brain and in the RTgill-W1 cell-line. A Rad1 isoform of 664bp was discovered in rainbow trout heart and brain. The 221aa protein, it could potential encode, is non-functional since there is a non-sense mutation at amino acid position 141. Two isoforms were isolated in RTgill-W1, one of 426bp which encodes for a 141aa protein and one of

405bp which encodes for a 134aa protein. Both proteins have a predicted molecular weight at around 16kDa which is very close to the 18kDa protein detected in RTgill-W1 western blots. The predicted start and end of the deletions found in each isoform are different which suggests that alternative splicing of rtRad1 may play a role in producing many different Rad1 proteins, similar to the human TCL6 gene (Sammeth *et al.,* 2008). Furthermore, the agarose gel containing the RT-PCR reaction amplifying the ORF from RTgill-W1 (Figure 2.19) shows many amplified products that could not be excised but could potentially be more splice variants. Alternative splicing of a rainbow trout gene that creates a functional protein has been seen before with the 14-3-3 family of regulatory proteins which are involved in many cell-cycle pathways such as apoptosis (Wanna *et al.,* 2010). The Teleost Alternative Splicing Database (http://www.animalgenome.org/catfish/tasd/index.html) is a website that allows users to search the archive for alternative splicing of genes in teleost (Lu *et al.,* 2010). Rad1 is currently not listed in the database and therefore could not be examined.

The 18kDa Rad1 protein appeared to increase in intensity with the increase of bleomycin on RTgill-W1 (Figure 2.13). The same 18kDa protein did not increase in the RTbrain-W1 samples that were dosed with bleomycin. However the levels could not be quantified since the bands on the western blots were touching each other. When the experiment was replicated this increase was not seen (Figure 2.14). When RTgill-W1 was treated with hydroxyurea for a 6-day time-course the 18kDa protein was detected in all the control samples and all the hydroxyurea samples. A higher molecular weight protein at 21kDa was detected in days 1, 3, 6 of the control samples but only day 1 of the hydroxyurea sample. Rad1 has been shown to be phosphorylated in response to hydroxyurea (Roos-Mattjus *et al.,* 2002) and in *Xenopus* this phosphorylation occurs at position T5 in an ATR-depended manner (Lupardus and Cimprich, 2006). Furthermore, the small isofroms isolated from RTgill-W1, band "C" and "D", both contain the T5 predicted phosphorylation site. Thus the 21kDa band could be a phosphorylated form of the 18kDa Rad1 protein. Since the 21kDa protein disappears after days 3 and 6 of the hydroxyurea samples it appears that

Rad1 may be dephosphorylated in response to a genotoxic agent. Furthermore, the double band that appears could simply be two different Rad1 polypeptides (i.e. band C and D are both detected). This is the first time reported that an isoform of Rad1 appears to be functional and is modified in the presence of a damaging agent. However, this experiment needs to be replicated and this topic will be explored in section 2.4.1.

2.4.1 Future Work

Rainbow trout Rad1 needs to be characterized more thoroughly before it can be used as a genotoxicity biomarker. The genomic sequence should be determined and the introns should be analyzed to determine the different potential splice sites. The intronic sequence can be used to make an effective probe to determine the gene copy number using a Southern blot. One of the main questions is whether or not the 18kDa protein is a product of a spliced variant or a different gene completely. By analyzing the genomic sequence and after completion of a Southern blot the identity of Rad1 will be more concrete. Furthermore, it may be possible that there are more Rad1 isoforms still to be discovered. Hybridization screening of a rainbow trout cDNA library using a Rad1 probe could help identify any other Rad1 isoforms. A northern blot should be performed to determine the transcript levels of Rad1 in RTgill-W1, RTbrain-W1 and each of the rainbow trout tissues. Probes for the northern blot can be developed based on different regions of the Rad1 splice variants to identify which tissue the isoforms are more abundant in.

The bleomycin and hydroxyurea dose studies on RTgill-W1 should be replicated twice more to better identify the role of the 18kDa Rad1 protein, and the other isoforms, as a genotoxicity biomarker. Furthermore, a dose study using bleomcyin and hydroxyurea on whole rainbow trout should be completed to view the role of Rad1 *in vivo*. The concentration of the damaging agent will need to be determined as there is no reference in the literature of a dose study using bleomycin or hydroxyurea on whole fish. It would be a good idea to analyze both the mRNA and protein levels of Rad1 in these dose studies. RT-

PCR can be used to amplify the Rad1 open reading frame from all the dosed samples to determine if there is a change in expression of the different isoforms. Western blots should be run side-by-side to determine if the protein levels correlated with the transcript levels and whether or not protein modification occurs. A comparison of the *in vitro* model to the *in vivo* biology is critical when developing a novel assay.

Once the Rad1 isoforms are discovered monoclonal antibodies could be made for each recombinant protein. Each isoform-specific monoclonal could be labelled and immunofluorescence could be used to localize each isoform in the control and dosed cells. This will give a visual perspective of the role of each isoform in the presence of a genotoxic stress. Furthermore, transcription factors involved in telomere maintenance, such as TBP-related factor 1 (TRF1), could be labelled to determine if any of the Rad1 isoforms localize with telomeres in immortal cell-lines (Nabetani *et al.*, 2004).

2.5 Conclusion on rtRad1

Rainbow trout Rad1 is alternatively spliced and expression of the resultant isoforms appear to be tissue and cell-line specific. It appears that the Rad1 isoform expression in brain tissue is different than that of the RTbrain-W1 cell-line which raises a question as to why Rad1 is different between the *in vivo* and *in vitro* model. One difference is that the RTbrain-W1 is an immortal cell-line that contains telomerase activity, while the brain cells should not be immortal. Since Rad1 from other species has been shown to play an important role in telomere length then it may be possible that different rtRad1 isoforms may function in telomere maintenance which can help explain the difference seen in brain tissue. Furthermore, it appears that the 18kDa Rad1 isoform may play a role in the intra-S checkpoint since bleomycin damage has caused the protein levels to increase. Rainbow trout Rad1 needs to be characterized further before being used as a genotoxicity biomarker but the potential of this protein is evident.

Chapter 3
Characterization of Hus1 in Rainbow Trout

3.1 Introduction to Hus1

Analysis of numeroust *Schizosaccharomyces pombe* mutants that were hydroxyurea sensitive (Hus) led to the discovery of Hus1, a mutant that bypassed the intra-S checkpoint and failed to arrest the cell-cycle when treated with hydroxyurea (Enoch *et al.,* 1992). Hus1 is an evolutionarily conserved checkpoint protein that has been identified in *Homo sapiens*, *Mus musculus*, *Caenorhabditis elegans* and *Drosophila melanogaster* (Dean *et al.,* 1998). The role of Hus1 in *S. pombe* appears to be different than that of higher eukaryotes (Meyerkord *et al.,* 2008). In *S. pombe*, four forms of Hus1 have been discovered, Hus1A to Hus1D, and evidence suggest Hus1B plays the most important during a checkpoint response(Caspari *et al.,* 2000). In humans, two Hus1 paralogs have been identified, hHus1A and hHus1B, and it appears that both may have different roles that are equally important in the cell-cycle (Hang *et al.,* 2002). For example, when hHus1B was overexpressed in HEK 293T cells the percentage of dead cells was 99.54%, while none died when hHus1A was overexpressed (Hang *et al.,* 2002). This suggest that hHus1B may be specifically involved in the apoptosis pathway while hHus1A appears to be involved in the DNA damage repair pathway (Meyerkord *et al.,* 2008; Sohn and Cho, 2009).

3.1.1 The role of Hus1

The role of Hus1 has been investigated more thoroughly in mice than in any other higher eukaryote and will be discussed below. Evidence suggests that Hus1 plays an important role in the intra-S checkpoint by helping to activate ATR/CHK1 in the single-stranded DNA repair pathway (Weiss *et al.,* 2000; Weiss *et al.,* 2002; Weiss *et al.,* 2003). This evidence is supported since mice fibroblasts that are deficient in Hus1 have impaired regulation of the intra-S checkpoint when exposed to camptothecin, a DNA damaging agent (Wang *et al.,* 2004). In *Xenopus*, the potential phosphorylation sites of xHus1 were

mapped to positions S59, S219, T223 (Lupardus and Cimprich, 2006). Please refer to section 2.1.2, to see the role Hus1 plays in the 9-1-1 complex (Paek and Weinert, 2010). Please refer to section 2.1 to review the chaperone role of hRad1 with hHus1.

3.1.2 Hus1 and telomeres

As explained in section 2.1.3, the 9-1-1 complex has been identified as a key player in telomere maintenance (Francia *et al.*, 2007). For example, in *S. pombe* the Hus1 protein has been shown to associate with telomeres (Nakamura *et al.*, 2002). Furthermore, Hus1-deficient mouse embryonic fibroblasts (MEF) cells were shown to have half the mean telomere length compared to wild-type and showed to have reduce telomerase activity (Francia *et al.*, 2006). The role of Hus1 in telomere maintenance also correlates with results seen in *C. elegans* where Hus1 deficiency produces shorter telomeres (Hofmann *et al.*, 2002).

3.2 Materials and methods

3.2.1 Cloning rtHus1 open reading frame into an expression vector

The rainbow trout Hus1 sequence was available on NCBI [NM_001160574.1] and was used to design gene-specific sense (Hus1-ORF.For 5'-GGATCCATGAAGTTCCGAGC- 3') and antisense (Hus1-ORF.Rev 5'- AAGCTTCTAGGCCACCGCTGGGATGAAGTATTGC-3') primer-adapters. The restriction sites *BamH* I and *Hin*dIII were included in the sense and antisense primers, respectively. The above primer set would amplify the Hus1 ORF while including two different restriction sites to allow for directional cloning into pRSET(A) expression vector (Invitrogen: Carlsbad, CA). PCR was performed using 2.5µl of 10X Incubation Mix Taq Polymerase without $MgCl_2$, 0.5µl of 10mM each dNTP mix, 1µl of 25mM $MgCl_2$, 1µl of each primer (10µM), 0.1µl Taq DNA Polymerase (5U/µl) (MP Biomedical: Solon, OH), 0.5µl of rainbow trout thymus cDNA library (725ng/µl) and 18.4µl H_2O. The thermocyler (Bio-Rad DNA Engine: Mississauga, ON) conditions were as follows 95°C 5min, 35 cycles (95°C

45sec, 54°C 45sec, 72°C 1.15min) and 72°C 15min. The amplicon was gel-purified, cloned and sequenced as stated in section 2.2.1. The nucleotide sequence was translated into a protein sequence using the "Translate Tool" from ExPASy (http://expasy.org/tools/dna.html). The protein sequences from human [NM_004507.2] and house mouse [NM_008316.4] Hus1A homologs were aligned with the rtHus1 protein sequence using ClustalW.

The clone containing rtHus1 ORF (pGEM T-easy:rtHus1) and the pRSET (A) expression vector (Invitrogen: Carlsbad, CA) were both digested with *BamH*I and *Hin*dIII restriction enzymes and run on an agarose gel. Bands corresponding to rtHus1ORF(*B*/*H*) and pRSET(A)(*B*/*H*) were gel purified using using the QIAquick Gel Extraction Kit (Qiagen: Mississauga, ON) then ligated together using T4 DNA ligase (Promega: Madison, WI) as stated in section 2.2.3 and sequenced at TCAG Sequencing center (Toronto, ON) to verify that the ORF was in frame with the N-terminal 6x His-tag . The expression vector construct [pRSET(A):rtHus1ORF(*B*/*H*)] was transformed into into the *E. coli* bacterial strain, BL21 (DE3) pLysS (Promega: Madison, WI). During a pilot study it was revealed that over-expression of rtHus1 was minimal, potentially due to codon bias. Therefore the [pRSET(A):rtHus1ORF(*B*/*H*)] construct was transformed into BL21-CodonPlus®(DE3)-*RIPL* strain (Stratagene: Aurora, ON) to relieve the codon bias.

3.2.2 Expression and purification of rtHus1 recombinant protein

Overnight cultures were grown in 4ml Luria-Bertani (LB) media containing 50µg/ml ampicillin, 35µg/ml chloroamphenical, 10µg/ml streptomycin at 37°C and 220rpm shaking. Six 4ml overnight cultures were used to inoculate 1L of LB. At an OD600 of 0.4-0.6 cultures were induced by the addition of isopropyl-beta-D-thiogalactopyranoside at 0.1mM. After 18h of induction, cells were harvested by centrifugation at 10,000×*g* for 25 min.

Lysis buffer 1 (1X PBS (pH 7.4), 5% Triton X-100, 0.5mg Lysozyme and 5X "complete" Protease Inhibitor cocktail-EDTA free (Roche: Mississauga, ON) was added to the cells and then sonicated

(Microson™ Ultra Sonic Cell Disrupter, Misonix: Farmingdale, NY) on level 5 for 1min at 4°C. The supernatant (i.e. soluable fraction) was collected and removed after centrifugation of cells in a Sorvall® RC5B Plus centrifuge (Buckinghamshire, England) at 10,000×*g* for 25 min. Solubilizing buffer (1mM B-mercaptoethanol, 0.5M NaCl, 20mM Tris-HCl, 1% Tween 20, 7.5mM Imidazole, 6M Urea, 0.5mg Lysozyme and 5X "complete" Protease Inhibitor cocktail-EDTA free: pH 8) was added to remaining pellet (i.e. insoluble fraction) and sonicated on level 5 for 1 min at 4°C and set to rotate overnight at 4°C. The cells were centrifuged at 10,000×*g* for 25 min and the supernatant (the "solubilised insoluble fraction") was collected and purified using Ni-NTA_Agarose (Qiagen: Mississauga, ON) as per the manufacturer's instructions. To summarize, 50ml of the "solubilised insoluable" fraction was added to 1.5ml of equilibrated Ni-NTA resin on an econo-column (Bio-Rad Laboratories: Mississauga, ON) 4°C. The column was then subjected to 8 washes (1mM B-mercaptoethanol , 0.5M NaCl, 20mM Tris-HCl, 35mM Imidazole, 6M urea: pH 8) of 10X the volume of the resin. The recombinant protein was eluted in five 1ml aliquots of elution buffer (1mM B-mercaptoethanol , 0.5M NaCl, 20mM Tris-HCl, 0.5M Imidazole, 6M urea: pH 8)

Each elution was separated on a 12% sodium dodecyle sulfate (SDS) gel and stained with Coomassie blue to determine purity and background proteins. High purity elutions were dialyzed for 3hrs in a 4M Urea-1XPBS solution (pH 7.4), followed by a 3hr dialysis in a 2M Urea-1XPBS solution (pH 7.4), and followed by 3hr dialysis in a 1M Urea-1XPBS solution (pH 7.4). An overnight dialysis in 1XPBS (pH 7.4) was performed at 4°C, followed by a 3hr dialysis in 1XPBS (pH 7.4) at 4°C. A Bradford (Bio-Rad: Mississauga, ON) assay was performed following dialysis to determine the protein concentration. The dialyzed protein was concentrated using VivaSpin 6 10,000 MWCO columns (Sartorius Stedim Biotech: Aubagne, France) to 1mg/ml and stored at -80°C. One microgram of the final batch of recombinant rtHus1 (1mg/ml) was run on a 12% SDS gel and analyzed through Coomassie staining and western blots. Western blots using the primary antibodies (1) Anti-polyhistidine (Sigma: St. Louis, MO), (2) Anti-

Xpress™ (Invitrogen: Carlsbad, CA), (3) Anti-Human-Hus1A (ProteinTech Group: Chicago, IL- Catalog No: 11223-1-AP), (4) no primary antibody were used to confirm that the recombinant protein made was indeed rtHus1. The total amount of recombinant rtHus1 protein made was 17mg.

3.2.3 Immunization of rabbits and monitoring antibody titre.

Two female New Zealand white rabbits (Charles River Canada: Wilmington, MA) were inoculated with recombinant rtHus1 exactly as was described in section 2.2.5. The same procedures were used for each boost and titre check as were described in section 2.2.6.

3.2.4 Determining anti-rtHus1 antibody specificity

Results from the final bleed ELISA determined that serum diluted to 1:1000 from rabbit 1D1 was sufficient for anti-rtHus1 to recognize rtHus1 protein. The protein samples used were those mentioned in section 2.2.7. Protein lysates from rainbow trout spleen, heart, gill, brain, liver, head kidney, sperm, thymus and RTgill-W1 were boiled with 5X sample buffer (60mM Tris-HCl, pH 6.8, 25% glycerol, 2% SDS, 14.4mM β-mercaptoethanol, 2% bromophenol blue) and 5µg of each sample was loaded, run in four replicates on 12% SDS-PAGE gel, and transferred to 0.2 µm nitrocellulose membrane Bio-Rad: Mississauga, ON. Please refer to the Appendix section for the western blot protocol. The western blot membrane (1) was probed with Anti-actin (1:200; Sigma: MO, USA), (2) was probed with pre-immune serum (1:1000), (3) was probed with anti-rtHus1 (1:1000), (4) was probed with anti-rtHus1 (1:1000) that had been pre-incubated with 1mg of rtHus1 protein. Following the washes, the blots were probed with Goat anti-rabbit IgG antibody conjugated to alkaline phosphatase (Sigma, St. Louis, MO) at 1:3000 and detected with alkaline phosphatase detection solution. The blot was visualized using a Hewlett Packard ScanJet 3300C (Mississauga, ON) scanner and Adobe® Photoshop® 7.0.

3.2.5 Hus1 mRNA distribution in rainbow trout tissues

One microgram of spleen, heart, gill, brain, liver, head kidney, and RTgill-W1 cell-line RNA was transcribed into cDNA using *RevertAid™ H Minus First Strand* cDNA *Synthesis* Kit (Fermentus: On, Canada) according to the manufacturer's instructions. RT-PCR was performed using 2.5µl of 10X Incubation Mix Taq Polymerase without $MgCl_2$, 1µl of 10mM each dNTP mix, 1.5µl of 25mM $MgCl_2$, 1.5µl of each primer (10µM), 0.1µl Taq DNA Polymerase (5U/µl) (MP Biomedical: Solon, OH), 1µl of cDNA template and 15.9µl of H_2O. The sense (Hus1For2 5'-CGTCAGTCGTGTTGTCACCCATG-3') and antisense (Hus1Rev2 5'-GGCCACCGCTGGGATGAAG -3') primers were designed to amplify a 503bp fragment. The thermocyler (Bio-Rad DNA Engine: Mississauga, ON) conditions were as follows 95°C 5min, 30 cycles (95°C 40sec, 58°C 1min, 72°C 1.15min) and 72°C 15min. Equal amounts of each product (1 µl) were run on a 1% agarose gel containing 1X GelRed™ (Hayward, CA) visualized with a UV transilluminator and Alpha Imager HP program (Alpha Innotech Flourochem 8000 Chemiluminescence and Visable Imaging system: Santa Clara, CA).

3.3 Results

3.3.1 Cloning of rtHus1 open reading frame into an expression vector

PCR was performed to amplify the 852bp ORF of rtHus1 (Figure 3.1). A protein alignment with the rtHus1 ORF, *H. sapiens* and *M. musculus* Hus1 orthologs revealed highly conserved regions (Figure 3.2). The ORF was cloned into pGEM T-easy vector and then digested out using the restriction sites incorporated into the primers (*BamH*I and *Hin*dIII). The digested ORF and pRSET(A) were both gel purified and ligated together; using methods previously described for rtRad1 (Figure 2.6). The new construct was sequenced to confirm that proper ligation occurred and it was determined that the ORF was in frame with the 6XHIS and XPRESS™ epitope tag (Figure 3.2). The construct [pRSET(A):rtHus1ORF(*B*/*H*)] was transformed into BL21-CodonPlus®(DE3)-*RIPL* strain (Stratagene: Aurora, ON) to begin over expression of rtHus1 recombinant protein.

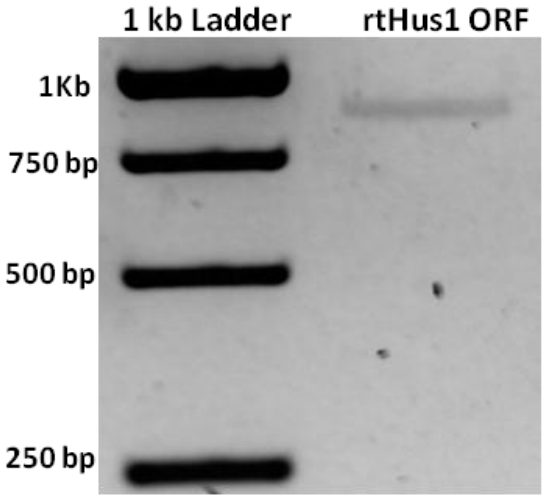

Figure 3.1: Amplification of rtHus1 open reading frame
The 852bp open reading frame (ORF) of rtHus1 was amplified using primer-adapters. The lanes of the 1% agarose gel are labeled.

A

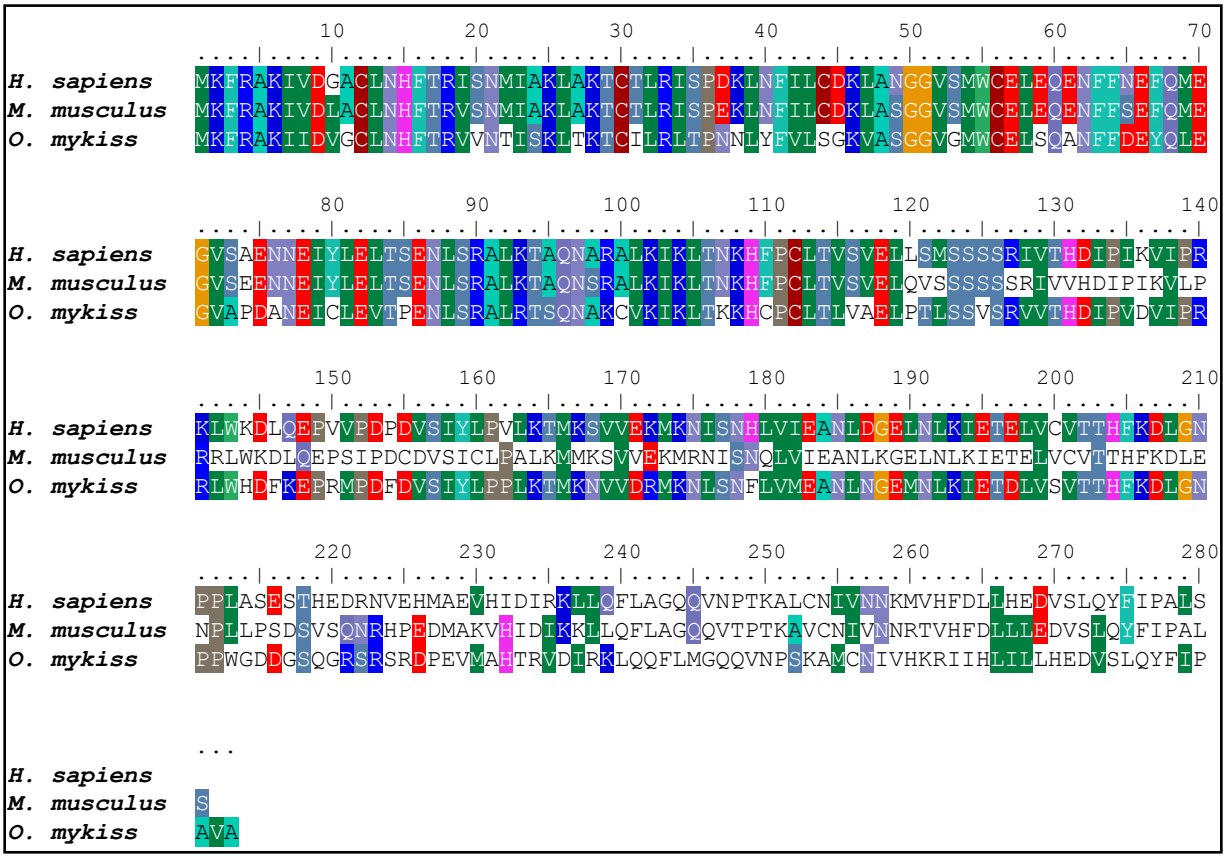

B

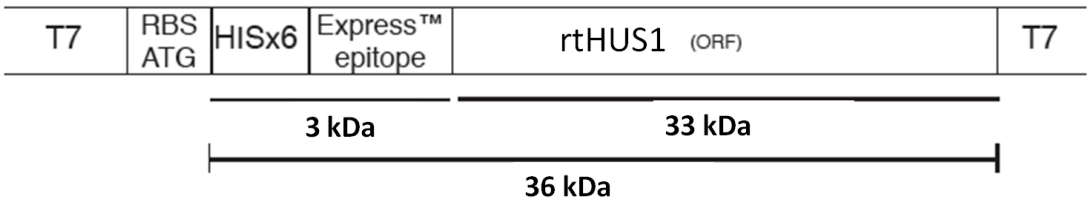

Figure 3.2: Hus1 protein alignment and diagram of the rtHus1 expression vector construct
(A) The protein sequences of rtHus1 and Hus1 homologs are aligned and the conserved regions are highlighted. The species names are listed to the left. **(B)** Diagram of the ligation construct created [pRSET(A):rtHus1ORF(*B*/*H*)]. Expected protein sizes of the N-terminal tags, rtHus1 ORF and the expected size of the rtHus1 recombinant protein are labeled.

3.3.2 Expression and purification of rtHus1 recombinant protein

The theoretical molecular weight of rtHus1 is 33kDa but due to the addition of the 6XHIS and Xpress™ epitope (3kDa) the recombinant protein ran at 36kDa (Figure 3.2B). Elutions which contained a thick band at 36kDa and with little background were collected and stored at -80°C (Figure 3.3). In the end, 18mg/ml of recombinant rtHus1 protein in 1XPBS (pH 7.4) was collected. A Coomassie stained gel containing 1µg/ml of the final stock of recombinant rtHus1 revealed the presence of a pure sample as there was no background bands present (Figure 3.4A). Four western blots containing 1µg/ml of the final stock of recombinant rtHus1 were probed with (1) anti-polyhistidine(Figure 3.4B), (2) anti-Xpress™ (Figure 3.4C) , (3) anti-Human-Hus1A (Figure 3.4D) and (4) no primary antibody (Figure 3.4E) confirm that the recombinant protein made was indeed rtHus1 and it was highly pure (Figure 3.4). The western blots from anti-polyhistidine, anti-Xpress™ identified a thick intense band at 36kDa which is the expected size of the recombinant rtHus1 protein. The anti-hHus1A western blot revealed two bands, one at 29kDa and one at 45kDa, which may represent cross reactivity with non-specific proteins. None the less, there was a strong 36kDa band visible in the coomassie stained gel and in the anti-polyhistidine and anti-Xpress western blots.

3.3.3 Analysis of anti-rtHus1 antibody titre

The highly pure rtHus1 recombinant protein was used to inoculate two rabbits to develop anti-rtHus1 antibodies. The titre was monitored prior to each boost and it was revealed that anti-rtHus1 was being produced at a high titre for each rabbit (Figure 3.5). For each rabbit, there was an increase in titre strength from boost one to boost three. However, the final bleed had a titre that was lower than that of the previous boost. Both rabbits produced very strong antibodies that can be used at 1:1000 dilution for western blots. Serum for rabbit #1 was used for all westerns as it had a little less background than rabbit #2 (data not shown).

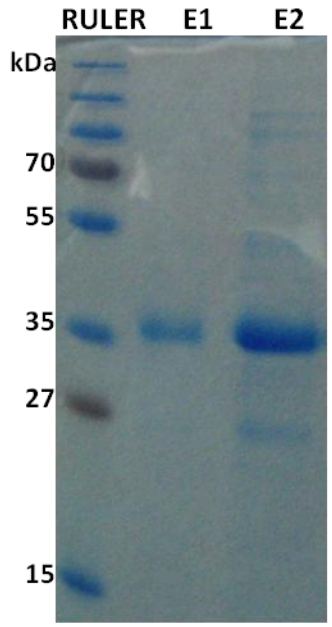

Figure 3.3: Coomassie staining of rtHus1 recombinant protein elution fractions
Ten micrograms of each elution was run on a 12% SDS-PAGE and stained with Coomassie Brilliant Blue G-250. Elution fractions 1-2 are labeled as E1 and E2, respectively. The expected size of the rtHus1 recombinant protein (36kDa) is seen in both E1 and E2.

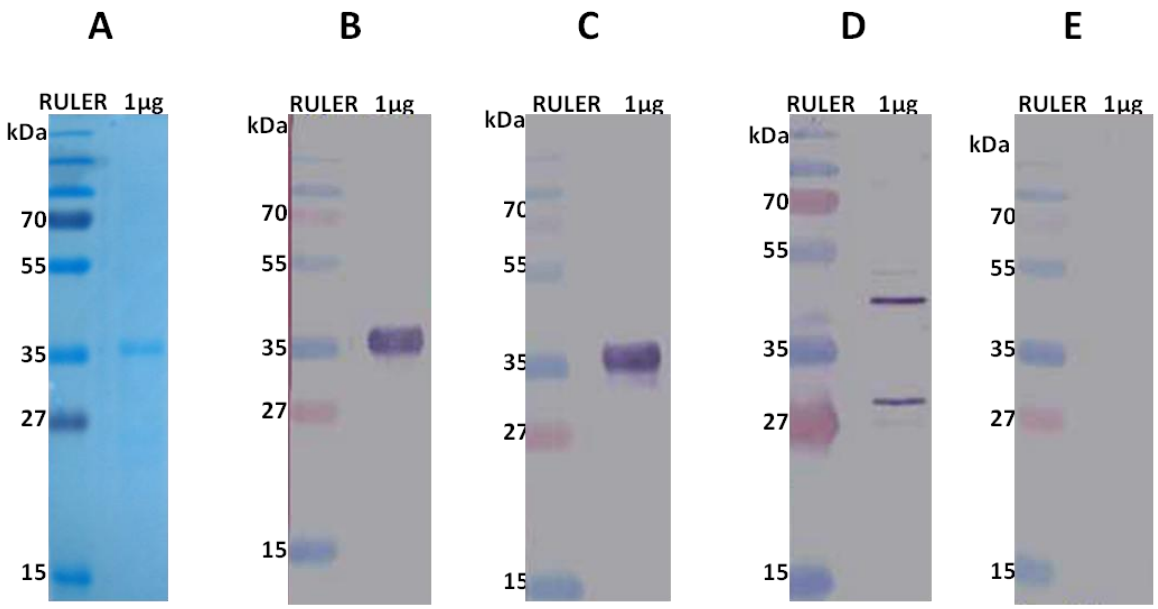

Figure 3.4: Analysis of the rtHus1 recombinant protein
One microgram of the final batch of recombinant rtHus1 was run on a 12% SDS-PAGE and analyzed through Coomassie staining (A) and western blot (B-E). **(A)** Comassie staining revealed a clear band at 36kDa with no background proteins visible. **(B)** A western blot probed with Anti-polyhistidine was used to detect the 6XHIS-TAG on the recombinant protein (36kDa). **(C)** A western blot showing the detection of the Xpress™ epitope tag on the recombinant protein (36kDa) using the primary antibody Anti-Xpress™. **(D)** A western blot probed with Anti-Human-Hus1A was used to detect the rtHus1 recombinant protein. A 36kDa band was not detected but rather proteins at 29kDa and one at 45kDa were detected. **(E)** Western blot showing that with no primary antibody added there were no proteins detected.

A

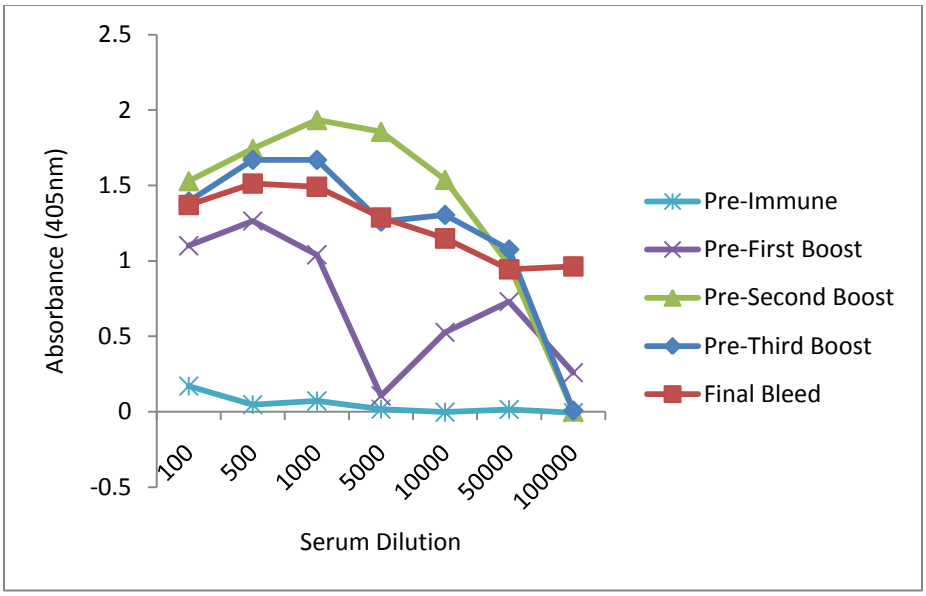

B

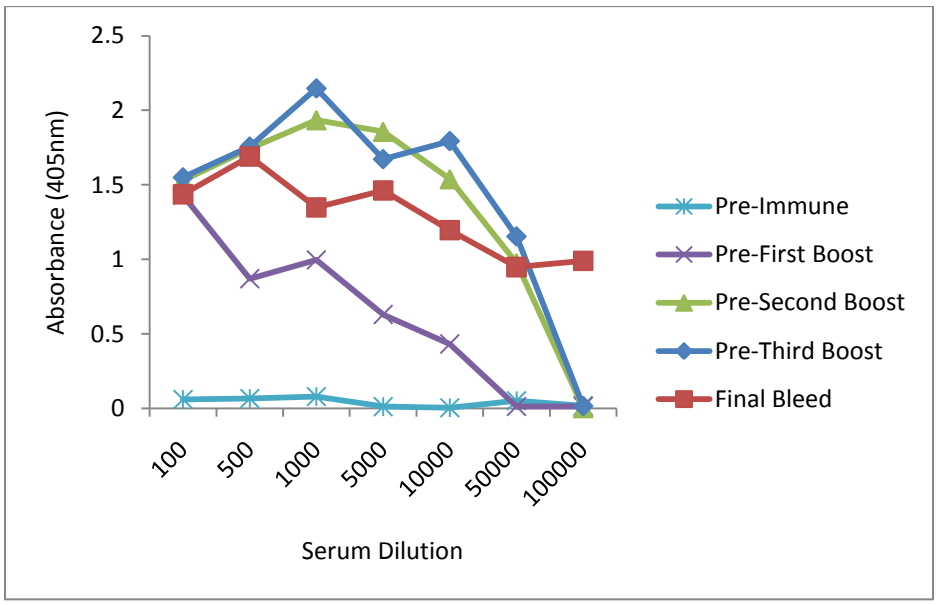

Figure 3.5: ELISA of anti-rtHus1 antiserum samples from rabbits #1 and #2
Serum was taken prior to each boost, as well as the final bleed, to examine the antibody's titre. **(A)** The dilution series of rabbit#1 shows that each boost had a high titre against the recombinant rtHus1 protein. **(B)** Serum from rabbit #2 had similar results to rabbit#1. For both rabbits, the final bleed had a titre that was less than that of the previous boost.

3.3.4 Determining anti-rtHus1 specificity

Anti-rtHus1 antiserum from rabbit #1 recognizes protein at different sizes than the predicted size of rtHus1. To confirm that these bands are rtHus1 and to confirm the specificity of the polyclonal antibodies four western blots were completed. Blot one had untreated final bleed anti-rtHus1 antiserum, blot two used anti-rtHus1 antiserum that was pre-incubated with 1mg recombinant rtHus1, blot three used antiserum prior to inoculation, and blot four used anti-actin as a control. Figure 3.6 shows that when anti-rtHus1 antiserum is blocked with the recombinant protein, that bands around 36kDa and 100kDa that were there prior to being blocked are no longer present. This is due to the excess recombinant protein blocking the anti-rtHus1 antibodies. This helps confirm that the bands that appear on the western blots probed with anti-rtHus1 are highly likely to be rtHus1. Furthermore, the blot with the pre-immune antiserum shows that there was only a small amount of background. Ponceau S staining is shown as a loading control.

The predicted size of Hus1 (33kDa) was not seen in any of the tissues nor cell-lines examined. In spleen, gill, liver, head kidney, sperm and RTgill-W1 no intense bands were visualized but only background bands. In heart and thymus an intense band at 100kDa appears whereas in brain a strong band at 36kDa was visible. The band at 36kDa is close to that of the expected size and could indeed be Hus1. The 100kDa band could be Hus1 trimers or may potentially be Hus1 in the 9-1-1 complex that has remained associated even though denaturing of proteins has occurred. Furthermore, the Ponceau S staining reveals that only a small amount of protein was loaded. The results need to be replicated to accurately depict the tissue distribution of Hus1 in rainbow trout.

3.3.5 Hus1 mRNA distribution in rainbow trout tissues

RT-PCR was used to determine the rtHus1 mRNA levels, using high-quality RNA (Figure 2.12A) from spleen, heart, gill, brain, liver, head kidney, RTgill-W1. The primers used created an amplicon of 503bp that was seen in each of the aforementioned tissues (Figure 3.7). Furthermore, since there are Hus1

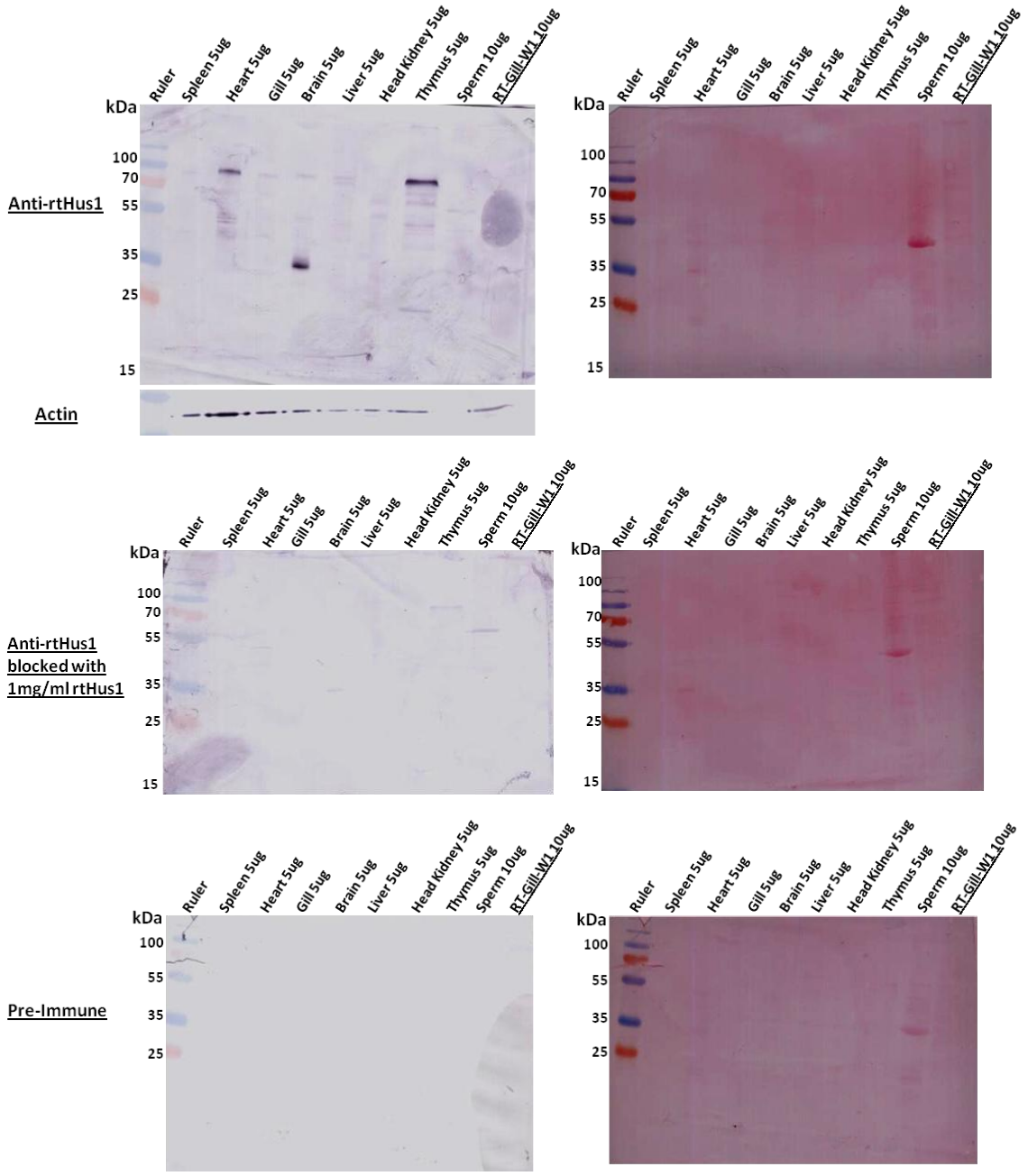

Figure 3.6: Analyzing the specificity of the anti-rtHus1 antibody
Western blots were used to verify the specificity of anti-rtHus1 antibody. Rainbow trout Hus1 protein was detected with the anti-rtHus1 antibody (1:1000) and anti-actin (1:500) was used as a control. Detection of Hus1 protein was absent when the anti-rtHus1 antiserum was pre-incubated (blocked) with 1mg of the recombinant rtHus1 protein. Pre-immune antiserum detected only a few background bands. Ponceau S staining is shown to the right of the western blot and is shown as a loading control.

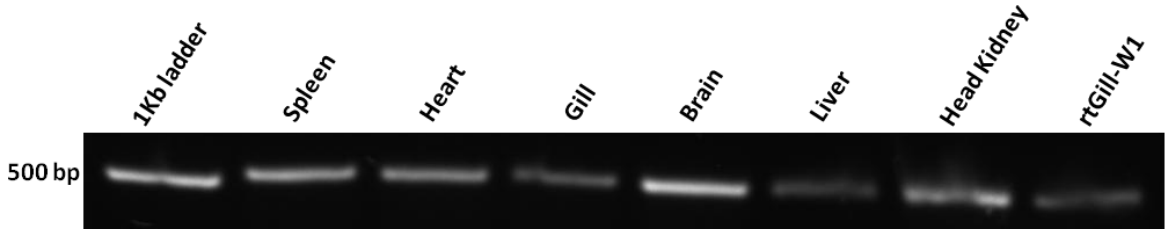

Figure 3.7: Expression of Hus1 mRNA transcripts in various rainbow trout tissues
The products of the RT-PCR were run on a 1% agarose gel and the lanes corresponding to the template cDNA used are labeled. Hus1 was detected in every sample.

isoforms in humans, it is likely that isoforms of Hus1 are present in rainbow trout. Therefore, calculating the expression levels in each tissue may not be accurate since the isoform being amplified cannot be determined. However, the information is useful as now it is known that some form of Hus1 mRNA is expressed in each of the aforementioned tissues.

3.4 Discussion on rtHus1

The open reading frame of rtHus1 was cloned, expressed as a recombinant protein and used to make anti-rtHus1 polyclonal antibodies. The anti-rtHus1 antiserum works effectively at a 1:1000 dilution on western blots and shows little background. Different sizes of rtHus1 protein were detected in heart, brain and thymus suggesting that alternative forms of Hus1 may exist in rainbow trout. A 100kDa protein was detected in heart and thymus while a 35kDa protein was detected in the brain. The 35kDa protein is close to the expected rtHus1 size of 33kDa while the 100kDa protein could be trimers. RT-PCR was used to amplify a portion of rtHus1 in spleen, heart, gill, brain, liver, head kidney and RTgill-W1 suggesting that a form of Hus1 is expressed in each of these tissues. Paralogs of Hus1 have been discovered in other species and these paralogs play an important role in the cell-cycle (Hang *et al.,* 2002). Four different human Hus1 transcripts were detected in a northern blot using RNA from the following samples: spleen, thymus, prostate, testis, uterus, small intestine, colon and leukocytes (Hang *et al.,* 2002). Five different mouse Hus1 transcripts were detected in a northern blot using RNA from various sections of mouse embryos and mouse tissue, including spleen (Weiss *et al.,* 1999). The detection of Hus1 in rainbow trout spleen correlates with the results from the human and mouse northern blots. Hus1 protein has not been characterized in mammalian tissues and this is the first time that Hus1 has been characterized in teleosts.

3.4.1 Future work

RT-PCR should be used to determine if any Hus1 splice variants exist, as well, a northern blot should be completed to determine the RNA transcript level. Since different sized hHus1 and mHus1 transcripts have

been observed (Weiss *et al.*, 1999; Hang *et al.*, 2002) it is expected that different variants will exist in rainbow trout. Furthermore, a Southern blot needs to be completed to determine the genome copy number of Hus1. The expression levels of rtHus1 and any protein modifications should be monitored during a genotoxic study to determine the usefulness of Hus1 as a genotoxicity biomarker. Whole rainbow trout and cell-lines, such as RTgill-W1 and RTbrain-W1, should be treated with hydroxyurea and the protein levels of rtHus1 should be examined on a western blot. Hus1 is sensitive to hydroxyurea and in *Xenopus*, Hus1 has been shown to become phosphorylated in the presence of hydroxyurea in an ATR-dependent manner (Lupardus and Cimprich, 2006). It is important to characterize the gene thoroughly so that it can better be used as a genotoxicity biomarker.

3.5 Conclusion on rtHus1

The use of Hus1 as a genotoxicity biomarker can be explored now that an anti-rtHus1 antibody has been developed. The characterization of Hus1 and any alternative spliced forms needs to be explored thoroughly to better understand the function of Hus1 in rainbow trout. Overall, Hus1 is a useful addition to the list of antibodies made from checkpoint proteins in rainbow trout and the involvement of Hus1 with DNA repair, the 9-1-1 complex and telomere maintenance shows that this protein plays a very important role in the cell-cycle.

Chapter 4
General Conclusions

4.1 Future directions

The 9-1-1 complex has been characterized in other organisms and has shown to play an important role in the cell-cycle checkpoints and in telomere maintenance (Roos-Mattjus *et al.,* 2002; Parrilla-Castellar *et al.,* 2004; Sorensen *et al.,* 2004). It would be interesting to determine whether Rad9, Rad1 and Hus1 form the 9-1-1 complex in rainbow trout and whether the formation of the 9-1-1 complex is tissue specific. Furthermore, it would be fascinating to see if rtRad1 isforms or rtHus1 are able to interact with each other. Paralogs of Rad1 have not been characterized in the literature but a paralog of hHus1, hHus1B, is unable to associate with Rad9 and Rad1 and is unable to form the 9-1-1 complex (Hang *et al.,* 2002). Since the cDNA sequence and polyclonal antibodies of rtRad1 and rtHus1 are available then characterizing the 9-1-1 complex in rainbow trout can be very easy. The rtRad1 and rtHus1 antibodies can be used to immunoprecipitate the 9-1-1 complex which can then be used to determine the crystal structure of the complex (Volkmer and Karnitz, 1999). Furthermore, the open reading frame of rtRad9 has been cloned into pGEM T-easy vector (Promega: Madison, WI) and subcloned into XL1-Blue MRF' (data not shown). Since all three genes of the 9-1-1 complex (Rad9, Rad1 and Hus1) have been cloned in rainbow trout then they can be combined in tri-cistronic cloning and can be overexpressed. The recombinant 9-1-1 complex can be purified and used to make anit-rt911complex antiserum. The antiserum could be used for genotoxic testing and could be added to the panel of checkpoint proteins used as genotoxicity biomarker.

From an evolutionary standpoint it would be very beneficial to create a phylogenetic tree for Rad1 and Hus1 using the rainbow trout sequences. It would be interesting to see how conserved these genes are with other teleost and mammals. Furthermore, a phylogenetic tree should be made of the different Rad1 isoforms found in rainbow trout, humans, mouse and any other species (Dean *et al.,* 1998). This will help

determine the evolution of each isoform and why it may have been kept or eliminated from species (Yeang, 2008).

4.2 General conclusions

The development of anti-rtRad1 and anti-rtHus1 polyclonal antibodies adds to the collection of antibodies made from rainbow trout checkpoint proteins thus far, such as CHK2 and p53. Once Rad1 and Hus1 are further characterized then they can be thoroughly assessed as genotoxicity biomarkers.

References

Adams S. M., Bevelhimer M. S., Greeley M. S., Levine D. A. and Teh S. J. (1999). Ecological risk assessment in a large river-reservoir: 6. Bioindicators of fish population health. 4**(18):** 628-640.

Ashwell S. Zabludoff S. (2008). DNA damage detection and repair pathways--recent advances with inhibitors of checkpoint kinases in cancer therapy. *Clin.Cancer Res.* 13**(14):** 4032-4037.

Bluyssen H. A., van Os R. I., Naus N. C., Jaspers I., Hoeijmakers J. H. and de Klein A. (1998). A human and mouse homolog of the Schizosaccharomyces pombe rad1+ cell cycle checkpoint control gene. *Genomics* 2**(54):** 331-337.

Borlado L. R. Mendez J. (2008). CDC6: from DNA replication to cell cycle checkpoints and oncogenesis. *Carcinogenesis* 2**(29):** 237-243.

Broderick R. Nasheuer H. P. (2009). Regulation of Cdc45 in the cell cycle and after DNA damage. *Biochem.Soc.Trans.* Pt 4**(37):** 926-930.

Bryan T. M. Reddel R. R. (1997). Telomere dynamics and telomerase activity in in vitro immortalised human cells. *Eur.J.Cancer* 5**(33):** 767-773.

Bryan T. M., Englezou A., Gupta J., Bacchetti S. and Reddel R. R. (1995). Telomere elongation in immortal human cells without detectable telomerase activity. *EMBO J.* 17**(14):** 4240-4248.

Bucher N. Britten C. D. (2008). G2 checkpoint abrogation and checkpoint kinase-1 targeting in the treatment of cancer. *Br.J.Cancer* 3**(98):** 523-528.

Carr A. M. Hoekstra M. F. (1995). The cellular responses to DNA damage. *Trends Cell Biol.* 1**(5):** 32-40.

Carvan M. J.,3rd, Gallagher E. P., Goksoyr A., Hahn M. E. and Larsson D. G. (2007). Fish models in toxicology. *Zebrafish* 1**(4):** 9-20.

Caspari T., Dahlen M., Kanter-Smoler G., Lindsay H. D., Hofmann K., Papadimitriou K., Sunnerhagen P. and Carr A. M. (2000). Characterization of Schizosaccharomyces pombe Hus1: a PCNA-related protein that associates with Rad1 and Rad9. *Mol.Cell.Biol.* 4**(20):** 1254-1262.

Cerquaglia C., Diaco M., Nucera G., La Regina M., Montalto M. and Manna R. (2005). Pharmacological and clinical basis of treatment of Familial Mediterranean Fever (FMF) with colchicine or analogues: an update. *Curr.Drug Targets Inflamm.Allergy* 1**(4):** 117-124.

Clarke P. R. Allan L. A. (2009). Cell-cycle control in the face of damage--a matter of life or death. *Trends Cell Biol.* 3**(19):** 89-98.

Claussen C. A. Long E. C. (1999). Nucleic Acid recognition by metal complexes of bleomycin. *Chem.Rev.* 9**(99):** 2797-2816.

Coller H. A. (2007). What's taking so long? S-phase entry from quiescence versus proliferation. *Nat.Rev.Mol.Cell Biol.* 8**(8):** 667-670.

Collins A. R., Oscoz A. A., Brunborg G., Gaivao I., Giovannelli L., Kruszewski M., Smith C. C. and Stetina R. (2008). The comet assay: topical issues. *Mutagenesis* 3**(23):** 143-151.

Dahlen M., Olsson T., Kanter-Smoler G., Ramne A. and Sunnerhagen P. (1998). Regulation of telomere length by checkpoint genes in Schizosaccharomyces pombe. *Mol.Biol.Cell* 3**(9):** 611-621.

Dean F. B., Lian L. and O'Donnell M. (1998). cDNA cloning and gene mapping of human homologs for Schizosaccharomyces pombe rad17, rad1, and hus1 and cloning of homologs from mouse, Caenorhabditis elegans, and Drosophila melanogaster. *Genomics* 3**(54):** 424-436.

Eliezer Y., Argaman L., Rhie A., Doherty A. J. and Goldberg M. (2009). The direct interaction between 53BP1 and MDC1 is required for the recruitment of 53BP1 to sites of damage. *J.Biol.Chem.* 1**(284):** 426-435.

Enoch T., Carr A. M. and Nurse P. (1992). Fission yeast genes involved in coupling mitosis to completion of DNA replication. *Genes Dev.* 11**(6):** 2035-2046.

Fairchild J. F., Feltz K. P., Sappington L. C., Allert A. L., Nelson K. J. and Valle J. (2009). An ecological risk assessment of the acute and chronic toxicity of the herbicide picloram to the threatened bull trout (Salvelinus confluentus) and the rainbow trout (Onchorhyncus mykiss). *Arch.Environ.Contam.Toxicol.* 4**(56):** 761-769.

Francia S., Weiss R. S. and d'Adda di Fagagna F. (2007). Need telomere maintenance? Call 911. *Cell.Div.***(2):** 3.

Francia S., Weiss R. S., Hande M. P., Freire R. and d'Adda di Fagagna F. (2006). Telomere and telomerase modulation by the mammalian Rad9/Rad1/Hus1 DNA-damage-checkpoint complex. *Curr.Biol.* 15**(16):** 1551-1558.

Freire R., Murguia J. R., Tarsounas M., Lowndes N. F., Moens P. B. and Jackson S. P. (1998). Human and mouse homologs of Schizosaccharomyces pombe rad1(+) and Saccharomyces cerevisiae RAD17: linkage to checkpoint control and mammalian meiosis. *Genes Dev.* 16**(12):** 2560-2573.

Fryer J. L. Lannan C. N. (1994). Three decades of fish cell culture: a current listing of cell lines derived from fishes. 2**(16):** 87-94.

Furuya K., Miyabe I., Tsutsui Y., Paderi F., Kakusho N., Masai H., Niki H. and Carr A. M. (2010). DDK Phosphorylates Checkpoint Clamp Component Rad9 and Promotes Its Release from Damaged Chromatin. *Mol.Cell* 4**(40):** 606-618.

Grossenbacher-Grunder A. M. Thuriaux P. (1981). Spontaneous and UV-induced recombination in radiation-sensitive mutants of Schizosaccharomyces pombe. *Mutat.Res.* 1**(81):** 37-48.

Hagting A., Den Elzen N., Vodermaier H. C., Waizenegger I. C., Peters J. M. and Pines J. (2002). Human securin proteolysis is controlled by the spindle checkpoint and reveals when the APC/C switches from activation by Cdc20 to Cdh1. *J.Cell Biol.* 7**(157):** 1125-1137.

Han L., Hu Z., Liu Y., Wang X., Hopkins K. M., Lieberman H. B. and Hang H. (2010). Mouse Rad1 deletion enhances susceptibility for skin tumor development. *Mol.Cancer*.**(9):** 67.

Hang H., Zhang Y., Dunbrack R. L.,Jr, Wang C. and Lieberman H. B. (2002). Identification and characterization of a paralog of human cell cycle checkpoint gene HUS1. *Genomics* 4**(79):** 487-492.

Hartwell L. H. Kastan M. B. (1994). Cell cycle control and cancer. *Science* 5192**(266):** 1821-1828.

Hartwell L. H. Weinert T. A. (1989). Checkpoints: controls that ensure the order of cell cycle events. *Science* 4930**(246):** 629-634.

HAYFLICK L. MOORHEAD P. S. (1961). The serial cultivation of human diploid cell strains. *Exp.Cell Res.***(25):** 585-621.

Hirai I., Sasaki T. and Wang H. G. (2004). Human hRad1 but not hRad9 protects hHus1 from ubiquitin-proteasomal degradation. *Oncogene* 30**(23):** 5124-5130.

Hirai I. Wang H. G. (2002). A role of the C-terminal region of human Rad9 (hRad9) in nuclear transport of the hRad9 checkpoint complex. *J.Biol.Chem.* 28**(277):** 25722-25727.

Hofmann E. R., Milstein S., Boulton S. J., Ye M., Hofmann J. J., Stergiou L., Gartner A., Vidal M. and Hengartner M. O. (2002). Caenorhabditis elegans HUS-1 is a DNA damage checkpoint protein required for genome stability and EGL-1-mediated apoptosis. *Curr.Biol.* 22**(12):** 1908-1918.

Houtgraaf J. H., Versmissen J. and van der Giessen W. J. (2006). A concise review of DNA damage checkpoints and repair in mammalian cells. *Cardiovasc.Revasc Med.* 3**(7):** 165-172.

Huang J., Yuan H., Lu C., Liu X., Cao X. and Wan M. (2007). Jab1 mediates protein degradation of the Rad9-Rad1-Hus1 checkpoint complex. *J.Mol.Biol.* 2**(371):** 514-527.

Jegou T., Chung I., Heuvelman G., Wachsmuth M., Gorisch S. M., Greulich-Bode K. M., Boukamp P., Lichter P. and Rippe K. (2009). Dynamics of telomeres and promyelocytic leukemia nuclear bodies in a telomerase-negative human cell line. *Mol.Biol.Cell* 7**(20):** 2070-2082.

Johnson A. C., Williams R. J., Simpson P. and Kanda R. (2007). What difference might sewage treatment performance make to endocrine disruption in rivers? *Environ.Pollut.* 1**(147):** 194-202.

Johnson D. G. Walker C. L. (1999). Cyclins and cell cycle checkpoints. *Annu.Rev.Pharmacol.Toxicol.***(39):** 295-312.

Kidd K. A., Blanchfield P. J., Mills K. H., Palace V. P., Evans R. E., Lazorchak J. M. and Flick R. W. (2007). Collapse of a fish population after exposure to a synthetic estrogen. *Proc.Natl.Acad.Sci.U.S.A.* 21**(104):** 8897-8901.

Kilarski W. (1967). The fine structure of striated muscles in teleosts. *Z.Zellforsch.Mikrosk.Anat.* 4**(79):** 562-580.

Koc A., Wheeler L. J., Mathews C. K. and Merrill G. F. (2004). Hydroxyurea arrests DNA replication by a mechanism that preserves basal dNTP pools. *J.Biol.Chem.* 1**(279):** 223-230.

Lehmann A. R. Fuchs R. P. (2006). Gaps and forks in DNA replication: Rediscovering old models. *DNA Repair (Amst)* 12**(5):** 1495-1498.

Li H., Mitchell J. R. and Hasty P. (2008). DNA double-strand breaks: a potential causative factor for mammalian aging? *Mech.Ageing Dev.* 7-8**(129):** 416-424.

Long K. E., Sunnerhagen P. and Subramani S. (1994). The Schizosaccharomyces pombe rad1 gene consists of three exons and the cDNA sequence is partially homologous to the Ustilago maydis REC1 cDNA. *Gene* 1**(148):** 155-159.

Lu J., Peatman E., Wang W., Yang Q., Abernathy J., Wang S., Kucuktas H. and Liu Z. (2010). Alternative splicing in teleost fish genomes: same-species and cross-species analysis and comparisons. *Mol.Genet.Genomics* 6**(283):** 531-539.

Lupardus P. J. Cimprich K. A. (2006). Phosphorylation of Xenopus Rad1 and Hus1 defines a readout for ATR activation that is independent of Claspin and the Rad9 carboxy terminus. *Mol.Biol.Cell* 4**(17):** 1559-1569.

Malumbres M. Barbacid M. (2009). Cell cycle, CDKs and cancer: a changing paradigm. *Nat.Rev.Cancer.* 3**(9):** 153-166.

Marathi U. K., Dahlen M., Sunnerhagen P., Romero A. V., Ramagli L. S., Siciliano M. J., Li L. and Legerski R. J. (1998). RAD1, a human structural homolog of the Schizosaccharomyces pombe RAD1 cell cycle checkpoint gene. *Genomics* 2**(54):** 344-347.

Maya-Mendoza A., Tang C. W., Pombo A. and Jackson D. A. (2009). Mechanisms regulating S phase progression in mammalian cells. *Front.Biosci.***(14):** 4199-4213.

McArt D. G., McKerr G., Howard C. V., Saetzler K. and Wasson G. R. (2009). Modelling the comet assay. *Biochem.Soc.Trans.* Pt 4**(37):** 914-917.

Meyerkord C. L., Takahashi Y., Araya R., Takada N., Weiss R. S. and Wang H. G. (2008). Loss of Hus1 sensitizes cells to etoposide-induced apoptosis by regulating BH3-only proteins. *Oncogene* 58**(27):** 7248-7259.

Musacchio A. Salmon E. D. (2007). The spindle-assembly checkpoint in space and time. *Nat.Rev.Mol.Cell Biol.* 5**(8):** 379-393.

Nabetani A., Yokoyama O. and Ishikawa F. (2004). Localization of hRad9, hHus1, hRad1, and hRad17 and caffeine-sensitive DNA replication at the alternative lengthening of telomeres-associated promyelocytic leukemia body. *J.Biol.Chem.* 24**(279):** 25849-25857.

Nabhan C., Gartenhaus R. B. and Tallman M. S. (2004). Purine nucleoside analogues and combination therapies in B-cell chronic lymphocytic leukemia: dawn of a new era. *Leuk.Res.* 5**(28):** 429-442.

Nakamura T. M., Moser B. A. and Russell P. (2002). Telomere binding of checkpoint sensor and DNA repair proteins contributes to maintenance of functional fission yeast telomeres. *Genetics* 4**(161):** 1437-1452.

Niida H. Nakanishi M. (2006). DNA damage checkpoints in mammals. *Mutagenesis* 1**(21):** 3-9.

Nitiss J. L. (2009). Targeting DNA topoisomerase II in cancer chemotherapy. *Nat.Rev.Cancer.* 5**(9):** 338-350.

Nogueira P., Lourenco J., Rodriguez E., Pacheco M., Santos C., Rotchell J. M. and Mendo S. (2009). Transcript profiling and DNA damage in the European eel (Anguilla anguilla L.) exposed to 7,12-dimethylbenz[a]anthracene. *Aquat.Toxicol.* 2**(94):** 123-130.

Nyberg K. A., Michelson R. J., Putnam C. W. and Weinert T. A. (2002). Toward maintaining the genome: DNA damage and replication checkpoints. *Annu.Rev.Genet.***(36):** 617-656.

Paek A. L. Weinert T. (2010). Choreography of the 9-1-1 Checkpoint Complex: DDK Puts a Check on the Checkpoints. *Mol.Cell* 4**(40):** 505-506.

Parker A. E., Van de Weyer I., Laus M. C., Oostveen I., Yon J., Verhasselt P. and Luyten W. H. (1998). A human homologue of the Schizosaccharomyces pombe rad1+ checkpoint gene encodes an exonuclease. *J.Biol.Chem.* 29**(273):** 18332-18339.

Parrilla-Castellar E. R., Arlander S. J. and Karnitz L. (2004). Dial 9-1-1 for DNA damage: the Rad9-Hus1-Rad1 (9-1-1) clamp complex. *DNA Repair (Amst)* 8-9**(3):** 1009-1014.

Peters G. J., van der Wilt C. L., van Moorsel C. J., Kroep J. R., Bergman A. M. and Ackland S. P. (2000). Basis for effective combination cancer chemotherapy with antimetabolites. *Pharmacol.Ther.* 2-3**(87):** 227-253.

Pichardo S., Jos A., Zurita J. L., Salguero M., Camean A. M. and Repetto G. (2007). Acute and subacute toxic effects produced by microcystin-YR on the fish cell lines RTG-2 and PLHC-1. *Toxicol.In.Vitro.* 8**(21):** 1460-1467.

Prakash L. (1976). Effect of Genes Controlling Radiation Sensitivity on Chemically Induced Mutations in SACCHAROMYCES CEREVISIAE. *Genetics* 2**(83):** 285-301.

Reguart N., Cardona A. F., Carrasco E., Gomez P., Taron M. and Rosell R. (2008). BRCA1: a new genomic marker for non-small-cell lung cancer. *Clin.Lung Cancer.* 6**(9):** 331-339.

Rexroad C. E.,3rd, Palti Y., Gahr S. A. and Vallejo R. L. (2008). A second generation genetic map for rainbow trout (Oncorhynchus mykiss). *BMC Genet.***(9):** 74.

Roos-Mattjus P., Vroman B. T., Burtelow M. A., Rauen M., Eapen A. K. and Karnitz L. M. (2002). Genotoxin-induced Rad9-Hus1-Rad1 (9-1-1) chromatin association is an early checkpoint signaling event. *J.Biol.Chem.* 46**(277):** 43809-43812.

Rowley R., Subramani S. and Young P. G. (1992). Checkpoint controls in Schizosaccharomyces pombe: rad1. *EMBO J.* 4**(11):** 1335-1342.

Sammeth M., Foissac S. and Guigo R. (2008). A general definition and nomenclature for alternative splicing events. *PLoS Comput.Biol.* 8**(4):** e1000147.

Sancar A., Lindsey-Boltz L. A., Unsal-Kacmaz K. and Linn S. (2004). Molecular mechanisms of mammalian DNA repair and the DNA damage checkpoints. *Annu.Rev.Biochem.***(73):** 39-85.

Shimada M. Nakanishi M. (2006). DNA damage checkpoints and cancer. *J.Mol.Histol.* 5-7**(37):** 253-260.

Siede W., Nusspaumer G., Portillo V., Rodriguez R. and Friedberg E. C. (1996). Cloning and characterization of RAD17, a gene controlling cell cycle responses to DNA damage in Saccharomyces cerevisiae. *Nucleic Acids Res.* 9**(24):** 1669-1675.

Singh N. P., McCoy M. T., Tice R. R. and Schneider E. L. (1988). A simple technique for quantitation of low levels of DNA damage in individual cells. *Exp.Cell Res.* 1**(175):** 184-191.

Sinha R. P. Hader D. P. (2002). UV-induced DNA damage and repair: a review. *Photochem.Photobiol.Sci.* 4**(1):** 225-236.

Sohn S. Y. Cho Y. (2009). Crystal structure of the human rad9-hus1-rad1 clamp. *J.Mol.Biol.* 3**(390):** 490-502.

Sorensen C. S., Syljuasen R. G., Lukas J. and Bartek J. (2004). ATR, Claspin and the Rad9-Rad1-Hus1 complex regulate Chk1 and Cdc25A in the absence of DNA damage. *Cell.Cycle* 7**(3):** 941-945.

Steel G. G. (1986). Autoradiographic analysis of the cell cycle: Howard and Pelc to the present day. *Int.J.Radiat.Biol.Relat.Stud.Phys.Chem.Med.* 2**(49):** 227-235.

Steighner R. J. Povirk L. F. (1990). Bleomycin-induced DNA lesions at mutational hot spots: implications for the mechanism of double-strand cleavage. *Proc.Natl.Acad.Sci.U.S.A.* 21**(87):** 8350-8354.

Steinmoeller J. D., Fujiki K., Arya A., Muller K. M., Bols N. C., Dixon B. and Duncker B. P. (2009). Characterization of rainbow trout CHK2 and its potential as a genotoxicity biomarker. *Comp.Biochem.Physiol.C.Toxicol.Pharmacol.* 4**(149):** 491-499.

Stephan H., Concannon C., Kremmer E., Carty M. P. and Nasheuer H. P. (2009). Ionizing radiation-dependent and independent phosphorylation of the 32-kDa subunit of replication protein A during mitosis. *Nucleic Acids Res.* 18**(37):** 6028-6041.

Sullivan M. Morgan D. O. (2007). Finishing mitosis, one step at a time. *Nat.Rev.Mol.Cell Biol.* 11**(8):** 894-903.

Sun A., Bagella L., Tutton S., Romano G. and Giordano A. (2007). From G0 to S phase: a view of the roles played by the retinoblastoma (Rb) family members in the Rb-E2F pathway. *J.Cell.Biochem.* 6**(102):** 1400-1404.

Sunnerhagen P., Seaton B. L., Nasim A. and Subramani S. (1990). Cloning and analysis of a gene involved in DNA repair and recombination, the rad1 gene of Schizosaccharomyces pombe. *Mol.Cell.Biol.* 7**(10):** 3750-3760.

Udell C. M., Lee S. K. and Davey S. (1998). HRAD1 and MRAD1 encode mammalian homologues of the fission yeast rad1(+) cell cycle checkpoint control gene. *Nucleic Acids Res.* 17**(26):** 3971-3976.

Vandenbroucke I. I., Vandesompele J., Paepe A. D. and Messiaen L. (2001). Quantification of splice variants using real-time PCR. *Nucleic Acids Res.* 13**(29):** E68-8.

Venclovas C., Colvin M. E. and Thelen M. P. (2002). Molecular modeling-based analysis of interactions in the RFC-dependent clamp-loading process. *Protein Sci.* 10**(11):** 2403-2416.

Volkmer E. Karnitz L. M. (1999). Human homologs of Schizosaccharomyces pombe rad1, hus1, and rad9 form a DNA damage-responsive protein complex. *J.Biol.Chem.* 2**(274):** 567-570.

Walsh C. T., Garneau-Tsodikova S. and Gatto G. J.,Jr. (2005). Protein posttranslational modifications: the chemistry of proteome diversifications. *Angew.Chem.Int.Ed Engl.* 45**(44):** 7342-7372.

Walworth N., Davey S. and Beach D. (1993). Fission yeast chk1 protein kinase links the rad checkpoint pathway to cdc2. *Nature* 6427**(363):** 368-371.

Wang J. C. (1991). DNA topoisomerases: why so many? *J.Biol.Chem.* 11**(266):** 6659-6662.

Wang T. H., Wang H. S. and Soong Y. K. (2000). Paclitaxel-induced cell death: where the cell cycle and apoptosis come together. *Cancer* 11**(88):** 2619-2628.

Wang X., Guan J., Hu B., Weiss R. S., Iliakis G. and Wang Y. (2004). Involvement of Hus1 in the chain elongation step of DNA replication after exposure to camptothecin or ionizing radiation. *Nucleic Acids Res.* 2**(32):** 767-775.

Wang Y., Ji P., Liu J., Broaddus R. R., Xue F. and Zhang W. (2009). Centrosome-associated regulators of the G(2)/M checkpoint as targets for cancer therapy. *Mol.Cancer.***(8):** 8.

Wanna W., Rexroad C. E.,3rd and Yao J. (2010). Identification of a functional splice variant of 14-3-3E1 in rainbow trout. *Mar.Biotechnol.(NY)* 1**(12):** 70-80.

Wassmur B., Grans J., Kling P. and Celander M. C. (2010). Interactions of pharmaceuticals and other xenobiotics on hepatic pregnane X receptor and cytochrome P450 3A signaling pathway in rainbow trout (Oncorhynchus mykiss). *Aquat.Toxicol.* 1**(100):** 91-100.

Weiss R. S., Leder P. and Vaziri C. (2003). Critical role for mouse Hus1 in an S-phase DNA damage cell cycle checkpoint. *Mol.Cell.Biol.* 3**(23):** 791-803.

Weiss R. S., Matsuoka S., Elledge S. J. and Leder P. (2002). Hus1 acts upstream of chk1 in a mammalian DNA damage response pathway. *Curr.Biol.* 1**(12):** 73-77.

Weiss R. S., Leder P. and Enoch T. (2000). A conserved role for the Hus1 checkpoint protein in eukaryotic genome maintenance. *Cold Spring Harb.Symp.Quant.Biol.***(65):** 457-466.

Weiss R. S., Kostrub C. F., Enoch T. and Leder P. (1999). Mouse Hus1, a homolog of the Schizosaccharomyces pombe hus1+ cell cycle checkpoint gene. *Genomics* 1**(59):** 32-39.

Wilson K. A. Stern D. F. (2008). NFBD1/MDC1, 53BP1 and BRCA1 have both redundant and unique roles in the ATM pathway. *Cell.Cycle* 22**(7):** 3584-3594.

Wollmann Y., Schmidt U., Wieland G. D., Zipfel P. F., Saluz H. P. and Hanel F. (2007). The DNA topoisomerase IIbeta binding protein 1 (TopBP1) interacts with poly (ADP-ribose) polymerase (PARP-1). *J.Cell.Biochem.* 1**(102):** 171-182.

Wood K. W., Chua P., Sutton D. and Jackson J. R. (2008). Centromere-associated protein E: a motor that puts the brakes on the mitotic checkpoint. *Clin.Cancer Res.* 23**(14):** 7588-7592.

Xu M., Bai L., Gong Y., Xie W., Hang H. and Jiang T. (2009). Structure and functional implications of the human rad9-hus1-rad1 cell cycle checkpoint complex. *J.Biol.Chem.* 31**(284):** 20457-20461.

Yanagida M. (2009). Clearing the way for mitosis: is cohesin a target? *Nat.Rev.Mol.Cell Biol.* 7**(10):** 489-496.

Yeang C. H. (2008). Identifying coevolving partners from paralogous gene families. *Evol.Bioinform Online***(4):** 97-107.

Yen T. J. Kao G. D. (2005). Mitotic checkpoint, aneuploidy and cancer. *Adv.Exp.Med.Biol.***(570):** 477-499.

Appendix A
Western Blot Protocol

Once the SDS-PAGE has finished running it is placed in transfer buffer (25mM Tris base, 192mM Glycine, 20% methanol) for 20min, shaking at low speed. The 0.2 µm nitrocellulose membrane (Bio-Rad: Mississauga, ON) is also placed in transfer buffer and this process is necessary to equilibrate the membrane and the SDS-PAGE. Then the following is set up on a Semi-dry transfer unit (Bio-Rad: Mississauga, ON) from bottom to top, thick filter (Bio-Rad: Mississauga, ON), membrane, SDS-PAGE and thick filter paper. A plastic tube is used to roll over each layer as to remove air bubbles that may interfere with the transfer. The lid is put onto the semi-dry transfer unit, according to the manufacturer's instructions, and the power source is set at 20V for 25min. After the transfer the membrane is stained with Ponceau S (0.1% Ponceau S and 5% glacial acetic acid) for 10min on a shaker and then rinsed three times with deionized water until background staining is removed and all that remains stained is the protein. The stained membrane is then scanned using a Hewlett Packard ScanJet 3300C (Mississauga, ON) scanner and Adobe® Photoshop® 7.0. The membrane is then placed in blocking solution [5% Carnation skim milk powder in TBS-T (0.14M NaCl, 2.7mM KCl, 25mM Tris, 1% Tween 20; pH 7.5)] for 1hr, shaking at room temperature as to block unoccupied protein sites. The blocking solution is then removed and the primary antibody (which has been diluted in blocking solution) is added and left in for 1hr, shaking at room temperature. After the 1hr incubation, the antibody is removed and the membrane is washed with TBS-T two times for 10sec, one time for 15min and then two times for 10min. The secondary antibody is added (usually at 1:3000 dilution) and probed for 1hr, shaking at room temperature. After the 1hr incubation the membrane is washed with TBS-T once for 30sec, once for 15min and then twice at 5min. The membrane is placed in an alkaline phosphate (AP) detection solution [(0.1M Tris, 0.1M NaCl, 0.05M MgCl2; pH 9.5)

with 0.33mg/ml nitro blue tetrazolium (NBT) and 0.165 mg/ml bromochloroindolyl phosphate BCIP)] until bands are detected (around 5min). The detection was stopped with the addition of deionized water.

Appendix B
TRIzol® Method for RNA Extraction

For RNA extraction, 120mg of tissue was placed in 1ml of TRIzol® (Invitrogen: Carlsbad, CA) and homogenized using a hand held electric pestle. Another 500µl TRIzol® was added and left to sit for 5min on ice, followed by the addition of 200µl chloroform. After incubating on ice for 10min the samples were centrifuged at 12,000x g for 15 min 4°C. The transparent upper phase layer was removed and placed into a new centrifuge tube containing 500µl isopropyl alcohol. The tubes were inverted twice, incubated on ice for 10min then centrifuged at 12,000xg for 15 min 4°C. The supernatant was removed and 1ml 75% ethanol made in diethyl pyrocarbonate (DEPC) water was added to the RNA to remove trace elements. The sample was centrifuging at 7500xg for 5 min at 4°C and the supernatant was removed. Once dry, the RNA pellet was resuspended in DEPC water. The isolated RNA was subjected to DNase disgestion and "RNA cleanup" according to the protocol of *QIAGEN® RNeasy®* mini kit (Qiagen: Mississauga, ON). The concentration of RNA was determined using a NANODROP® Spetrophotometer ND-100 (Thermo Scientific: Wilmington, DE) and the quality of RNA was evaluated by running 10µg of each sample on a formaldehyde-agarose gel. The RNA samples were stored at -80°C.